TU WIEN

TECHNISCHE UNIVERSITÄT WIEN

Diplomarbeit

Construction of a Corrosion-Resistant 15 L-Pilot-Bioreactor for the Cultivation of Extremely Halophilic Microorganisms

ausgeführt zum Zwecke der Erlangung des akademischen Grades eines

Diplom-Ingenieurs

unter der Leitung von

Univ. Prof. Dipl.-Ing. Dr. techn. Christoph Herwig

(E166 Institut für Verfahrenstechnik, Umwelttechnik und Techn. Biowissenschaften)

Projektass. Dipl.-Ing. Nicole Mahler

(E166 Institut für Verfahrenstechnik, Umwelttechnik und Techn. Biowissenschaften)

eingereicht an der Technischen Universität Wien

Institut für Verfahrenstechnik, Umwelttechnik und Technische Biowissenschaften

von

Pascal Deringer, BSc

Matr. Nr. 1127198

Mandlgasse 25-27/15

1120 Wien

Wien, im Juni 2016

_____

Pascal Deringer

Ich habe zur Kenntnis genommen, dass ich zur Drucklegung meiner Arbeit unter der Bezeichnung

Diplomarbeit

nur mit Bewilligung der Prüfungskommission berechtigt bin.

Ich erkläre weiters an Eides statt, dass ich meine Diplomarbeit nach den anerkannten Grundsätzen für wissenschaftliche Abhandlungen selbstständig ausgeführt habe und alle verwendeten Hilfsmittel, insbesondere die zugrunde gelegte Literatur, genannt habe.

Weiters erkläre ich, dass ich dieses Diplomarbeitsthema bisher weder im In- noch Ausland (einer Beurteilerin/einem Beurteiler zur Begutachtung) in irgendeiner Form als Prüfungsarbeit vorgelegt habe und dass diese Arbeit mit der vom Begutachter beurteilten Arbeit übereinstimmt.

Wien, im Juni 2016

_____
Pascal Deringer

Abstract

Halophiles are microorganisms that can thrive in hostile, hypersaline environments, for example in salt lakes. Due to adaptation to their extreme living conditions they have developed unique features that offer a huge biotechnological potential: halophiles can grow on an exceptionally large variety of substrates and allow cost-effective, non-sterile continuous production of bioproducts.

Potential biotechnological applications of halophilic organisms are for example industrial wastewater treatment and the production of carotenoids, biopolymers or the unique photoactive biomolecule bacteriorhodopsin. However, only a few halophilic organisms are currently commercially used because efficient and economical biotechnological processes for their cultivation on industrial scale have not been developed yet.

A process for biotechnological treatment of industrial waste water by halophiles has been developed by the department of bioprocess engineering at Vienna University of Technology in recent years in a 1 L lab-scale bioreactor. To make this process available for the industry, it has to be scaled up and its simplicity, robustness as well as efficiency have to be demonstrated.

For this reason, a worldwide unique pilot plant on 15 L-scale for the cultivation of halophiles with high productivity is constructed that is customized to the special requirements of these microorganisms. To reduce shear stress to the cells, an airlift bioreactor is used. Due to the high corrosiveness of the medium, the corrosion-resistant nickel-based alloy 2.4602 (Hastelloy C-22) and plastic components are utilized. The bioreactor can be operated at increased pressures to enhance the solubility of oxygen in the medium. Moreover, a cell retention loop is attached to the vessel to increase the productivity of the slow growing halophiles. The process can be operated in batch as well as in continuous mode and allows online monitoring of the main process parameters.

The targets of this master thesis are the construction of the novel bioreactor setup and to make it operational for subsequent research on the biotechnological application of halophiles. The thesis includes the design, specification, installation and testing of the pilot plant as well as documentation. The main challenge is the selection and especially the combination of equipment that is feasible for the highly corrosive medium as well as pressure-resistant. After implementation of the pilot plant, test fermentations with a halophilic strain are performed to demonstrate the operability of the system.

Table of Contents

1   Introduction

Halophiles are organisms that can thrive in hypersaline environments, for example in salt lakes. As a result of adaptation to their extreme living conditions they have developed unique features. Especially the extremely halophilic Archaea have a huge biotechnological potential since they can grow on an exceptionally large variety of substrates and allow cost-effective, non-sterile continuous production of valuable bioproducts. Potential biotechnological applications of halophiles are for example industrial wastewater treatment and the production of carotenoids, biopolymers or the unique photoactive biomolecule bacteriorhodopsin.

The industry has been targeting their commercial use for quite some time, but only a few industrial-scale processes with halophiles exist at the present time [1]. This is because recent scientific studies mainly deal with the isolation of novel halophilic microorganisms and their special characteristics or future applications, but not with the development of efficient and economical biotechnological processes for their cultivation on industrial-scale [1]. Since these studies were mostly carried out with shake flask cultures, little is known about the optimal culture conditions of halophiles in bioreactors [2]. Out of the few experiments that were actually executed in bioreactors, the majority have focused on conventional stirred tank reactors which are not optimal for the cultivation of halophiles on larger scale. Most recent tests in reactors were mostly carried out in batch mode as well as on a small scale, far fewer studies deal with continuous cultures although their ability to perform long-lasting fermentations without the risk of contamination is one of the great advantages these organisms offer. Almost no studies face the production of halophiles at larger scales, for example pilot plants. [1]

To make halophilic microorganisms a beneficial host organism for future applications, more quantitative studies on the cultivation of extreme halophiles have to be executed [2] and mathematical models, which would be useful tools to systematize the analysis of this type of biological processes, have to be developed [1].

When dealing with halophiles, one is confronted with the following drawbacks:
- Due to the corrosiveness of the culture medium with salt concentrations of up to 25%, conventional stainless steels are not suitable. Instead, all components in contact with the brine have to consist of alternative, corrosion-resistant materials such as plastics, glass, ceramic or special non-iron alloys.
- The oxygen solubility in the medium decreases with rising salinity and must therefore be particularly well monitored or improved by specific measures.
- Halophiles have a low specific growth rate.
- The high shear sensitivity of halophilic cells allows only limited turbulence or flow rates in the process.

The development of biotechnological processes for the cultivation of halophilic microorganisms has been executed by the department of bioprocess engineering at Vienna University of Technology in recent years. A special 1 L corrosion-resistant stirred tank reactor made of borosilicate glass with a stirrer consisting of the polymer PEEK (polyetheretherketone) was used for continuous studies on industrial waste water treatment [2]. This new technology was designed to improve the economic viability of industrial processes by the so-called "Waste-to-Value"-principle. Thereby, a saline waste water stream containing various carbon sources is continuously fed into the fermenter and converted into biomass, CO_2 and a target product by the halophiles inside the reactor. Treated effluent is continuously removed from the system. To increase the productivity of the slow growing halophiles, the process was extended by a cell retention system. The 1 L lab-scale setup is depicted on the left side of Figure 1.

Valuable knowledge in dealing with highly saline media and the cultivation of halophilic microorganisms was obtained by these tests. However, to make this process available for the industry, this process technology has to be scaled up and particularly its simplicity, robustness and efficiency have to be demonstrated. For this reason, a worldwide unique pilot plant for the cultivation of halophiles with high productivity was constructed that is customized to the special requirements of halophiles and aims to close the gap between the cultivation of halophilic microorganisms on laboratory scale and the industrial-scale production.

Compared to previous studies, a completely new approach was chosen. First, the reactor volume was increased to 15 L pilot-scale to achieve a more scalable setup. This size allows the implementation of a setup that is much closer to industrial application. The reactor vessel was made of the exceptionally corrosion-resistant nickel-based alloy 2.4602 (Hastelloy C-22; HAYNES International Inc., USA). Moreover, instead of a conventional stirred tank reactor, the pilot reactor was designed as an airlift reactor with external circulation. Airlift reactors are a special type of bubble column reactor and ensure a sufficient oxygen transfer from the gas into the broth at very low shear rates. The external circulation loop, made of PVDF (polyvinylidene fluoride) piping, is directly coupled with a cell retention system by means of a hallow fiber microfiltration membrane module to increase the productivity of the slow-growing halophiles. However, to overcome the pressure drop created by the membrane, an additional pump is required to generate the desired liquid circulation in the system. That way, an external loop airlift reactor with "forced" circulation is created. Furthermore, the reactor can be pressurized to enhance the solubility of oxygen in the medium. Thereby, a major drawback of the use of halophilic microorganisms, low oxygen solubility in salt-containing media, can be compensated. However, in order to pressurize the reactor, all equipment parts (reactor, tubing, sensors, membrane module) had to be designed to withstand

overpressure. Moreover, further safety measures by means of a safety valve had to be taken. The process can be operated in batch, continuous as well as in cell retention mode and allows online process monitoring of the main process parameters (temperature, pressures, pH-value, dissolved oxygen concentration, transmembrane pressure, flow rates, off-gas composition, etc.). For demonstrative purposes, e.g. to bring it to fairs, the pilot plant was executed as a mobile, compact system, which means that it was placed on custom made wheeled rack that fits through normal doors.

The pilot plant was dimensioned by scaling the 1 L lab-scale process [2] up to 15 L. The setup based on a user requirements specification and a process flow diagram provided by Nicole Mahler and Christoph Herwig of the research group bioprocess engineering [3]. The targets this master thesis were the construction of the novel bioreactor setup as well as to make it operational for subsequent research on halophiles. The thesis included the design, specification, installation and testing of the pilot plant as well as documentation. During the first phase, the reactor, cell retention loop plus other main process parts were dimensioned and an automation concept was created. The aim of the second phase was the specification of the equipment parts so that they met the demands for pressure and corrosion resistance. Once all components were specified, they were inquired and bought. After testing the operability of the individual components, the pilot plant was completely assembled and all control signals (from pumps, online sensors, control valves, balances etc.) were integrated into the existing process control system of the Vienna University of Technology. Next, integrity tests of the whole system were performed with water, followed by test fermentations in batch and continuous mode, in which a halophilic strain was successfully cultivated and hence the operability of the plant could be demonstrated. Lastly, all equipment parts, the construction, circuit diagram and the process control signal assignment were documented and an operating manual was written. A comparison of the 1 L lab-scale and 15 L pilot bioreactor setup at the time of the submission of this thesis is shown in Figure 1:

Figure 1: 1 L Lab-scale (left) and 15 L Pilot-scale (right) Bioreactor Setups

2 Theory

2.1 Halophiles

Halophilic microorganisms are specialized in living in hypersaline environments, whereas organisms capable of growth in the absence of salt, but tolerating variable salinities are considered to be halotolerant [4]. Both have the ability to balance the osmotic pressure of their habitat and resist the denaturing effects of salts [2]. As a result of adaptation to their extreme environment they have, like many other extremophiles, evolved unique properties of considerable biotechnological and thus commercial significance [5].

Halophilic microorganisms' natural habitats are crystallizer ponds of solar salterns or hypersaline soda lakes [2]. These are typical examples of generally hostile environments in which low microbial species diversity can be found. The spectrum of organisms that thrive in such saline habitats is mainly determined by the parameters salinity, O_2-solubility and ionic composition [4].

Figure 2: Solar Saltern at Salinas de S'Avall, Mallorca, Spain [6]

Halophiles can be classified as slightly (up to 5% NaCl-concentration), moderately (5-15% NaCl-conc.) or extremely halophilic (above 20% NaCl-conc.), depending on their requirement for sodium chloride concentration [2]. They are mainly represented by the halobacteria (extremely halophilic aerobic Archaea), the moderate halophiles (Bacteria) and several eukaryotic algae [4].

Especially the extremely halophilic aerobic Archaea are very promising for future biotechnological use since they are able of growing on an exceptionally large variety substrates, can produce unique, thus valuable substances and lastly, offer the possibility for non-sterile, continuous cultivation. Although their ecology and physiology are widely identified on the microbiological level, little emphasis has been laid on quantitative bioprocess development with extreme halophiles [2].

2.1.1 Characteristics of Extremely Halophilic Archaea

The use of halophilic microorganisms offers some unique advantages compared to conventional biotechnologically used strains. Their suitability for cost-effective, non-sterile cultivation may even make extremely halophilic Archaea suitable for non-biotechnological industrial environments [2].

Halophilic microorganisms are able to live in environments which are generally hostile. Due to the high osmotic pressure of hypersaline environments, almost no competition to other organisms and hence low risk of contamination occurs [2]. This allows the work under non-sterile conditions and to carry out long-lasting continuous cultivations without the danger of infections. Unlike continuous cultures with plant and mammalian cells that require the addition of antibiotics to prevent them from being overgrown by other, faster growing bacteria, a natural selection takes place in halophilic cultures [3]. Such non-sterile continuous processes allow the best utilization of the investment costs. If the systems do not need to be autoclaved costly, the processes can be designed simpler and less expensive - an argument that is even more significant if one moves from laboratory to industrial-scale [3].

Another special feature of halophiles is that they are capable of growing on an exceptionally large variety of different carbon compounds, for example organic acids (e.g. acetate, lactate), diverse sugars, sugar alcohols and even glycerol. They also show a remarkable resistance to organic substances which have an inhibitory or even toxic effect on many other organisms and therefore can even grow on aromatic compounds like phenol [2]. Moreover, halophilic microorganisms allow a very simple purification of intracellular products through the automatic lysis of the cells in water due to an osmotic shock.

However, the downsides of the use of halophilic organisms are the high corrosiveness and the lower oxygen solubility of their media as well as their small specific growth rate and high shear sensitivity.

Since halophiles require hypersaline environments of up to 30% or 5 M sodium chloride concentration, these organisms cannot be cultivated in conventional reactors made of stainless steel because of the corrosiveness of saline media. All components in contact with the brine have to consist of alternative, corrosion-resistant materials [5].

The oxygen solubility in water decreases with increasing salinity. Compared to pure water, only 40% of the initial amount of oxygen can be dissolved in a solution with a NaCl-concentration of 20% [7]. To ensure sufficient oxygen transfer from the gas into the broth and allow high outputs, additional measures have to be taken when using saline media, for example more mixing or turbulence in the reactor, higher oxygen content in the inlet air or increased pressure.

High biological activity and volumetric productivity are considered as prerequisites for efficient bioprocesses. Extremely halophilic Archaea and other halophiles have, however, low growth rates, for which reason they are so far not commonly used in industrial bioprocesses [8]. For example, the halophilic archaeon *Haloferax mediterranei* proliferates with a rate of 0.04 to 0.08 h^{-1}, depending on the used substrate. By contrast, Escherichia coli, a commonly utilized bacterium in biotechnology, has a maximum growth rate of 2 h^{-1} at 40°C [3]. To overcome this physiological limit and to achieve increased volumetric productivity, the produced biomass must be retained in the bioreactor [8]. For this reason, a cell retention system for halophiles by means of a microfiltration membrane has been developed by the Vienna University of Technology. This process is described in Chapter 2.4.

Furthermore, the high shear sensitivity of the halophilic Achaea only allows limited turbulence and flow rates in the process. This has to be considered when selecting the reactor type, pipe dimensions as well as other process parts, such as the membrane, pumps and valves.

Halophiles can produce valuable substances for use in food and pharmaceutical industries. The secondary metabolites of halophilic organisms are for example carotenoids, which are used as food additives and in the pharmaceutical industry, or biopolymers. In addition, they can be used for the production of recombinant products. Further actual and potential halophiles-derived products are listed in Chapter 2.1.2.

2.1.2 Biotechnological Applications and Products of Halophiles

Although halophilic microorganisms offer a multitude of actual and potential applications in biotechnology [5] as they are easy to grow and the necessity for aseptic conditions is decreased to a minimum [4], only a few processes are currently commercially established, namely the production of β-carotene by the algae *Dunaliella salina,* as well as carotenoids produced by *Halobacterium salinarum*, which function as antioxidants and food colorants [9]. Especially the extremely halophilic Archaea offer a great variety of possible process applications that have not been industrialised yet.

An example is the bacteriorhodopsin formation by *Halobacterium salinarum,* promising multiple possible applications by converting light energy to electrical or chemical energy [9]. The usage of this photoactive molecule for photovoltaic is currently investigated. Thereby a sustainable alternative to conventional solar cells could be developed. At present, bacteriorhodopsin is commercially used in bio-photosensors for the identification of security features or data storage with light [3], for example by the German company Actilor GmbH.

Polyhydroxyalkanoates (PHA) are intracellularly accumulated bacterial storage compounds and their properties are comparable to those of polyethylene and polypropylene. Such biodegradable plastics could replace oil-delivered thermoplastics in some fields [5]. The accumulation of PHAs as energy reserves within *Haloferax mediterranei* and *Halomonas boliviensis* is known, but so far no industrial attempt for the production of these plastics has been made [9].

Haloferax mediterranei along with some other halophiles is also known to produce extracellular polysaccharides which could be utilized as gelling or thickening agents in food industry. [9]

Another example is the use of biosurfactant-producing halophilic microorganisms for the accelerated remediation of oil-polluted saline environments. By decreasing surface tension, biosurfactants increase the solubility and thus mobility of hydrophobic hydrocarbons, which may promote degradation. *Bacillus licheniformis* produces the most effective surfactant lychenisin. [5]

Since halophile microorganisms are capable of growing on a large variety of carbon sources, another possible application is the biological treatment of saline industrial waste effluents [2][4] as well as degradation of toxic compounds and even detoxification of chemical warfare agents [5].

2.2   Waste to Value

A possible application of halophiles is the biotechnological utilization of waste streams - the so-called "Waste-to-Value"-principle. Waste streams from various industrial processes, such as in the chemical-, pharmaceutical-, pulp- , paper- and food industry, often contain large amounts of organic carbon that have be reduced before they can be reused or even be disposed of. To make these processes more economic, these waste streams must be either disposed of inexpensively or, even better, converted into useful substances.

At the department of bioprocess engineering, a new technology has been developed to improve the economic viability of these production processes by biotechnologically purifying hyper saline wastewater. The principle is based on the use of extremely halophilic Archaea. These can grow on an exceptionally large amount of different carbon sources, such as organic acids, sugars and even aromatic compounds [3]. When cultivating these microorganisms on the industrial saline effluents, they metabolically degrade these substances and thereby lead to a reduction of the total organic carbon (TOC) content, an indicator of the pollution of waste water. The halophilic wastewater treatment is based on the same basic principle as each sewage plant: impurities are converted into CO_2 and biomass by the metabolism of the cells and then the biomass is removed from the waste stream [3].

But the potential of halophilic Archaea goes beyond the mere reduction of waste materials, since they are capable to use them as nutrients and convert them into economically valuable organic products while simultaneously purifying the industrial effluent by reducing its TOC. This process is called "Waste-to-Value"-principle. The purified waste stream can then be disposed of or recycled [3]. The products of halophilic organisms are for example carotenoids, or biopolymers (PHAs), previously described in Chapter 2.1.2.

This method can also be used for industrial effluents that do not contain salt by adding NaCl to the stream until a sufficient concentration for the cultivation of a halophilic organism is reached. However, most of the time the added salt would have to be removed from the stream again before the effluent can be disposed of or recycled. Therefore directly using saline waste water is far more cost efficient. The following picture shows a schematic representation of the "Waste-to-value"-principle:
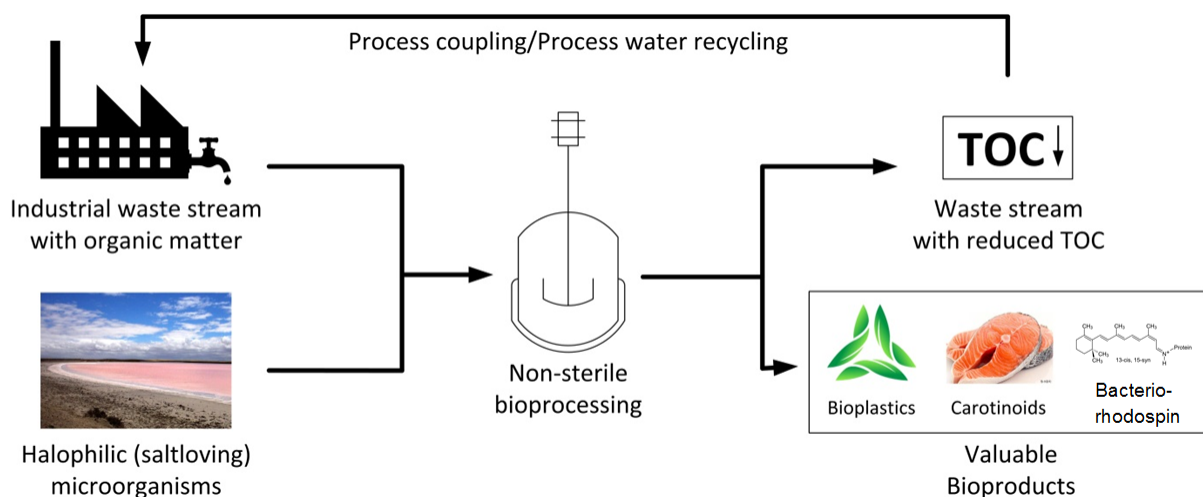
Figure 3: Schematic Representation of the "Waste-to-Value"-Principle

The biological process for treating hypersaline wastewater can be a financially rewarding alternative to conventionally used chemical methods, like precipitation or flocculation. It is possible to deplete carbohydrates greatly and achieve residual concentrations that are well below the ones reached with chemical processes. Biological treatment requires fewer resources as temperature of only up to 40°C are necessary and less chemicals are needed. Furthermore, it contributes to a sustainable wastewater treatment concept, especially if it is possible to integrate purified substances back into the process or converting materials previously declared as waste into valuable substances. Thus, these "Waste-to-value"-processes offer the opportunity to reduce resource consumption to a minimum. [3]

2.3   Bioreactor Setup for Halophilic Microorganisms

Batch operation mode is the preferred strategy to operate in pharmaceutical, biotechnological, and food industry due to its simplicity, the large amount of experience with this system and low risk of contamination. However, the drawbacks of this mode are high labour and processing costs, as well as low operating efficiencies due to frequent start-ups and shut-downs. [1]

Continuous culture can outperform batch culture by eliminating the down time for cleaning and sterilization and the long lag phases before the organisms enter a brief period of high productivity. Furthermore, it allows constant product quality and higher productivity and overall low labour cost. On the contrary, its major drawback is the higher risk of contamination, which has traditionally restricted this operation mode to academic investigation. However, since the risk for contamination of extremophilic continuous cultures is relatively small, long-term, steady-state operation is possible [1].

Another crucial aspect of the cultivation of extremophiles on bioreactor-scale is the selection of an adequate bioreactor configuration [1]. Gas-liquid reactors should achieve efficient mixing of reactor contents and intensive contact of the two phases. In the classical type of gas-liquid reactor, the stirred tank, this is accomplished by a mechanical agitator, mostly Rushton turbines [10]. The stirrer is the main gas-dispersing tool, and its speed and design have both a pronounced effect on mass transfer. [1]

When selecting the bioreactor type, a balancing act between critical shear rates of the cells and the mixing quality has to be performed. Therefore, alternative bioreactor configurations such as airlift or horizontal rotating-drum bioreactors have been suggested for the cultivation of halophiles, which are shear-sensitive and slow-growing microorganisms [1][11]. To ensure a sufficient oxygen transfer rate (OTR) from the gas into the broth at very low shear rates, the pilot reactor was designed as an airlift reactor (ALR), instead of a conventional stirred tank reactor (STR).

Airlift reactors, a special modification of bubble column reactors, do not need a mechanical device for dispersing the gas phase because they are pneumatically agitated by the ascending bubbles. The contacting of gas and liquid is done by feeding the gas stream through distributing devices, so-called spargers, such as perforated or porous plates [10]. The mass transfer in these reactors depends mainly on the aeration rate and the reactor height. ALRs provide good mixing, an efficient OTR, low shear forces and have a relatively simple design [12]. A detailed study of the pros and cons of airlift reactors is given in Chapter 2.3.1.

2.3.1 Airlift Reactors

In airlift reactors a circulating flow of liquid is produced by aerating only the riser section separated from the rest of the reactor (downcomer) [10]. ALRs can be divided into two main types based on their structure: baffled or internal-loop vessels, in which baffles or a draft tube placed strategically in a single vessel create the channels required for the circulation, and external loop vessels, in which circulation takes place through separate conduits [10][13]. Both setups are displayed in Figure 4.
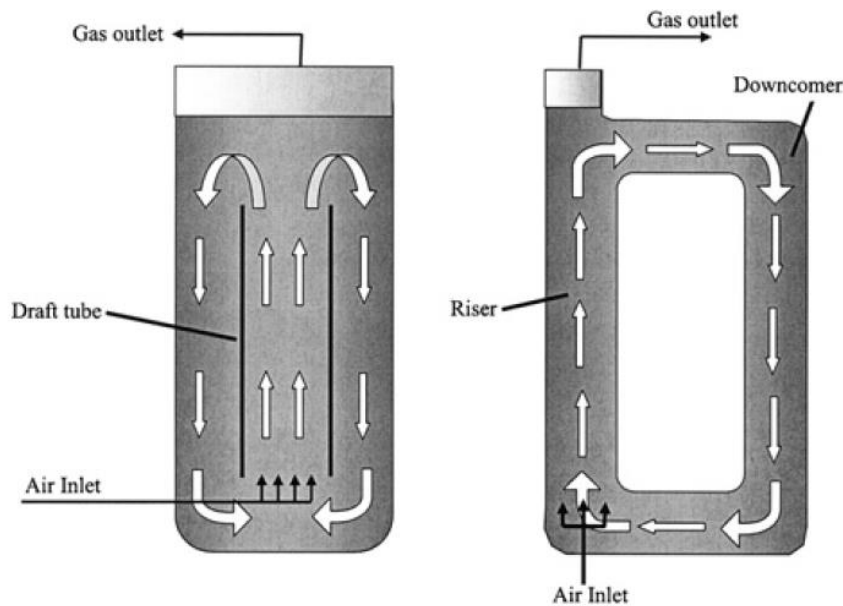
Figure 4: Airlift Bioreactor with Internal (left) and External (right) Circulation [14]

The main difference between ALRs and bubble columns is the type of fluid flow, which mainly depends on the geometry of the system. In bubble columns, gas is injected at the bottom and random mixing is produced by the ascending bubbles. In the ALR, the major patterns of fluid circulation are determined by the design of the reactor, which has a channel for gas-liquid upward flow, the riser, and a separate channel for the downward flow, the downcomer. The two channels are linked at the bottom and at the top to form a closed loop. The gas is usually injected near the bottom of the riser. [13]

The aerated liquid in the riser is at least partially degassed at the top of the reactor. As shown in Figure 5, airlift reactors therefore often have larger diameters on the top end to act as gas separators [12]. Due to the density difference between gas-liquid dispersion in the riser and relatively gas-free liquid in the downcomer, hydrostatic pressure in these two regions is different, which induces a circulating flow of liquid in the reactor loop [10]. This circulation acts additionally to the pneumatic agitation by the upward gas flow and thus increases the quality of mixing, turbulence and mass transfer in the reactor. Figure 5 shows an airlift bioreactor setup with an internal circulation.

$$D_s/D \simeq 2$$
$$H/D = 5 - 10$$
$$D_a/D \geq 0.71$$

Figure 5: Standard Airlift Reactor with Internal Draft Tube [12]

Airlift reactors offer several advantages over stirred tank reactors, such as being more energy efficient, better heat transfer, not having a mixer shaft, which eliminates one source of potential contamination, and finally having a less harsh hydrodynamic environment, in other words applying lower shear forces to the cells [14].

Since airlift reactors do not require a mechanical stirrer, the energy demand is significantly reduced. Hence, they require only about one third of the energy needed for stirred tank reactors. Furthermore, the turbulence of two-phase flow in airlift reactors not only produces favourable conditions for mass transfer, it can also be used for suspending solid particles. [10]

However, to achieve efficient mixing as well as mass- and heat transfer, airlift reactors have to be very high [10], with a height to diameter ratio (H/D) varying between 5 and 10. The OTR increases with the height of the reactor. Compared to STRs (H/D of 2 to 3), jackets along the vessel cylinder of airlift reactors have therefore much better heat transfer rates. [12]

The mechanical agitation required to provide a homogeneous environment in an STR presents three possible mechanisms of cell damage: first, the direct contact between cells and the impeller blades, second, the contact between cells and other stationary bioreactor components such as baffles and third, the bubble burst caused by the

vortices created by the impeller. In an airlift bioreactor, these problems are all eliminated by the absence of a stirrer. [14]

For the growth of microorganisms, ALRs are considered to be superior to traditional stirred-tank fermenters, mainly because of different fluid dynamics. In conventional stirred tanks, the energy required for the movement of the fluids is introduced at a single point in the reactor, via the stirrer. Consequently, energy dissipation is very high in the immediate surroundings of the stirrer and decreases away from it toward the walls. Similarly, shear will be greatest near the stirrer. This results in a wide variation of shear forces. For example, the maximum shear gradient in a stirred tank with a flat-blade turbine has been reported to be approximately 14 times larger than the mean shear gradient. By contrast, there are no local points of energy dissipation and shear distribution is homogeneous throughout an ALR, thus there is a relatively constant environment. [13]

The overall energy dissipation into the medium is lower in ALRs than in STRs, which must be especially considered for upscaling, because the heat dissipation is usually more problematic in large vessels due to a smaller volume to surface ratio.

Another advantage of airlift reactors is their mechanical simplicity. The absence of a mixing shaft and of the associated sealing, which are generally problematic in regard to sterility, makes them suitable for processes involving slow-growing cultures, such as animal and plant cells, for which the risk of contamination is large, as well as for long lasting continuous fermentations. [13]

Furthermore, due to their relatively simple design, ALRs are well suited for very large applications in production-scale of up to 500 m³ [12]. Besides, their simple structure is advantageous in terms of corrosion resistance since no moving parts, such as the impeller and its shaft in STRs, come into contact with the medium [10]. ALRs are appropriate for large processes involving low-value products, where energy efficiency may be the key point for design, for example when used as reactors for wastewater treatment. That is because the mass transfer rates for a given energy input of ALRs are superior to mechanically agitated reactors. [13]

However, the disadvantages of ALRs are lower maximum possible oxygen transfer rates and the requirement for a minimum liquid volume for proper operation. The high OTRs of stirred tank reactors cannot be reached in bubble or even airlift reactors by far [12]. According to Präve [15], the volumetric mass transfer coefficient (k_La-value) in a stirred tank is about 60% higher than in an airlift reactor with the same working volume and the same aeration rate. Furthermore, the changes in liquid volume in airlift reactors are limited to the region of the gas separator, since the liquid height must always be sufficient to allow liquid recirculation in the reactor and must therefore be above the separation between the riser and the downcomer. [13]

The external loop of the pilot airlift reactor is combined with a microfiltration membrane module for cell retention. The membrane significantly increases the flow resistance in the loop and presumably hinders the formation of the circulation flow that is inherent to ALRs. Therefore, a pump is required to overcome the pressure drop created by the microfiltration membrane and to circulate the liquid in the system. That way, an external loop airlift reactor with "forced" circulation is created. This method is less cost efficient, but offers the advantage that the flow rate of the circulating fluid can be controlled in a wider range than in a free system.

Airlift reactors are popular in modern bioprocess research and development. These reactors are particularly suitable for biological processes in which a high mass transfer rate is required, but excessive power input may damage the cells due to shear effects. ALRs also have very appealing characteristics for bioprocesses for low-value products in which efficiency of energy utilization may become the key point for design. Such is the case for ALRs for wastewater treatment. [13]

Airlift reactors are currently used as fermenters in biotechnological processes mainly because of their simple construction. On industrial-scale they are nowadays utilized for the production of single cell proteins, ethanol and aerobic waste water treatment [10]. Furthermore, they are primarily recommended for the cultivation of plant and animal cells [11][16].

2.4　　Cell Retention

The main operation modes in biotechnology are batch, fed-batch and continuous (steady state) fermentations. Cell retention is an advancement of the continuous operation mode for the purpose of increasing the productivity of a bioprocess. A schematic representation of these four states is shown in Figure 6:

(A) Batch　　**(B) Fed-Batch**　　**(C) Steady State**　　**(D) Cell Retention**

F_M　　　　F_B　　F_P
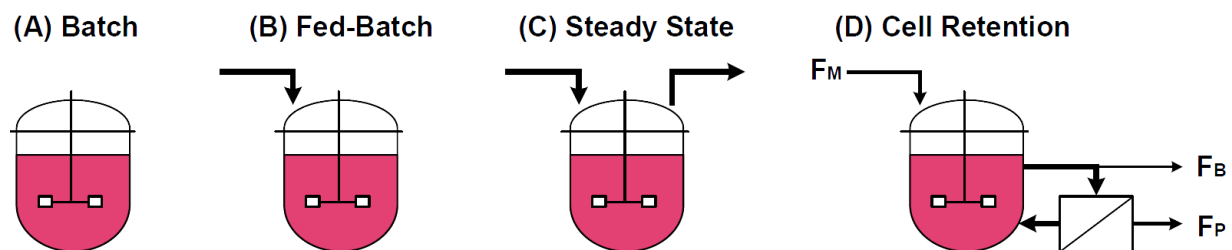
Figure 6: Main Operation Modes in Bioprocessing

Increasing volumetric productivity of a biological system to obtain the maximal amount of desired bioproduct in a given time period is of highest importance for research and industry [8]. Extremely halophilic Archaea and other halophiles have, however, low growth rates. To overcome this physiological limit and to realize high productivity, cell retention systems are used to retain the produced biomass in the bioreactor and achieve high cell densities [8].

The volumetric productivity of a bioprocess is not only dependent on the performance of the selected microorganism, but also on the available biomass concentrations x in the system. But in many cases x remains small in free culture systems. Therefore, by using immobilization or cell retention systems, the cells can be utilized much longer than they would have been available in a free system. Cell retention techniques are for example growing the cells on carrier materials, flotation, sedimentation as well as membrane filtration. [11]

The functionality of cell retention with a microfiltration membrane is described below. A schematic representation of this system is given in Figure 7. This configuration has been used for the experiments on the cultivation of halophiles by the department of bioprocess engineering at TU Vienna in the last years.
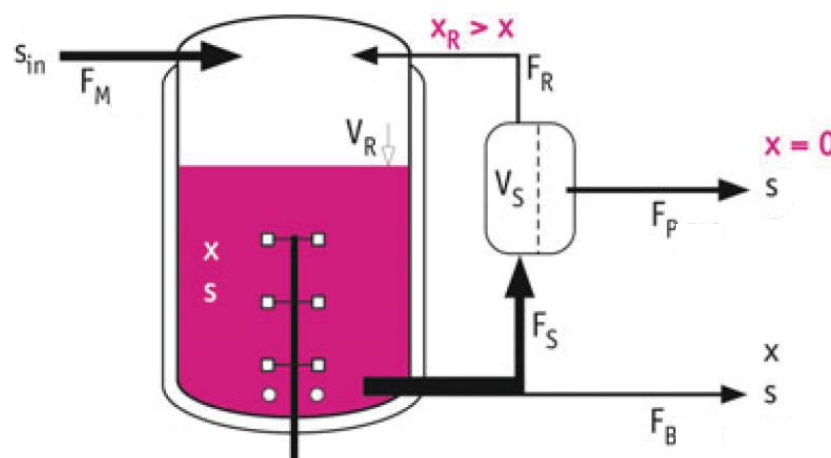
Figure 7: Cell Retention System with Microfiltration Membrane [11]

A continuous feed flow F_M with a substrate concentration s_{in} enters the reactor. At the same time, a constant stream of cell suspension is pumped out of the bioreactor and forced through a microfiltration membrane, where it is separated into a filtrate or permeate flow F_P and a cell suspension stream F_R with a slightly higher biomass concentration than in the reactor itself ($x_R > x$). Most of the cell suspension is then recirculated into the reactor, while the cell-free filtrate F_P ($x = 0$) and a small part of the cell suspension, the so-called bleed flow F_B, are removed from the system.

This bleed stream is necessary because when only cell-free stream is harvested, the biomass concentration in the bioreactor would constantly rise. Hence, the specific growth rate would continuously decrease and the physiological conditions in the bioreactor would no longer be constant. By using the so-called "feed and bleed"-strategy with an outgoing bleed stream F_B, the biomass concentration and thereby the specific growth rate in the bioreactor can be maintained constant. This is advantageous regarding process controllability for long term bioprocessing. [8]

During batch fermentations (Figure 6, A), the microorganisms proliferate with their maximum specific growth rate μ_{max}, a physiological constant. However, in continuous processes (Figure 6, C), the specific growth rate μ equals the dilution rate D, which is the ratio of feed flow F_M to reactor volume V_R, when a steady state has been reached.

$$\mu = D = \frac{F_M}{V_R} \ [h^{-1}]$$

Eq. 1 [11]

Therefore, when increasing the feed flow at constant reactor volume and substrate concentration in the feed, the growth rate μ rises as well and thus more biomass is produced in the same period [3]. As a result, the physiological factor μ can be adjusted by the operative variable D to a certain extent [11], which is a significant advantage regarding process control. However, since the growth rate of a microorganism is limited by the physiological constant μ_{max}, the dilution rate can only be increased to this value. Above, the cells wash out and growth is no longer possible [3].

Through cell retention, the specific growth rate μ can be decoupled from the dilution rate D, allowing much higher dilution rates in comparison to the free system without retention. The reason for that is the increased biomass concentration, shown in Eq. 4. By introducing the recirculation ratio R, the ratio of permeate to feed flow,

$$R = \frac{F_P}{F_M}$$

Eq. 2 [11]

where R = 1 means total cell retention and R = 0 equals normal continuous mode, and adapting the biomass balance, a new correlation between growth rate and dilution rate can be found:

$$\mu = (1 - R) * D \ [h^{-1}]$$

Eq. 3 [11]

Now D can be increased well above μ_{max} when the recirculation ratio is raised at the same time, therefore making μ more independent from the dilution rate. The biomass concentration x in the reactor is increased by the factor $(1 - R)^{-1}$ compared to the free system without cell retention, as the following equation shows. $Y_{X/S}$ stands for biomass yield, s_{in} is the substrate concentration in the feed and s the concentration in the media, that is usually below the detection limit.

$$x = Y_{X/S} \frac{s_{in} - s}{1 - R} \left[\frac{g}{L}\right]$$

Eq. 4 [11]

The experiments by the department of bioprocess engineering showed that D and hence the productivity of continuous processes could be increased tenfold compared to free continuous operation by using a microfiltration membrane cell retention

system and that this value could possibly be increased even further [3]. Chmiel [11] stated that the productivity could in fact be enhanced by the factor 100.

However, besides higher equipment costs, another drawback of cell retention systems is that the oxygen demand rises significantly with increasing biomass concentration. Furthermore, higher cell concentration enhances the viscosity of the suspension and thereby decreases the oxygen mass transfer from the gas into the liquid [3]. Therefore, the dissolved oxygen concentration has to be particularly well monitored in reactors when cell retention systems are utilized.

2.4.1 Cross Flow Filtration

In the lab-scale and the pilot process for the cultivation of halophiles, the microfiltration membrane module has the task to retain the biomass in the system to increase the volumetric productivity (cell retention). A hollow fiber cross flow filtration cartridge is used in the lab-scale plant.

Dead-end filtration is the classical filtration technique where the feed stream flows perpendicular to the membrane surface and the whole liquid has to pass through the membrane. However, this method is not suitable for cell retention, as the two components, medium and cells, do not have to be totally separated but a small cell-free filtrate stream has to be continuously removed from the system. Instead, cross flow filtration is feasible.

Cross flow filtration (CFF) or tangential flow filtration is a filtration technique in which the solution passes tangentially along the surface of the filter. The CFF-principle is shown in Figure 8. A pressure difference across the filter drives a part of the liquid and components that are smaller than the pores through the filter (permeate), while the remainder (retentate), which contains all components larger than the filter pores, is recirculated to the feed reservoir tank. [17][18]
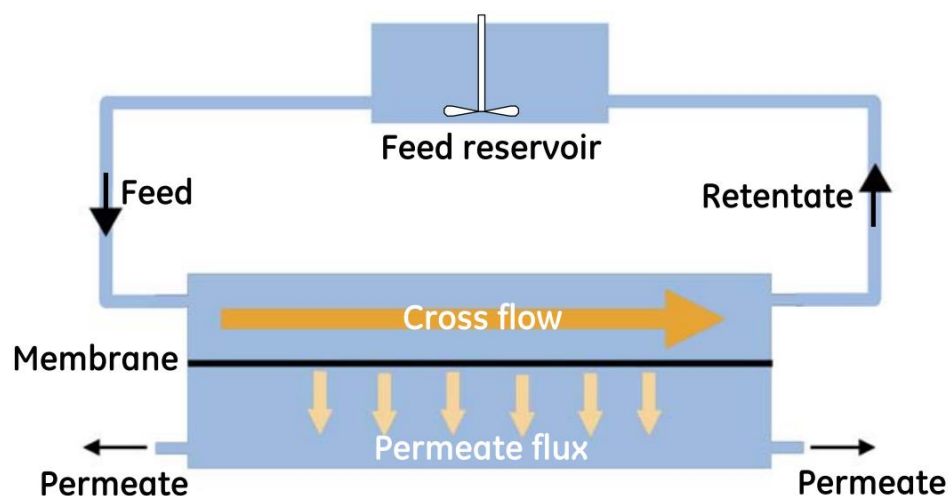
Figure 8: Principle of Cross Flow Filtration [18]

Two basic filter configurations are generally used for cross flow filtration: hollow fibre modules or cartridges as well as cassette modules [18]. Both types are depicted in Figure 9:
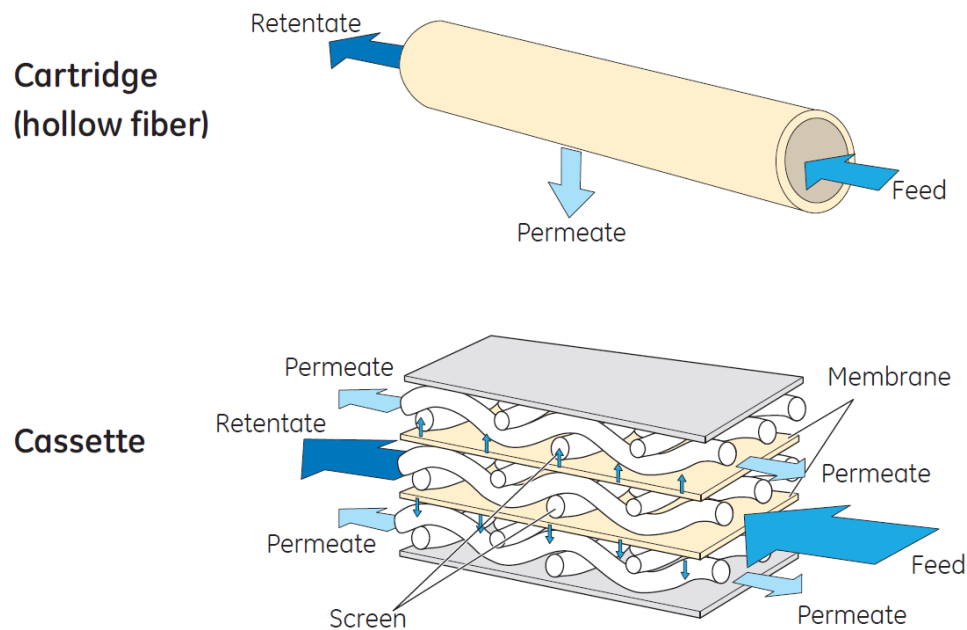
Figure 9: Filter Configurations for Cross Flow Filtration [18]

In hollow fiber filters, the feed stream passes through a set of parallel hollow fibers and the permeate is collected outside of the fibers. These filters are characterized by their fiber length and number, lumen diameter as well as filter pore size. In cassette filters, several flat membrane sheets are held apart from each other and from the cassette housing by support screens. The feed stream passes through the space between two sheets and permeate is collected on the opposite side of the sheets. Cassettes are characterized by their flow path length, channel height, as well as membrane pore size. [18]

For cell harvesting via microfiltration, the company GE Healthcare Life Sciences [18] recommends hollow fiber filtration. Compared to cassette modules, cartridges usually induce lower shear rates. Furthermore, the shear rate in hollow fibres can be easily calculated since it is only dependent on the fiber diameter and the flow rate through the lumen of a single fiber. Besides, hollow fiber modules can be cleaned from fouling by backflushing liquid from the permeate side. However, cassette modules are generally suitable for higher transmembrane pressures.

2.5 Corrosion-Resistant Bioreactor Materials for Extreme Halophiles

Materials for the construction of bioreactors that are suitable for the cultivation of extremely halophilic Archaea have to be durably corrosion-resistant to aqueous sodium chloride solutions with concentrations of up to 30% at relatively low temperatures. Appropriate materials for that purpose are glass, ceramics, polymers and special, non-iron alloys. However, due to high brittleness and low pressure resistance, glass and ceramics are not qualified for use as reactor materials at elevated pressures.

Most polymers have an excellent resistance to chemicals, but they leach over time when in contact with them. In order to use plastic in a bioreactor system, one has to choose a polymer that only leaches to a sufficiently small extend. These plastics are specified by organizations like the USA Food and Drug Administration (FDA) and are for example polyethylene (PE), polypropylene (PP), polysulfone (PSU), polyetheretherketone (PEEK), Polytetrafluoroethylene (PTFE) and polyvinylidene fluoride (PVDF) [19][20]. The drawbacks of plastics are that they have a significantly lower strength and temperature resistance than metals. Furthermore, their strength drastically decreases with rising temperature. However, PEEK, PTFE and PVDF are applicable for relatively high temperatures of up to 200°C and are therefore even able to be autoclaved. Hence, these three materials are the most suitable polymers for the use in bioreactors and have already been utilized in small scale plants [2][21]. But compared to other polymers, these three materials are considerably more expensive, albeit still cheaper than metals with sufficient corrosion resistance for hypersaline media. Furthermore, the yield strength of polymer materials can be significantly increased by using glass fibre reinforced plastic (GRP), allowing the construction of larger vessels and higher pressures. GRP-constructions are very cost efficient and are therefore promising for the use in large scale applications like waste water treatment, however, FDA-approval is more complicated for glass fibre reinforced plastics [22].

Metals have much better mechanical properties than plastics. Besides, they offer excellent weldability and fabricability. However, they are vulnerable to corrosion, especially in environments containing chloride ions. Only metals or alloys with passivity, which are protected by a durable, adherent oxide film on their surface, are resistant to chloride solutions or exhibit only very low rates of corrosion. Such materials are aluminium, chrome, nickel, titanium, cobalt, tantalum and their alloys. Even steel can be passivized by alloying passive metals like chrome, thereby creating so-called stainless steel. However, materials that exhibit passivity are especially prone to localized (pitting and crevice) corrosion in solutions that contain chloride ions. While various stainless steels are capable of being used in

environment containing low NaCl-concentrations like seawater, only non-iron materials such as the nickel-based alloys Hastelloy C-22 (HAYNES International Inc., USA) are suitable for a medium containing up to 25% NaCl without being affected by local corrosion. However, the high costs of these special materials usually limit their large scale application. [23][24]

A short study of the corrosion mechanisms of metals is given in Chapter 2.5.1 and a summary of the characteristics of the nickel-based alloy Hastelloy C-22, which was chosen for the construction of the bioreactor, is shown in Chapter 2.5.2.

2.5.1 Corrosion of Metals

Corrosion is the chemical or electrochemical reaction between a material, usually a metal, and its environment that leads to deterioration of the material and/or its properties. [23]

Corrosion can be classified as uniform corrosion and localized corrosion. Uniform corrosion occurs over the entire exposed surface and leads to thinning of materials, for example rusting of iron. Uniform corrosion rates of most materials in a variety of environments are already established and available in corrosion handbooks. In plant design, the uniform corrosion rate is usually minded by providing a corrosion allowance that takes the design life of the plant into account. However, one has to consider that corrosion products can enter the medium, which might not be acceptable, especially in biotechnological applications. Materials resistant to uniform corrosion for specific applications are available, too. These are mainly metals that protect themselves by passivation like stainless steels, aluminium as well as nickel- , cobalt- and titan-based alloys. When anodic reactions get concentrated at certain specific regions, they result in localized corrosion for example crevice corrosion, pitting corrosion, intergranular corrosion and stress corrosion cracking. [23]

Crevice Corrosion: occurs in openings too narrow for convective streams, but allowing ionic diffusion to take place. It is associated with a small volume of stagnant solution, caused by holes, gasket surfaces and crevices left by design, like under bolt heads. Crevice corrosion takes place by an autocatalytic anodic reaction inside the crevice geometry and leads to local lowering of pH down to 2 and concentration of chloride. However, crevice corrosion damage usually occurs after an incubation time and can be delayed or avoided by increasing the flow rate of the process solution. All materials are prone to crevice corrosion. [23]

Pitting Corrosion: propagates by a mechanism similar to crevice corrosion. It is called the self-initiating form of crevice corrosion and occurs on open surfaces. Materials showing passivity (stainless steels, nickel-based alloys, etc.) are especially prone to pitting corrosion. [23]

The simplified mechanisms of crevice and pitting corrosion are depicted in Figure 10:
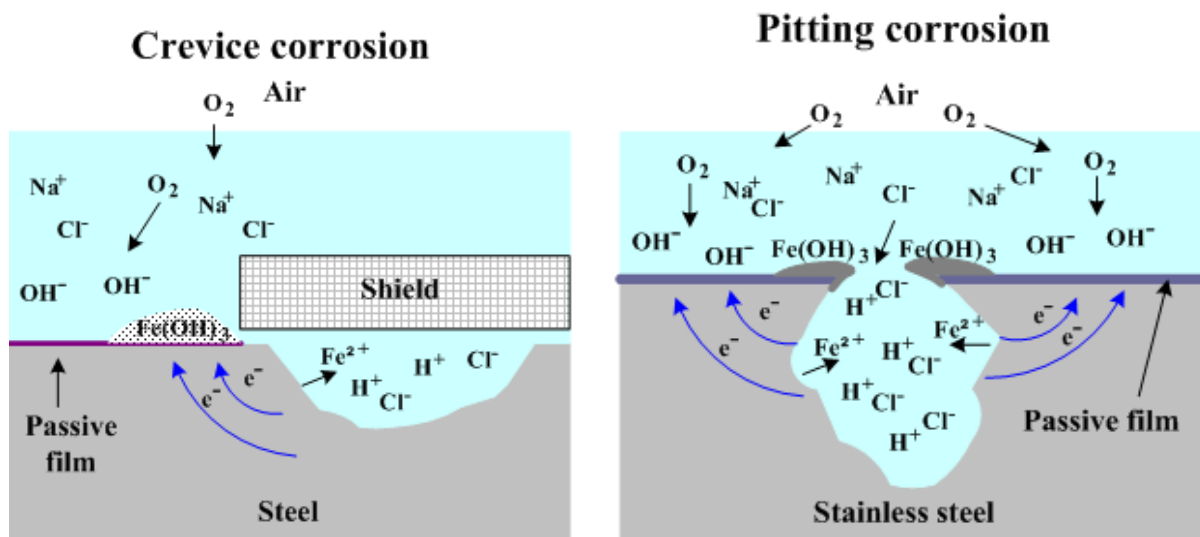
Figure 10: Mechanisms of Crevice and Pitting Corrosion [25]

Materials that exhibit passivity are especially vulnerable to pitting corrosion, whereas crevice corrosion can affect materials that exhibit passivity as well as those that do not. Both forms of corrosion can occur if the medium contains smallest amounts of halides or other aggressive anions. The resistance to pitting corrosion improves when the passive film becomes stronger. In stainless steels, higher amounts of chromium and molybdenum in the material make the passive film more protective. Nickel-based alloys are inherently more resistant to pitting and crevice corrosion than stainless steels. In fact, some nickel-based alloys (Hastelloy C-22) are known not to pit even when exposed to a boiling solution of 25% NaCl. [23]

Crevice and pitting corrosion are very common in the chemical industry and can occur on materials that are usually resistant to uniform corrosion when the medium contains dissolved chloride ions or other halides. When selecting a material for a corrosive environment one should ensure that it is uniform corrosion that would be the degradation mechanism and not localized corrosion. Therefore, the resistance to local corrosion is the main attribute that has to be considered when selecting a metal for use in a corrosive environment. [23]

The critical pitting temperature is an indicator of the susceptibility of materials to pitting corrosion. Higher values of the critical pitting temperature indicate lower vulnerability to pitting corrosion. For example, the critical pitting temperature of the stainless steel 1.4435 in 6% $FeCl_3$-solution is at about 20°C, while the one of the nickel-based 2.4856 is at about 90°C. Thus, only the latter is suitable for processes with this medium at ambient temperatures. [23]

2.5.2 Hastelloy C-22 (HAYNES International Inc., USA)

Hastelloy C-22 alloy (2.4602, alloy 22) is a most versatile nickel-based chromium-molybdenum-tungsten alloy with improved resistance to both uniform and localized corrosion as well as to a variety of industrial chemicals [26]. It is one of the few materials that are resistant to the corrosion of hydrogen chloride, hypochlorite and chlorine dioxide. However, the high cost of Hastelloy C-22 has limited its large-scale application. But in the recent decades, Hastelloy C-22 coating has been developed which can be applied to various constructions in marine environment and chemical facilities for protection against corrosion [27]. Other applications are flue gas desulfurization, refineries, pulp and paper industry as well as chemical waste incineration [26]. The nominal chemical composition of Hastelloy C-22 in weight percent is given in Table 1:

Table 1: Hastelloy C-22: Nominal Chemical Composition in Weight Percent [26]

Ni	Co	Cr	Mo	W	Fe	Si	Mn	C	V
56	2.5	22	13	3	3	0.08	0.50	0.010	0.35

Hastelloy C-22 has outstanding resistance to pitting and crevice corrosion (extraordinarily high critical pitting temperature) as well as stress corrosion cracking. It has excellent resistance to oxidizing aqueous media including wet chlorine, seawater, brine solutions and mixtures containing nitric acid or oxidizing acids with chloride ions. Also, C-22 alloy offers optimum resistance to environments where reducing and oxidizing conditions are encountered in process streams. Because of such versatility, it can be used in multi-purpose plants. It resists the formation of grain-boundary precipitates in the weld heat-affected zone, thus making it suitable for most chemical process applications in the as-welded condition. Due to its superior weldability it is used as overalloy filler wire and weld overlay consumables to improve corrosion resistance of welds. [26]

2.6   Oxygen Transfer in Airlift-Bioreactors

The gas-liquid mass transfer of oxygen into the broth is a most important parameter in bioprocessing. The transfer is based on convection and molecular diffusion and is driven by a concentration difference of oxygen between the phases. In bioreactors, oxygen is usually supplied by gassing the medium. O_2 is thereby transferred from gas bubbles through the phase boundary into the bulk liquid, the broth, with lower concentration of oxygen.

The characteristic variable of oxygen mass transfer is the oxygen transfer rate (OTR), described in Eq. 5. Since the mass transfer resistance on the gas side is usually negligible small compared to the one on the liquid side, it is excluded from the calculation of the OTR. Thus, the oxygen transfer rate is only determined by the

specific mass transfer coefficient of the liquid phase k_L, the specific contact area a and the driving force of the transport, the difference between the mean oxygen concentration of the bulk liquid c_{O2} and its O_2-concentration in equilibrium c_{O2}^*:

$$\text{OTR} = k_L a * (c_{O2}^* - c_{O2}) \left[\frac{g}{L * h} \right]$$

Eq. 5

The dissolved oxygen concentration in equilibrium c_{O2}^* is calculated by using Henry's law, where H_{O2} is the Henry constant of the liquid phase and p_{O2} the partial pressure of oxygen in the gas phase:

$$c_{O2}^* = \frac{p_{O2}}{H_{O2}} \left[\frac{g}{L} \right]$$

Eq. 6

According to Dalton's law, the partial pressure of oxygen can be determined by multiplying the total pressure p_{tot} with the amount-of-substance fraction of oxygen in the gas, approximately 21% for air:

$$p_{O2} = p_{tot} * y_{O2} \; [bar]$$

Eq. 7

Eq. 7 shows that the partial pressure of oxygen proportionally increases with rising total pressure. Therefore, by pressurizing a bioreactor, the maximum equilibrium concentration of dissolved oxygen in the liquid c_{O2}^* and thus the driving force of the mass transfer $(c_{O2}^* - c_{O2})$ is increased, leading to a higher OTR. Another possibility to raise the oxygen transfer rate is by increasing p_{O2} in the gas phase by using pure oxygen or O_2-enriched air for gassing.

Furthermore, as Eq. 5 shows, the OTR is proportional to the $k_L a$-value, the volumetric mass transfer coefficient. While the transfer coefficient k_L is mostly dependant on the properties of the liquid phase like, temperature, viscosity or the presence of surface-active substances, the specific contact area a can be altered by process parameters, such as gassing rate, energy input and pressure. The contact area correlates with the size of the gas bubbles and therefore increases with decreasing bubble diameter. In stirred tank reactors, the impeller is the main gas-dispersing tool and its speed and design determine the bubble size [1].

By contrast, in airlift reactors, the $k_L a$-value is directly proportional to the reactor height and the aeration rate, which determines the gas holdup [12]. The gas holdup or voidage ε is the main parameter to characterize the hydrodynamics in a bubble column. It determines the residence time of the bubbles in the liquid and usually increases with the gassing rate depending on the flow regime and the sparger design. The gas holdup is defined as ratio of gas bubble volume V_G dispersed in the liquid phase to the total volume V_{tot} of both phases and can be easily determined in practice by measuring the fluid level in a cylindrical reactor before (H_L) and while gassing (H_{tot}).

$$\varepsilon = \frac{V_G}{V_{tot}} = \frac{H_{tot} - H_L}{H_{tot}} \, [\%]$$

<div align="right">Eq. 8</div>

Increasing the operating pressure at constant gas flow leads to higher gas holdup in a bubble reactor. The reason for this is the decrease of bubble coalescence under high pressure and the formation of smaller bubbles on the gas distributor as a result of higher gas density. In addition, the gas holdup is increased due to the lower density difference between liquid and gas phase. This results in a lower speed of the rising of gas bubbles and hence longer residence time. [28]

Therefore, pressurization of ALRs is particularly advantageous as it increases the OTR in two ways: on the one hand, the driving force of the mass transfer $(c_{O2}^* - c_{O2})$ is raised, and on the other hand the increased pressure increases the gas holdup, allowing longer mass transfer.

Lastly, it has to be mentioned that the mass transfer in airlift reactor is dependent on the geometry of the gas-dispersing tool, the sparger, as well since it can influence the flow regime of the gas bubbles.

The homogeneous regime (uniform bubbly flow) is produced by spargers with small orifices at low gas flow and is characterized by equally-sized, non-coalescing bubbles. They are small, spherical and rise almost vertically, hence increase gas holdup. The heterogeneous regime (turbulent) is produced by spargers with large orifices at any gas flow or by ones with small orifices at high gas flow. Populations of large and highly non-uniform bubbles with a strong tendency to coalesce are generated in both cases. Strong convective motions of liquid within the whole column occur that lead to liquid circulations and decrease the gas holdup. This regime is usually present in airlift reactors due to their inherent fluid circulation. [29]

Increased pressure shifts the transition from homogeneous to heterogeneous flow regime to higher gas flow rates [28]. In uniform bubbly flow, the spargers with the smallest orifices produce the highest mass transfer rates, while the sparger's pore size hardly influences the mass transfer in heterogeneous flow [30]. Due to the latter, the pore size of spargers used for ALRs is usually of little importance.

3 Design Phase

The pilot plant was initially dimensioned by Nicole Mahler and Christoph Herwig of the research group bioprocess engineering of the Vienna University of Technology. They scaled the 1 L lab-scale bioreactor used by Bettina Lorantfy [2] up to 15 L and created a user requirements specification (URS; see Appendix 1) and a process flow diagram (PFD). Based on these two documents, the author designed and specified the pilot plant.

3.1 1 L Lab-scale Bioreactor

The lab-scale bioreactor system for waste water treatment with halophiles was designed and optimized by Lorantfy [2][8] and Ruschitzka [8][9]. The bioprocess can be carried out under non-sterile conditions. The system consists of a fully instrumented corrosion-resistant 2 L Labfors stirred tank bioreactor (Infors AG, Switzerland) made of borosilicate glass with a working volume of 1 L. Due to the corrosivity of the medium, the reactor lid, stirrer as well as the ports consist of the polymer PEEK. The connection lines are made of silicone tubing. The additional medium and harvest tanks are borosilicate glass flasks or made of plastic. For cell retention, a polysulfone (PSU) hollow fiber microfiltration membrane cartridge with an area of 420 cm² and a pore size of 0.2 µm is used. The membrane is placed in an external loop, directly attached to the reactor. This setup is depicted in Figure 11:
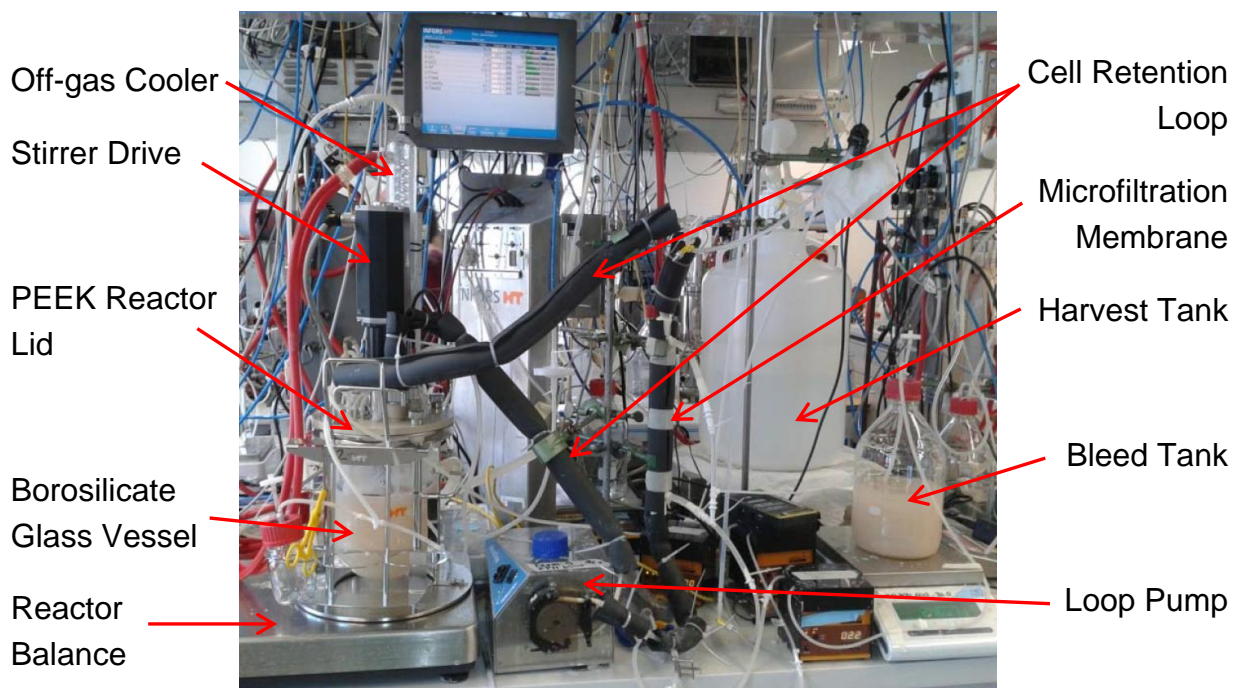
Figure 11: 1 L Lab-Scale Bioreactor Setup

The setup is equipped with a temperature as well as a pH-probe and the dissolved oxygen concentration in the bioreactor is measured by a Clark-sensor (Oxyferm, Hamilton Bonaduz, Switzerland), made of the stainless steel 1.4435. The reactor volume, feed, base and acid consumption are continuously monitored with laboratory scales with 0.1 g resolution. The inlet air flow is adjusted via a mass flow controller (MFC) to avoid oxygen limited process conditions. [2][9]

The reactor temperature is adjusted by a water jacket. For pH-control, acid or base are automatically added to the reactor when needed. The on-line data monitoring and process control is executed by the process control system (PCS) Lucullus (Applikon Biotechnology B.V., Netherlands). The PCS controls the stirrer speed, temperature, pH-value as well as the flow rates, which are determined by weight signals. The process flow diagram of the continuous process for waste water treatment with halophiles in the 1 L lab-scale reactor is depicted in Figure 12.
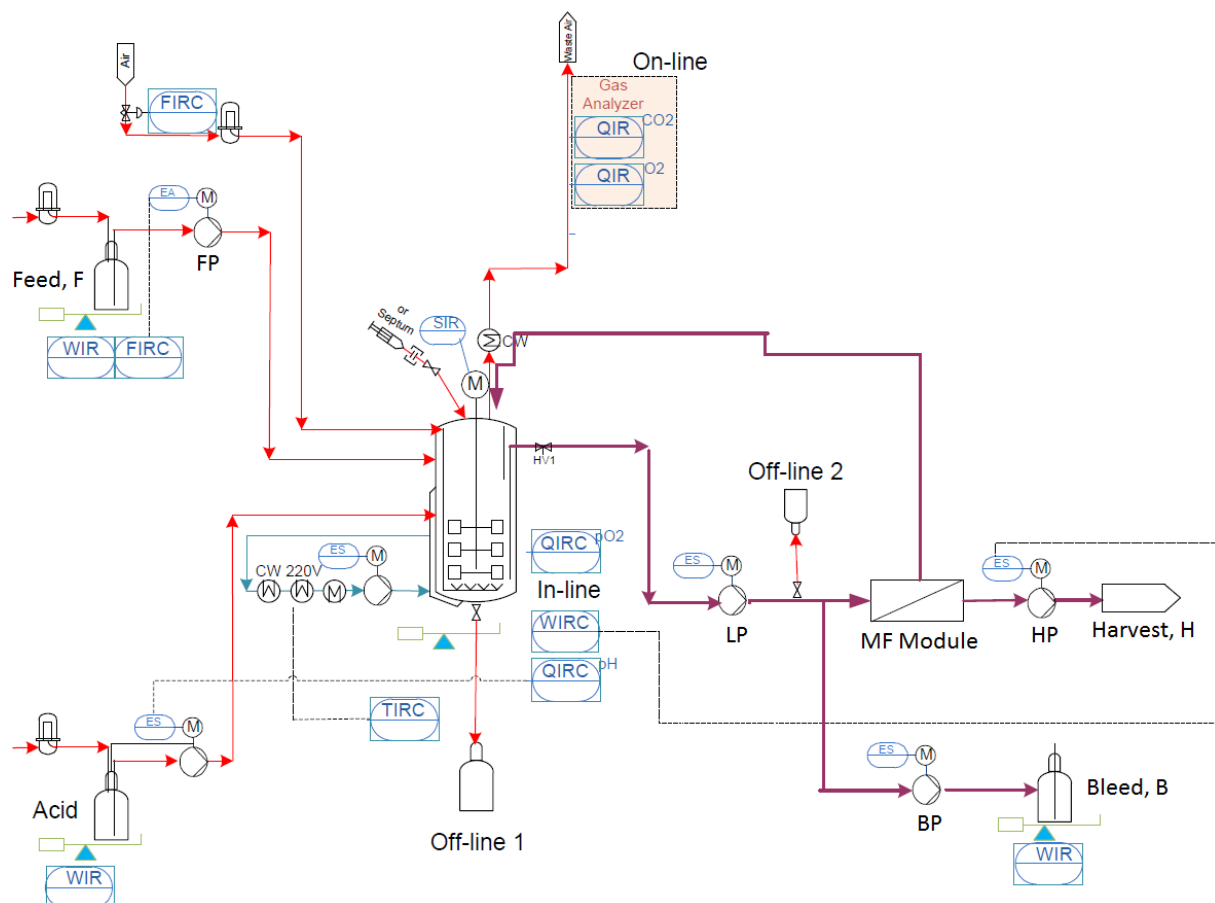
Figure 12: Process Flow Diagram: 1L lab-scale Bioprocess for Halophiles [9]

The untreated brine is fed into the reactor via the feed pump (FP). The inlet air enters the reactor below the impeller via a glass tube and is dispersed by the stirrer. The off-gas is cooled and dehumidified by a reflux condenser and then lead through a gas analyser that measures the O_2- and CO_2-composition of the gas. [9]

Cell suspension is continuously pumped out of the reactor by the loop pump (LP) and into the external cell retention loop. There, the cross flow microfiltration membrane module (MF) separates the medium in a filtrate and cell suspension stream. The filtrate, cell-free brine, leaves the reactor as harvest stream (H), while most of the broth returns to the reactor via a circulation line. A fraction of the reactor broth, the bleed stream (B), is separated and pumped out of the system via the bleed pump (BP). Filtrate and bleed flows are transferred into separate containers for product recovery. The loop-, feed-, harvest- and bleed pumps are peristaltic pumps with analogue control. [9]

During continuous fermentation, the feed and bleed flows are constant, while the harvest flow is used for level control, which means to keep the reactor volume constant. The harvest pump (HP) works as a step controller to keep the reactor weight in a range of ±10 g from the initial weight. Whenever the reactor weight exceeds its target value (set at 1 L reactor volume) by 10 g, the HP is activated and filtrate is removed from the system until the weight signal has sunk by 20 g. [9]

A representation of this 2-point-level-control process is depicted in Figure 13.
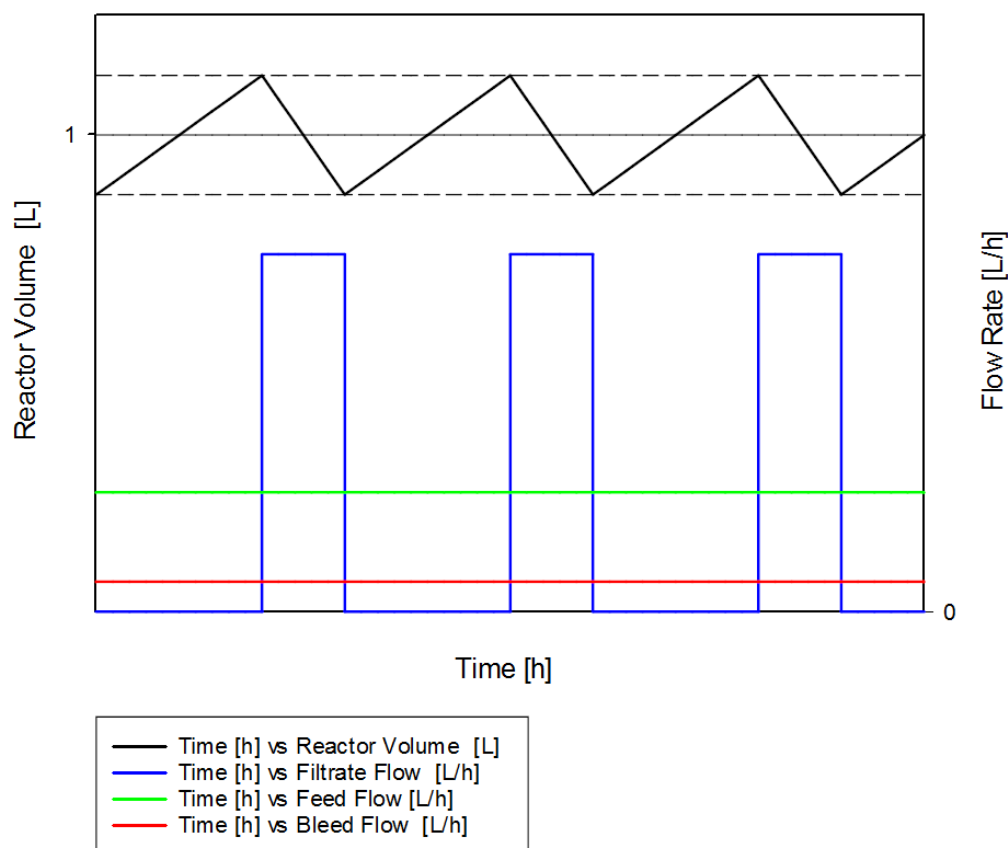
Figure 13: 1 L Lab-scale Bioreactor: Level Control Representation

3.2 Upscale to 15 L Pilot-Scale

The lab-scale plant was designed for waste water treatment of the extremely halophilic archaeon *Haloferax mediterranei.* When using glycerol as substrate, this organism has a specific growth rate μ of approximately 0.015 h^{-1} before overflow metabolism is reached [2]. By using a cell retention system, the productivity is increased tenfold, allowing a dilution rate of 0.15 h^{-1}. At a given reactor volume of 1 L, the system can thus be fed with 0.15 L waste water per hour, according to Eq. 1. After choosing a constant biomass concentration in the reactor, for example 3 g/L, the flow rates of bleed and harvest (filtrate) result from a mass balance. By contrast, loop flow is relatively variable. It must be considerably higher than the sum of filtrate and bleed flow and was eventually chosen to be about 7 L/h, so that the membrane could be operated optimally.

To upscale the 1 L bioreactor reactor setup to 15 L pilot-scale, the mass flows were multiplied by the factor 15. The results of this calculation are shown in the stream list in the PFD in Appendix 2 as well as in Table 2. The mass flows were converted into flow rates by using the actual densities of the different media.

During the upscale process, the different reactor type of the pilot plant (airlift reactor) compared to the lab-scale model was considered by increasing the aeration rate range. The experiments in the lab-scale reactor showed that gassing rates of 0.1 L/min (0.1 vvm) were usually sufficient. However, especially when high biomass concentrations were present, the dissolved oxygen concentration was hard to increase, even though the aeration rate and the stirrer speed were increased. This resulted in the need for a new bioreactor type and eventually an airlift reactor was chosen therefore. However, since these bubble reactors cannot achieve as high oxygen transfer rates as stirred tank reactors, the new pilot plant had to be able to be operated with significantly higher aeration rate. The upper limit for the flow was chosen to be 30 L/min (2 vvm), the maximum feasible aeration rate on laboratory scale [8].

Table 2: Upscaled Stream List for Pilot Plant

Stream	Stream No. in PFD	Flow Rate
Feed	1	1.92 L/h
Harvest/ Filtrate	12	1.44 L/h
Bleed	13	0.48 L/h
Loop	8	105 L/h
Inlet Air	4	1.5-30 L/min

3.3   User Requirements Specification (URS)

After scaling the 1 L lab-scale bioreactor up to 15 L, Mahler and Herwig created an initial user requirements specification, which can be found in Appendix 1, and a preliminary process flow diagram. These two documents were used for inquiry of the equipment. A summary of the main parameters of the URS is given in Table 3.

Table 3: Summary of the User Requirements Specification

Operating Range of the Pilot Plant	
Working Volume of the Reactor	15 L
Fermentation Temperature	20 - 50°C (± 0.2°C)
Fermentation Pressure	3 barg (± 0.1 barg)
Gassing Rate of Process Air via Sparger	1.5 - 30 L/min (0.1 - 2 vvm)
pH	2 - 12 (± 0.05) usually pH 7
Dissolved Oxygen Concentration	0 - 100 % (± 1%)
NaCl-Concentration	5 - 25%
Feed Addition (Stream 1)	0 - 3 L/h
Product Stream 1 / Filtrate (Stream 12)	0 - 3 L/h
Product Stream 2 / Bleed (Stream 13)	0 - 1 L/h
Acid Addition (Stream 2)	0 - 0.1 L/h
Base Addition (Stream 3)	0 - 0.1 L/h
Anti-Foam Addition	Manual Addition max. 2 mL/h
Size of the Storage Tanks	
Acid Tank (B1)	5 L
Base Tank (B2)	5 L
Feed Tank (B3)	4 x 50 L
Filtrate Tank (B4)	4 x 50 L
Bleed Tank (B5)	50 L

3.4   Process Design of the Pilot Plant

The process flow diagram of the novel pilot plant differs from the one of the lab-scale reactor in Figure 12. The main differences from the original setup result from the novel reactor type (airlift reactor instead of conventional stirred tank reactor), the pilot vessel's ability to be pressurized as well as from different measurement techniques and more possible process control due to the larger scale. A detailed study of all variations is given in Chapter 3.4.1.

3.4.1 Differences between Lab-scale and Pilot-scale Plant

- Instead of a conventional stirred tank reactor, the pilot plant is designed as an airlift reactor. Thus, the novel reactor does not have an impeller. Instead, it is pneumatically mixed by ascending gas bubbles, dispersed in the broth by a sparger at the bottom of the reactor. While stirred tank reactors are considered to be ideally mixed, meaning that no concentration gradient occurs in them, the concentrations in airlift reactors are more location-dependent, usually changing with the reactor height. All probes of the lab-scale reactor are placed on the lid and protrude into the vessel, whereas the airlift-pilot reactor's sensors have to be positioned laterally on the vessel as well to achieve representative measurement. For example, the dissolved oxygen- and the temperature sensor are installed laterally at mid-height of the vessel to measure the mean values.

- Since the pilot reactor has to be able to be operated at elevated pressure of up to 3 barg to enhance the oxygen mass transfer, it has to be equipped with pressure sensors and a safety valve for pressure relieve. Furthermore, a pressure control valve is required for process control.

- The pressurization of the plant requires fixed piping. However, unlike when working with flexible silicone hoses, the fixed tubing cannot be altered during operation. Therefore, the piping has to be implemented in a way that allows switching between the three operation modes of the plant (batch, continuous and cell retention mode) by adjusting shut-off valves. The membrane module has to be bypassed to operate in batch mode. In the two continuous modes, this bypass line is closed.

- For simplified process evaluation and safety reasons, the reactor volume has to be kept constant during fermentation. The filling volume of the 1 L reactor is indirectly controlled by a 2-point-control of the reactor weight. The scaled-up reactor is significantly heavier than the lab-scale one and is placed on a wheeled rack. These reasons make it very complicated to measure its weight by balances with sufficiently high accuracy. Therefore, a new method to maintain a constant reactor volume has to be introduced - a level sensor is implemented to directly measure the liquid level. This method would not have been possible on smaller scale due to lack of space.

- The flow rates of the 1 L reactor's outflowing streams (filtrate, bleed) are controlled by peristaltic pumps, whereas they are high enough to be controlled by control valves in the pilot plant, the typical method on industrial-scale.

- The larger scale of the cell retention loop allows the placement of probes in it. An additional dissolved oxygen sensor as well as a temperature sensor can be integrated into the piping. This makes it possible to monitor the change of state that occurs while the cell suspension passes through the loop and thereby improves process understanding. Furthermore, the larger diameter of the loop tubing allows the installation of pressure sensors in it. These are required to calculate the transmembrane pressure, the most important parameter to monitor membrane fouling. This enables further process control.

- Due to the higher off-gas flow, the gas stream has to be separated and only a part of it is used for the actual off-gas analysis.

3.4.2 Process Flow Diagram of the Pilot Plant

The full functionality of the pilot plant on the basis of the as-built process flow diagram in Appendix 2 is described below. All designations correspond to the ones used in the PFD and in the stock list in Appendix 4. The pilot plant requires a 230 V AC power supply, as well as a supply of compressed air and cooling water for operation.

The airlift reactor (C1) is gassed with compressed air. The inlet pressure is controlled by a pressure reducer valve (V1) that is directly mounted to the compressed air faucets in the laboratories of the department of bioprocess engineering. The air is then lead through a mass flow controller (FRC 019) which adjusts the flow rate to the desired value, controlled by the process control system Lucullus. The gas enters the reactor at the bottom through a check valve (V2) that prevents backflow of liquid into the gassing line. Via a sparger that protrudes into the reactor, the air is dispersed in the broth and gas bubbles ascend the reactor tube, providing the cells with oxygen. The gas leaves the reactor at the top through the off-gas port on the lid and is then lead through the off-gas cooler (W2), which is externally cooled by water. The cooler recovers water from the gas and thereby reduces its humidly, so that the off-gas analysis is not affected. The condensed water flows back into the reactor. The dried exhaust gas passes the pressure control valve (V3) which is used to adjust the reactor pressure to the desired value. The reactor pressure is measured by a probe (PIRC 005) placed on the lid. For safety reasons, a manometer (PI 004) as well as a pressure relief valve (V16) are mounted to the reactor lid, too. After passing V3, the off-gas is split. A small part of it flows to the external gas analyser that measures its CO_2- and O_2-concentration (QR 017, QR 018) and the rest goes directly to the air escape. The flows of these separate streams are controlled by two manual off-gas valves (V4, V5).

The pH-control of the system is performed by adding acid or base, respectively. The tanks for both liquids (B1, B2) are placed on balances (WIR 013, WIR 014) to monitor

their consumption and are added to the reactor by digital (On/Off) dosing pumps (P1, P2). Both mediums are fed into the reactor through ports on the lid and are from there led to the bottom of the airlift reactor by dosing pipes to increase mixture. The addition of culture medium (feed) happens in the same way. However, in this case, an analogue dosing pump (P3) is used so that the flow rate of the feed can be continuously adjusted. The dosing pumps for acid and base are switched on and off by the PCS, depending on the pH-value in the system. The pH-value is measured by a pH-probe (QIRC 009), placed in the circulation loop.

Three more sensors are placed on the reactor vessel. The level sensor (LRC 001), a point level switch, is mounted at exactly the height that corresponds to a working volume of 15 L in the reactor. This sensor indicates if the fluid level is above or below this certain mark and adjusts the feed or filtrate flow accordingly to maintain a constant level. Below, approximately at half reactor height, a dissolved oxygen sensor (QIRC 002) and a temperature probe (TIRC 003) are placed. The thermometer is used to control the electrical heating pad (W1) that jackets the reactor. A drain valve (V17) is placed at the lowest point of the airlift reactor to empty it.

The inlet of the cell retention loop is positioned at the top of the bioreactor tube but slightly below the level switch to ensure that the loop is always filled with liquid. Broth is continuously pumped out of the reactor by the loop pump (P4) through this port. The circulating loop stream enters the reactor again at the bottom, just above the sparger tube to be immediately mixed with the rest of the broth. The whole loop can be shut off by two valves (V6, V14), positioned at its in- and outlet. The loop pipes are slightly tilted so that they are drainable.

Before the loop stream enters the microfiltration membrane (F1), a junction occurs that bypasses it. Therefore, the flow can either be lead through the filter or bypass it, depending on position of the two shut-off valves (V8, V9) at the junction. Both lines are joined again at the 3-way ball valve (V11) at the bottom of the loop. Before and after the membrane module, pressure sensors (PIRC 006, PIRC 007) are positioned. Together with a third pressure sensor (PIRC 008) placed on the permeate side of the membrane, the transmembrane pressure (TMP) can be calculated from these three signals. The TMP can be adjusted by the TMP-control valve (V10), positioned after the retentate outlet of the membrane, or by the capacity of the loop pump. On the permeate side, the filtrate flow is lead through the filtrate valve (V12) and then into its storage tank (B4). The tank is placed on a balance (WIRC 015) to calculate the filtrate flow, adjusted by control valve V12. This variable filtrate flow is also used for level control.

Furthermore, a small part of the cell suspension in the loop, the bleed stream, is removed from the system and flows into a storage tank (V5) to maintain a constant

biomass concentration in the reactor. Again, this tank is placed on a balance (WIRC 016) to calculate the bleed flow and to adjust it to a constant value by the control valve V13. Besides, broth can be harvested by a manual sampling valve (V7) for offline analysis.

Downstream, just before the circulating stream flows back into the reactor, the pH-probe (QIRC 009), which simultaneously acts as a thermometer (TIRC 010), as well as a second dissolved oxygen sensor (QIRC 011) are placed in flow cells. The second DO-probe is necessary because it is assumed that the DO-concentration in the broth decreases while it passes through the loop tubing since no gassing occurs there. Thus, in order to avoid oxygen limitation in the loop, the DO-concentration has to be monitored there. The same principle applies to the temperature. Since the loop tubing is not heated, the temperature of the broth will sink while it flows through the non-insulated loop. Therefore, a second temperature signal is required to measure the impact of the cell retention loop.

Depending on the position of the valves V8, V9 and V11, the system can be operated in batch or continuous mode. The batch mode is run without the membrane by utilizing the bypass line. Furthermore, the membrane can be cleaned or exchanged during operation by temporarily using the bypass. By opening the bleed valve V13, "feed and bleed"-mode for constant biomass concentration can be achieved.

3.4.3 Process Control Approach

As the process flow diagram in Appendix 2 indicates, the pilot plant requires several control circuits for process control. The controlled parameters are:

- Temperature
- Pressure
- Dissolved Oxygen (DO) Concentration
- pH-Value
- Flow Rates of Feed, Filtrate and Bleed
- Liquid Level in the Reactor
- Transmembrane Pressure

Besides, an external gas analyser is used to measure the CO_2- and O_2-concentration of the off-gas. This analysis can be used as part of the "Process Analytical Technology" (PAT) concept, which is currently developed at the Vienna University of Technology, but is not integrated into process control.

Process control is realized by the process control system Lucullus (Applikon Biotechnology B.V., Netherlands). The full control approach of the pilot plant is described in the following. Possible safety measures against process failure are included as well.

3.4.3.1 Temperature Control

The temperature of the broth is controlled by the heating pad (W1) jacketing the reactor, which is PID-controlled. The temperature is measured both inside the reactor (TIRC 003) as well as at the end of the cell retention loop (TIRC 010) and is adjusted to the setpoint. Furthermore, a protection against overheating is implemented via Lucullus which shuts down the plant if the reactor temperature exceeds a certain input value.

3.4.3.2 Pressure Control

The reactor pressure is used to control the dissolved oxygen concentration and is adjusted by a proportional pressure control valve (V3) placed in the off-gas line. The reactor pressure is measured by a sensor (PIRC 005) mounted on the reactor lid and a PID controller adjusts the aperture of the valve so that the target pressure is reached. Although the reactor is equipped with a safety valve and can withstand high pressures, the remaining components are only designed for a maximum pressure of 3 barg and thus additional protection against unacceptable high pressure has to be implemented. Therefore, a control loop is realized which fully opens the pressure control valve when the measured pressure at any of the four sensors exceeds a certain value, but maximally 3 barg. However, in case of a blocked pressure valve, the pressure could still rise when the overpressure safety barrier is activated. For that reason, a timer could be implemented that shuts down the plant if the pressure limit is exceeded for a previously declared time period.

3.4.3.3 Control of the Oxygen Supply

The dissolved oxygen concentration can be increased by raising the reactor pressure or by increasing the aeration rate. It is measured by two DO-sensors. One is placed in the reactor vessel (QIRC 002) and the other (QIRC 011) is positioned at the end of the cell retention loop, the place where supposedly the lowest DO-concentration occurs. When the dissolved oxygen concentration falls below a certain level, the aeration rate can be increased by the MFC (FRC 019) to counteract. However, the control loop for oxygen supply is not automated since other facts like anti-foam agent addition have an impact on the DO-concentration as well. Therefore, the gassing rate is manually increased in case of oxygen limitation. However, an alarm could be implemented that is activated if the DO-concentration falls below a critical value.

3.4.3.4 pH-Control

This circuit consists of two separate control loops, an acid and a base control. Both are implemented as 2-point-control circuits. Depending on the pH-value, measured by the pH-sensor in the loop (QIRC 009), the acid (P1) and base (P2) dosing pumps are switched on and off at predefined thresholds.

A timer which sets an alarm if the pH-value is outside the previously set range for too long should be implemented as well. This could for example happen if all the acid in the tank has been consumed. Then, the alarm would notify the operator that it has to be refilled. However, since the acid/base storage should only be empty in case of emergency, it would be beneficial to inform the operator of this failure beforehand. A possible solution for that would be to set an alarm if the level in one of the tanks is too low. This could be measured by their weight signals. The same principle could also be applied to the feed tank.

3.4.3.5 Flow Control

The flow control is used to calculate the flow rates of feed, filtrate and bleed by using the progress of their weight signals, measured by balances, and to set them to the desired value by a PID-controller. The feed flow is controlled by adjusting the dosing pump's (P3) capacity while the flow rates of the filtrate and bleed stream are adjusted by the opening of their control valves (V12, V13).

3.4.3.6 Level Control

The level control is used to keep the filling level of the broth in the reactor at a constant height, equalling a working volume of 15 L. This is necessary for process evaluation and prevents the reactor and the off-gas tubing from flooding. Furthermore, a too low liquid level disables the circulating loop flow since the loop pump would suck air. In this case, the cell retention system would no longer be operational and the pH-value could not be measured.

Even during a batch operation, where usually no significant in- or outflowing streams occur, the fluid level still changes because of the following four mechanisms: first of all, the aeration rate influences the liquid height in the airlift reactor to a large extent. The higher the gassing rate, the larger the amount of gas bubbles dispersed in the liquid. These bubbles increase the total volume of the fluid inside the reactor - the gas holdup. This phenomenon has to be considered when changing the aeration rate because a too large rise could flood the reactor. Second of all, the supply of acid and base for pH-control increases the level of the broth and can be significant at high metabolic rates or cell densities. Besides, the water loss through the off-gas has to be considered, although this phenomenon is mostly taken care of by an off-gas cooler acting as a reflux condenser. Lastly, the slight decrease of the reactor volume due to sampling has to be minded.

In addition to the four previously mentioned mechanisms, the liquid level changes due to the inflowing feed as well as the outflowing filtrate and bleed streams during fermentation in continuous or "feed and bleed"-mode. In a steady state, these opposite flows are equal. However, because of inaccuracy of measurement and control, these streams differ in real operation. As a result, the reactor level gradually

changes. This deviation from the set level has to be compensated by the level control.

In the pilot plant the level is measured by a level switch (LRC 001), a device that detects two states. In air, the signal is "Off" and whenever the sensor is immersed in liquid, its digital signal switches to "On".

Two different level control approaches have to be implemented for batch and continuous mode. First, the level control for batch operation is described. It consists of two control circuits: "level too high" and "level too low". The level is maintained constant by either removing liquid from the system through the bleed valve (V13), or by supplying new medium via the feed pump (P3). A timer is implemented in order to check periodically if the signal of the level switch is either on ("level too high" → open bleed valve) or off ("level too low" → start feed pump) after a certain period of time and to start the corresponding countermeasure until the level signal switches to the other state. In batch mode the bleed flow has to be utilized for level control instead of the filtrate stream because in this case the loop flow runs through the bypass line instead of the membrane module. As a consequence, cells are removed from the system via the bleed stream whenever the level is too high. This has to be considered when choosing the timer period.

For continuous operation, the state "level too high" has to be avoided for safety purposes. Since the level switch can only detect if the liquid level is above or below the 15 L-threshold, the reactor should not be operated above this limit because when the sensor is activated, no statement can be made about how far the mark is exceeded and overflow could occur. Instead, the level should always be slightly below the threshold and whenever the level switch is activated a countermeasure has to be started to immediately reduce the level. However, the risk of overflow could be further reduced by installing a second level detector above the first one that shuts off the plant if activated. This method is commonly used on industrial-scale, but could not be applied to the pilot reactor due to lack of space.

To achieve permanent operation below the 15 L-limit in continuous mode, a slight imbalance of the in- and outflowing streams has to be realized in a way that the liquid level increases continuously and very slowly. In other words, the sum of filtrate and bleed stream has to be minimally smaller than the feed flow. Starting at a fluid height below the level sensor, the level slowly increases until the detector is immersed in the liquid and thus activated. Then, a countermeasure is started to quickly reduce the level below the 15 L-limit again. This could either be a temporary decline or even shutdown of the feed rate by adjusting the capacity of the feed pump (P3) or a short term rise of filtrate or bleed flow by increasing the aperture or even fully opening their control valves (V12, V13). However, for physiological reasons and to simplify process evaluation, the feed rate should remain constant during a continuous fermentation.

This applies to the bleed stream in the "feed and bleed"-mode, too. Besides, the utilization of the bleed stream for level control would decrease the biomass concentration in the broth. Hence, the only remaining tool for level control in continuous mode is to vary the filtrate flow.

However, two different methods are available for this control approach, one with intermittent filtrate flow and one with continuous flow (Figure 15). Both are operated with constant feed and bleed flow rates as well as with steadily rising liquid level. Schematic representations of both level control approaches are shown in Figure 14 (intermittent filtrate flow) and Figure 15 (continuous filtrate flow). The ends of the curves in both diagrams indicate an additional safety measure that prevents flooding. This procedure is described at the end of this chapter.
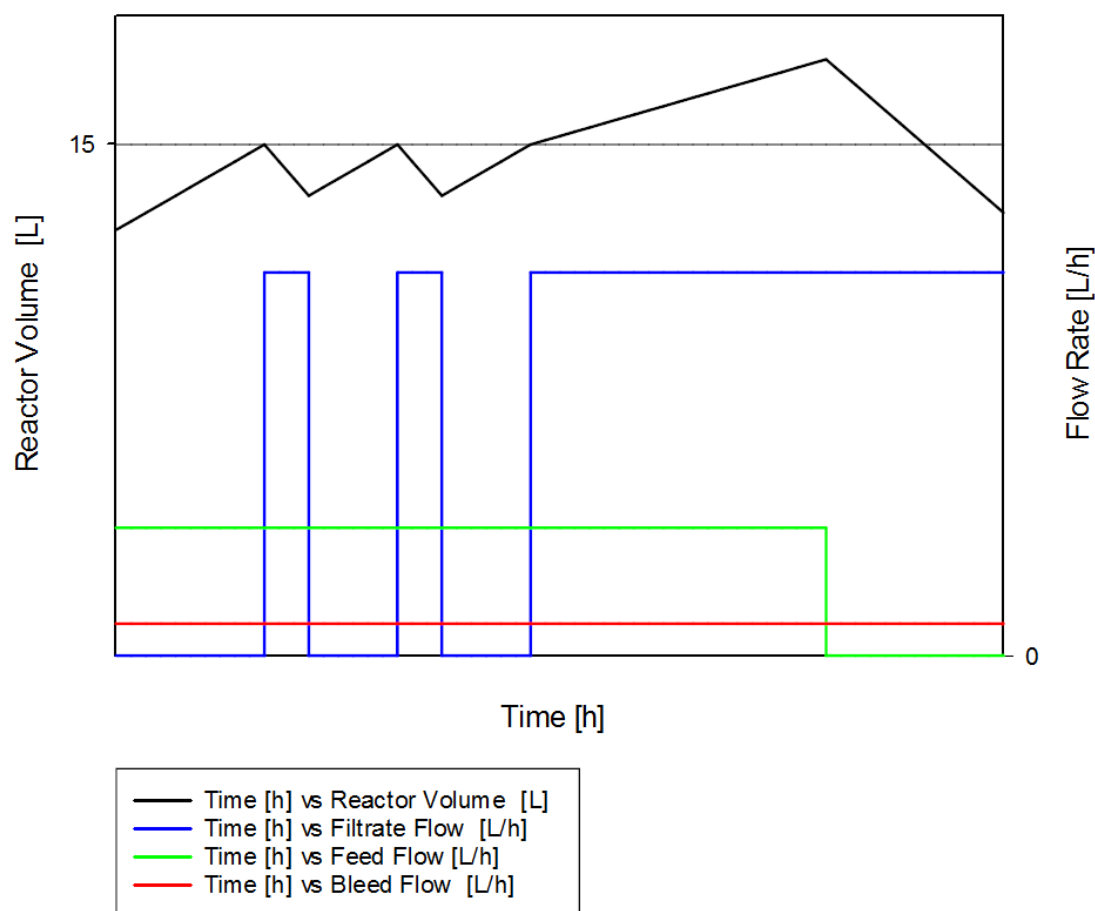
Figure 14: Level Control for Continuous Mode with Intermittent Filtrate Flow

When using the first approach with intermittent filtrate flow, the filtrate flow is normally deactivated. But whenever the level reaches the level switch, the filtrate valve (V12) is opened for a certain amount of time. During this period, the fluid level sinks below the 15 L-threshold again. Then, the valve is closed and the level rises again due to the incoming feed flow. The schematic representation of this control approach is depicted in Figure 14. It resembles the one used for the 1 L lab-scale bioreactor, shown in Figure 13. There, a 2-point control is utilized that keeps the reactor weight,

and thus the volume, between an upper and a lower limit. However, in case of the pilot plant, only one threshold exists that is defined by the position of the level switch. The sensor has to be the upper level limit of the liquid level to avoid overflowing. Instead of a lower limit, a timer has to be used to determine the time period in which the filtrate valve is opened, for example so that a volume of exactly 100 mL is removed from the system. However, since the filtrate flow rate is mainly dependent on the reactor pressure and TMP, these parameters have to be factored into the calculation of the opening time. This means that the opening time of the valve has to be decreased when the plant is operated at elevated pressures. Another possible solution for this problem would be to simply measure the outflowing filtrate stream by the filtrate balance (WIRC 015) and to close the control valve when a weight difference corresponding to volume that has to be drained is detected. However, this method has a higher inertia, which could be critical if short switches of the level state are present.
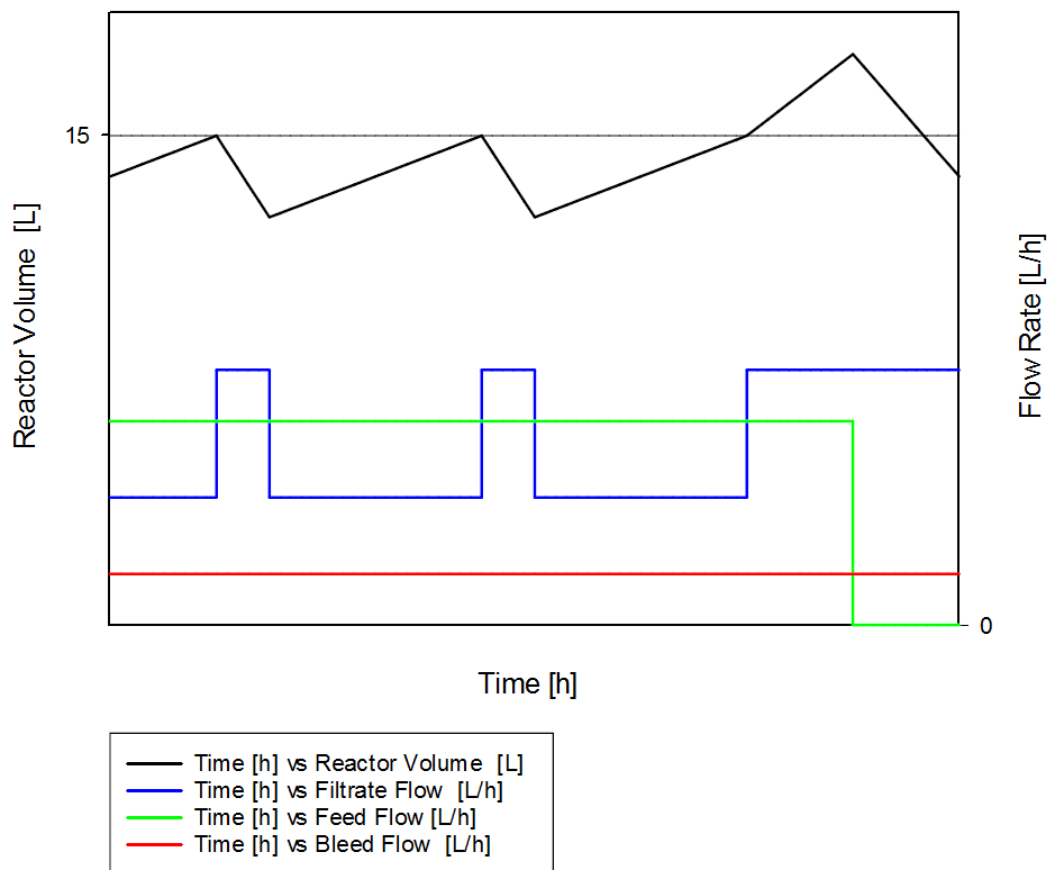
Figure 15: Level Control for Continuous Mode with Continuous Filtrate Flow

The second, far superior level control approach is the one with continuous filtrate flow. Thereby, a permanent filtrate flow is present besides the constant feed and bleed stream. However, the filtrate flow rate is slightly smaller than the mass balance would require it to be for steady state. Hence, the liquid level always increases continuously until the level switch is activated. Then, the flow rate of filtrate is

temporarily increased by adjusting the aperture of its control valve. But again, a controller with a timer is necessary to determine the time period in which the filtrate valve's opening is increased. It has to be independent from the reactor pressure as well. A schematic representation of this level control approach is shown in Figure 15.

The advantages of the approach with continuous filtrate flow over the one with intermittent flow are as follows: first, a "true" continuous state is reached, moreover, less switching operations are required and lastly, the total deviation from the 15 L-threshold is lower, resulting in a higher accuracy of process control. However, this approach is more complicated to implement and requires significantly higher accuracy of measurement and equipment like the control valves. For the test phase of the pilot plant, the level control approach with intermittent filtrate flow is acceptable, but the fully developed process should be operated with the more precise second method.

Furthermore, both level control approaches need a safety installation to prevent overflow of the reactor broth. Whenever the level switch is activated and the filtrate valve is opened, the liquid level in the reactor should sink. But in case of a process failure, for example when the filtrate valve is blocked, the level could still continue to rise when the state "level too high" is detected by the sensor. Therefore, an emergency timer has to be implemented that shuts down the feed flow if the level switch has been activated for a previously defined amount of time. This procedure is depicted at the end of both diagrams in Figure 14 and Figure 15.

3.4.3.7 Transmembrane Pressure Control

The transmembrane pressure (TMP) is the most important control parameter for membrane processes. It equals the force that presses the liquid through the membrane and is thus proportional to the filtrate flow. It is used to monitor the degree of membrane fouling. The TMP is calculated by Eq. 9, where p_1 is the liquid pressure before the membrane (feed side), p_2 the pressure after it (permeate side) and p_3 equals the pressure on the permeate side of the membrane. In order to determine the TMP of the pilot plant, three pressure sensors are placed at the above mentioned positions to measure the required parameters.

$$TMP = \frac{p_1 + p_2}{2} - p_3 \ [bar] \hspace{3cm} \text{Eq. 9}$$

In the pilot process, the transmembrane pressure is used to compensate the filtrate flow decrease by membrane fouling. Since the filtrate regulation by the control valve V12 can only reduce the maximum flow that passes the membrane, TMP-control is required to avoid that the filtrate flow rate sinks below the required value for steady state. In order to increase the permeate flow, the TMP has to be increased by decreasing the aperture of the retentate control valve (V10).

Another possibility to increase the permeate flow would be to increase the cross flow rate through the membrane by increasing the capacity of the loop pump (P4). The TMP-method is preferred because it is more accurate and cost effective. Moreover, higher loop pump flows lead to higher shear forces and therefore to more cell stress. However, a combination of both methods may be necessary in some cases, which is why both are implemented into the process control.

3.5   Equipment Design

The preliminary requirements of the equipment are specified in the user requirements specification in Appendix 1, which was created by Mahler and Herwig. The author modified them in consultation with the suppliers for the components. The result of this phase is the equipment specification, which is presented in Chapter 4. The revised equipment requirements are listed in the following subchapters. Dimensioning calculations for the loop tubing, microfiltration membrane and the off-gas cooler were performed, too.

3.5.1 Setup

Compared to the initial URS, the most significant alteration of the setup is the extension of the tanks for feed and filtrate. Their storage was originally planned to be executed by four 50 L tanks that would have had to be exchanged periodically. However, since the pilot plant allows a feed rate of approximately 50 L per day, these tanks would have had to be replaced once per day. Furthermore, because there is no mixing tank available at the laboratory of the department of bioprocess engineering, each 50 L batch of culture medium would have had to be produced separately.

For these reasons, the four 50 L tanks for both feed and filtrate were each replaced by a single 200 L storage tank. This offers the advantage that the plant can be operated autonomously for up to 4 days without the necessity of the physical presence of an operator. However, while the 50 L tanks could have been moved by one person, the larger tanks have to be stationary and have to be refilled or emptied by means of a pump. To produce 200 L culture medium at once, a separate mixing tank is needed that is equipped with an agitator and placed on a wheeled rack. In this mixing tank, the medium can be blended, rolled to the feed storage tank and then be transferred into it by a peristaltic pump. The filtrate tank has to be drained by this pump as well.

However, the increased storage volume requires larger balances with an increased measurement range suitable for a maximum load of 300 kg, which makes them far more expensive. Besides, the accuracy of smaller balances (usually 0.1 g in the laboratory) cannot be reached by far, as 2 g is the smallest practical readability of balances of that size. Furthermore, the larger dimensions of these balances make it impossible to place them on the movable reactor rack that should fit through normal

doors. Therefore, the pilot plant had to be split into two units. The first one, the moveable reactor skid, is placed on the wheeled rack and consists of the airlift reactor, cell retention loop with the membrane module as well as the pumps and probes. Furthermore, the switchboard is mounted to it and serves as power supply as well as a collecting point for all control signals. The media skid contains the balances and storage tanks for feed, filtrate, bleed, acid and base and is stationary. Power and signal lines of the balances are not connected to the switchboard of the reactor skid.

Furthermore, the installation site of the pilot plant was transferred to the fermenter-laboratory of the department bioprocess engineering (BD-building). Hence, the size of the reactor skid had to be reduced in order to fit into the lift. The maximum possible dimensions of the moveable rack were changed to a length of 1.50 m, width of 0.85 m and a height of 2 m.

3.5.2 Airlift Reactor

The airlift reactor was dimensioned by the reference of Krahe [12]. Figure 16 shows an internal-loop airlift reactor with typical proportions:
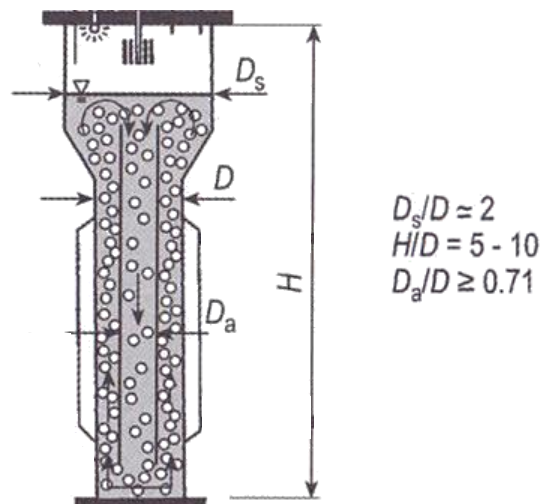
Figure 16: Airlift Reactor Geometry [12]

For efficient oxygen mass transfer, the airlift reactor had to be tall with a height to diameter ration between 5 and 10. That way, the residence time of the rising bubbles in the liquid and thus the OTR are optimal. The diameter of the top of the reactor vessel was doubled so that this area can act as a degassing zone and can compensate changes of the liquid height when the gassing rates and hence gas holdups are altered. Furthermore, that way, more space for placing equipment is available on the lid. The area ratio of riser and downcomer section is usually a most important parameter when designing an airlift reactor, since it determines the gas holdup, velocity of circulating flow and thus the hydrodynamics of the system [11]. In case of the airlift reactor for the pilot plant, an external loop is used, which means that the entire cross sectional area of the reactor tube can act as the gassed riser section,

while the diameter of the loop tubing determines the downcomer area. But the external loop of the pilot plant is combined with a membrane module for cell retention. The unification of these two methods is beneficial since they both require mostly the same equipment and can hence be combined very easily. However, the membrane significantly increases the flow resistance in the external loop and presumably hinders the formation of a free circulation flow that is created in airlift reactors by only gassing the riser section. Instead, a pump is used to overcome the pressure drop created by the microfiltration membrane and to circulate the liquid in the system. That way, an external loop airlift reactor with "forced" circulation is created, in which the circulation flow rate is not dependent on the actual area ratio of riser (reactor diameter) and downcomer section (loop tubing diameter) but on the capacity of the loop pump instead. Hence, the diameter of the loop tubing is insignificant for the hydrodynamics of the system. Moreover, the aeration and the loop flow are decoupled in this modification. The "forced" circulation offers the advantage that the flow rate can be controlled in a wider range than in a free system, but it is less cost efficient.

The operating range and the materials of the pilot reactor are specified in the URS and in Table 4:

Table 4: Operating Range of the Pilot Reactor

Properties	
Total Volume	ca. 20 L (considering gas holdup)
Working Volume	15 L
Allowable Gauge Pressure	-1 to 6 barg
Allowable Temperature	20 to 50°C
Materials	
Reactor, Tubing	GRP, Hastelloy C-22, glass or other materials resistant to 20% NaCl-concentrations
Bolts	A4-Quality (acid proof stainless steel grade)
Sealings	EPDM, Viton, PTFE

All required ports on the airlift bioreactor are specified in the initial URS as well. However, during the specification phase (Chapter 4) the positioning of these connections was modified, mainly due to the lack of space on the reactor lid. The final port configuration is displayed in Figure 17 and listed Table 5. All components attached to these ports have to be removable and the connections have to be closable by filler plugs.
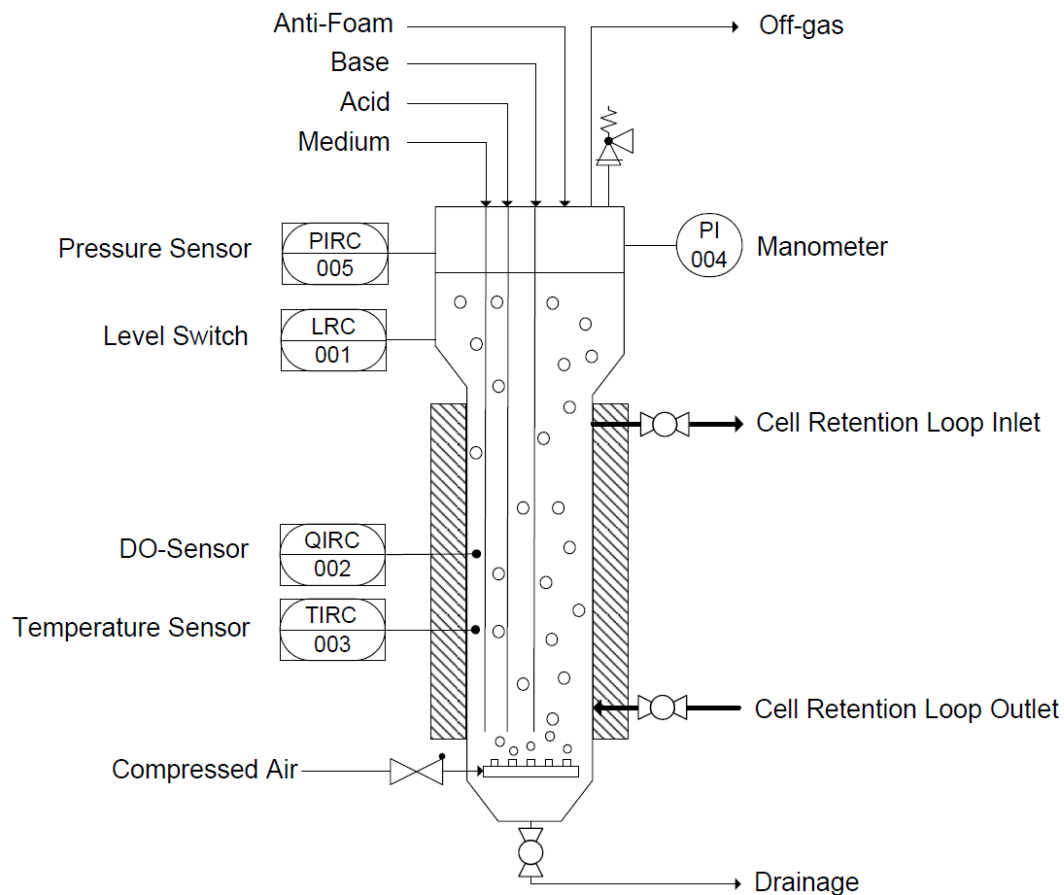
Figure 17: Required Ports on Airlift Reactor

Table 5: Required Ports on the Pilot Reactor and their Positions

Ports on the Lid	Position
Port for manual Anti-Foam Addition	-
Off-gas Port	-
Port for Feed Addition	-
Port for Acid Addition	-
Port for Base Addition	-
Port for Pressure Sensor	-
Port for Manometer	-
Port for a Safety valve	-
Excess Port for later Supplement	-
Gage Glass for Foam Control	-
Lateral Ports	
Port for Level Switch	At height equalling exactly 15 L volume
Port for DO-Sensor	Middle of reactor height
Port for Temperature Sensor	Middle of reactor height
Port for Gassing/Sparger	As low as possible
Port for Cell Retention Loop Inlet	Slightly below level switch
Port for Cell Retention Loop Outlet	Slightly above sparger
Ports on the bottom of the Vessel	
Port for Drainage	Lowest point of reactor

3.5.3 Piping

The maximum allowable flow velocity w_{max} of 1.5 m/s in the plant is specified in the URS. It is limited in order to prevent the cells from damage by too high shear forces. When using the flow rate of the circulating medium in the loop $\dot{V}_{Loop}$ from Table 2, the minimally required diameter of the loop tubing can be calculated by rearranging the continuity equation:

$$d_{min} = \sqrt{\frac{4 * \dot{V}_{Loop}}{w_{max} * \pi}} = 5 \; mm \qquad\qquad \text{Eq. 10}$$

The result of Eq. 10 is that the diameter of the loop piping has to be at least 5 mm wide to achieve acceptable shear rates. But then, the pipes must not be too wide, because larger diameters decrease the velocity and hence increase the residence time of the broth in the loop, which leads to a temperature drop and presumably oxygen limitation. Considering these facts, the inner loop tubing diameter was chosen to be 10 mm wide, which results in a flow velocity of about 0.37 m/s in the loop and allows sufficient safety margin for narrowings caused by valves. When estimating the length of the loop tubing with 4 m, the residence time of the broth in the tubing (without the membrane) is approximately 10 s. The required time to pass the membrane module will presumably be of similar size.

However, by default, some installations in the cell retention loop had to be used that have smaller apertures than the calculated diameter limit of 5 mm. This means that critical shear rates could occur locally in the loop. Especially the TMP-control valve and flow cells for the probes provide local narrowings. Flow cells are flow-through armatures that allow the positioning of sensors in tubing of smaller scale and are used to install the DO- and the pH-probe in the loop (see Chapter 4.2.2.).

A special requirement of the cell retention loop is that subsequent changes to the piping layout have to be made possible. Since the pilot reactor serves as a test plant, improvements as well as extensions to the system are likely to occur. This requires relatively flexible tubing that can be quickly altered. For that reason, the loop piping was chosen to be made of plastic (PEEK, PVDF or PTFE) tubes and fittings that are connected by compression- and screw joints. The position of compression fittings on a pipe can be easily altered. However, compared to fixed welded joints that are commonly used for steel piping, these two connection types are not suitable for hygienic design as they have small crevices and are not fully drainable. This makes these connection types hard to clean. But since halophiles can be cultivated under non-sterile conditions, hygienic design is not as important as for other microorganisms. Furthermore, the compression- and screw connections can be fully cleaned by dismounting them, which is permissible for the test plant.

To ensure drainability of the cell retention loop, the piping has to be inclined by at least 1°. The loop runs on two levels, one at the top and the other at the bottom of the vessel. The upper level was designed to be inclined downwards. By contrast, the lower level was planned to be tilted upwards so that gas bubbles that are carried away into the loop are forced to leave the piping and hence cannot affect the probes in the loop by forming air pads. However, that way, an additional drainage port has to be installed at the lowest point of the lower loop level.

To achieve sufficient cleanability, the junctions of the loop tubing (for bypass-, sampling- and bleed line) were designed according to the "3D"-rule to minimize dead spaces.

3.5.4 Membrane

A polysulfone (PSU) hollow fiber cross flow microfiltration membrane cartridge with an area of 420 cm² and a pore size of 0.2 µm is used for cell retention in the 1 L lab-scale plant. The same filtration configuration shall be used for the novel pilot process as well. The initial requirements for the membrane module for the pilot plant are listed in URS as well as in Table 6. The membrane area was scaled up from lab-scale by multiplying that size by the factor 15, resulting in a necessary membrane area of 6300 cm².

Table 6: Technical Specification of the Membrane Module according to the URS

Pore Diameter	0.2 µm
Membrane Area	min. 6300 cm²
Allowable Temperature	20 - 50°C
Allowable Pressure	3 barg
Transmembrane Pressure	max. 3 barg
Transmembrane Flow (Flux)	0 - 1.5 L/h
Cross Flow Rate	8 L/m²/min
Material	Resistant to solution with 25% NaCl-conc.

Cross flow microfiltration membrane modules for industrial applications are usually operated at cross flow or recirculation rates above 8 L/m²/min (retentate) and transmembrane flow rates, the so-called flux, over 10 L/m²/h (filtrate). These parameters are related to the membrane area and are used to characterize cross flow filtrations and to find optimal operating conditions. But on industrial-scale, microfiltration membranes are usually periodically cleaned by being backflushed from the permeate side to remove fouling. This method cannot be used for the pilot plant since cleaning lines and drainage are not available for filtration and the continuous operation should always be maintained. Furthermore, as a test plant, the setup has to be kept as simple as possible.

Instead, the membrane area of the pilot plant was designed to be large enough so that the membrane module can be operated for several weeks or even months without fouling that significantly limits its functionality. This could be achieved in the 1 L lab-scale plant with a cross flow filtration cartridge with a membrane area of 420 m². Ruschitzka [9] performed optimization studies on the membrane area for the lab-scale plant with the extremely halophilic archaeon *Haloferax mediterranei*. He executed long lasting, continuous cross flow filtrations without cleaning by backflushing. Ruschitzka measured the maximum flux rates at three different biomass concentrations before the membrane was blocked by fouling. He found out that the maximum feasible flux rate decreases with rising biomass concentration. His results are listed in Table 7:

Table 7: Feasible Flux Rates depending on Biomass Concentration [9]

Biomass Concentration [g/L]	Maximum feasible Flux Rate [L/m²/h)]
2	6.1
3	5.5
5	1.6

To avoid blockage by fouling, long lasting continuous cross flow filtration without periodic cleaning can be operated with a maximum flux rate of 1.6 L/m²/h according to Table 7 when a biomass concentration of 5 g/L is present in the reactor. This value is significantly smaller than flux rates for industrial applications with cleaning that are usually above 10 L/m²/h.

The required membrane area for a filtration process can be calculated for a given, transmembrane flow rate $\dot{V}_{TM}$ and the maximum feasible flux rate J by Eq. 11:

$$A_{Membrane} = \frac{\dot{V}_{TM}}{J} [m^2]$$

Eq. 11 [17]

Filtrate flows of up to 1.44 L/h occur in the pilot process. When using the maximum feasible flux rate of 1.6 L/m²/h for a biomass concentration of 5 g/L, determined by Ruschitzka, the required membrane area is 0.9 m². However, due to the larger size of the new membrane module and especially the fiber diameter, it was decided that the initially planned area of 0.63 m² would be sufficient for long-term application. This size would not be adequate for industrial applications, but offers the advantage that the membrane of the pilot plant can be operated for several weeks or even months without blocking through fouling. Furthermore, the filter can be manually cleaned from fouling or even exchanged during operation by temporarily using the bypass line. For comparison, in an industrial application with backflushing and a flux rate of 10 L/m²/h, a filtration area of 0.144 m² would be sufficient.

3.5.5 Off-gas Cooler

On laboratory scale, reflux condensers, so-called Liebig-coolers, are commonly used to cool the exhaust gas of bioreactors and recover most of its humidity by condensation. Thus, off-gas cooler prevent water loss and protect off-gas analysers from damage caused by water condensing inside of them. Furthermore, the water content influences the off-gas composition and has to be reduced for representative measurement. Liebig-coolers for laboratories are usually made of glass. Figure 18 shows the off-gas cooler used for the lab-scale bioreactor.
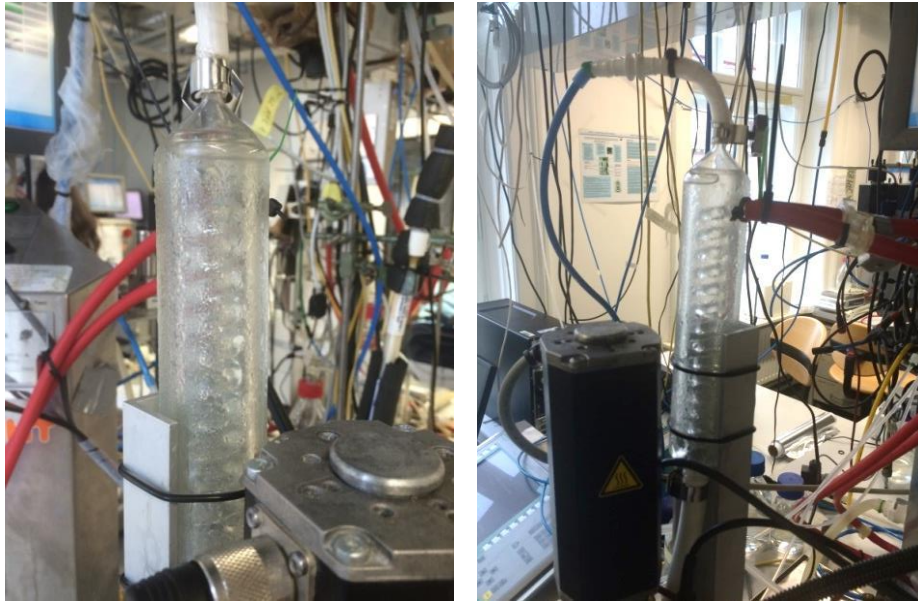
Figure 18: Reflux Condenser on the Lab-scale Bioreactor

However, such glass coolers cannot be utilized in the pilot plant because they are not resistant to overpressure due to high brittleness. Instead, a conventional heat exchanger or a reflux condenser made of a pressure-resistant material has to be used. Furthermore, those alternative devices have to be corrosion resistant, which limits this task mainly to polymers because alloys like Hastelloy C-22 are far more expensive for that application.

For this reason, a plastic gas-liquid tube bundle heat exchanger was dimensioned. The procedure for the calculation of the required heat transfer surface is covered below:

The water load Y of humid air is defined by the ratio of water mass per kg dry air:

$$Y = \frac{m_W}{m_G} \left[\frac{kg\ H_2O}{kg\ air} \right]$$

Eq. 12 [31]

The water load *Y* of saturated humid air above a water reservoir can be determined by Eq. 13 :

$$Y = 0.622 * \frac{p_S}{p_{tot} - p_S} \left[\frac{kg\ H_2O}{kg\ air} \right]$$

Eq. 13 [31]

Y depends on the saturated vapour pressure *p_s* as well as on the total pressure p_{tot} of the gas. The saturated vapour pressure and hence the maximum water load increases when the temperature rises. By contrast, *Y* and *p_s* decrease when the liquid contains ions, according to Raoult's law. For example, the saturated vapour pressure of an aqueous solution containing 20% NaCl is about 10% lower than in pure water. Besides, *Y* decreases with rising total pressure, as Eq. 13 indicates. Considering these three facts, the highest water load in the off-gas of the pilot plant is expected to occur at the maximum temperature, without overpressure and at low salt concentrations in the medium.

The specific enthalpy *h* of humid air is calculated by Eq. 14 . It is a function of the air temperature *θ* as well as of the water load *Y*. Furthermore, *h* depends on the specific heat capacity of dry air (c_{pA}), steam (c_{pS}) as well as on the enthalpy of vaporization Δh_V:

$$h = c_{pA} * \theta + Y * (\Delta h_V + 0.622 * c_{pS} * \theta) \left[\frac{kJ}{kg\ air} \right]$$

Eq. 14 [31]

To find the heat flow $\dot{Q}$ that is necessary to cool and dehumidify the off-gas to a desired water load, the specific enthalpy difference between the gas entering and leaving the cooler $(h_{in} - h_{out})$ has to be calculated. By multiplying this term with the gas flow rate $\dot{V}_G$ and the air density ρ_G, the heat flow can be determined according to Eq. 15:

$$\dot{Q} = (h_{in} - h_{out}) * \dot{V}_G * \rho_G [W]$$

Eq. 15

Then, the required heat exchange area can be calculated with Eq. 16, where *k* is the heat transfer coefficient and ΔT_{log} the middle logarithmic temperature difference between the two mediums.

$$A_{cooler} = \frac{\dot{Q}}{k * \Delta T_{log}} [m^2]$$

Eq. 16

Lastly, the previously described calculation of the heat exchange area was applied to the pilot process. For cost reasons, the cooler was not designed for the maximum possible operating conditions but for typical ones instead. The following assumptions were made:

A saturated humid air flow of 15 L/min enters the cooler at a temperature of 37°C and at 0 barg. Inside, heat is exchanged with cooling water of 8°C, whereby the gas is cooled down to 15°C and the water load Y of the gas is reduced to 0.01 kg water per kg dry air. The temperature change of the cooling water is negligible. Pure water is used for the calculation instead of saline solution. Thus, the influence of the dissolved ions in the medium is neglected, which is a conservative assumption. The heat transfer coefficient was estimated at 15 W/m²/K according to VDI Wärmeatlas [31]. This value is suggested for gas-liquid tube bundle heat exchangers at low gas pressures at unfavourable conditions and hence a very conservative estimation. The results of this calculation are:

- The saturated off-gas has a water load Y of 0.042 kg water per kg dry air.
- A heat flow $\dot{Q}$ of 31 W has to be extracted from the off-gas.
- A tube bundle heat exchanger with a heat transfer area of 0.135 m² is required.

For comparison, when the plant is operated with the maximum allowable temperature of 50°C, the previously calculated water load, heat flow and thus required heat transfer area are approximately doubled. When the maximum aeration rate of 30 L/min and the maximum allowable temperature of 50°C are used, the initial heat flow and required heat exchange are even quadrupled.

4 Equipment Specification

The preliminary requirements of the equipment are specified in the user requirement specifications in Appendix 1. In addition, the author performed dimensioning calculations and revised the initial requirements. Then, in consultation with the suppliers for the components, the equipment was specified and finally bought. The stocklist of all components used for the pilot plant can be found in Appendix 4. The materials and limits of use are listed in it as well. All abbreviations in this Chapter correspond to the ones used in the process flow diagram in Appendix 2 as well as in the stock list in Appendix 4.

The four main selection criteria for the plant's equipment parts in order of importance are:

1. Corrosion resistance
2. Pressure resistance
3. Connection type
4. Hygienic design/FDA-conformity

In biotechnological applications hygienic design is usually the most important requirement. But since halophiles do not need sterile environments for cultivation, hygienic plant design is beneficial for cleaning purposes, but not necessary for operability. Hence, a wider range and more cost efficient equipment was feasible for the pilot plant, for example threaded connections. Nevertheless, whenever possible, components with hygienic design were used.

A short description of the main equipment parts is given in the following subchapters. Especially their particular selection criteria and their integration or connection into the whole system are pointed out.

4.1 Reactor Skid: Airlift Reactor, Rack and Switchboard

The reactor skid was built by the Austrian plant construction firms Baumgartner & Co. GmbH and Möstl Anlagenbau GmbH. It consists of the airlift reactor, the wheeled rack with supports for piping, pumps and the membrane as well as the switchboard.

4.1.1 Airlift Reactor (C1)

The main characteristics of the pilot reactor vessel are specified in Table 8.

**Table 8: Specification of the Halophiles Pilot Reactor**

Allowable Operating Pressure	-1/+5 barg
Allowable Operating Temperature	0/+90°C
Total Volume	21.2 L
Material	2.4602
Empty Weight	63 kg
Test Pressure	7.3 barg

The reactor parts that are wetted by the corrosive medium (vessel, nozzles and lid) are made of electropolished Hastelloy C-22 alloy (2.4602). The rest of the construction (rack, insulation housing that covers the reactor vessel and the switchboard housing) do not have direct contact to the medium and therefore consist of the common stainless steel type 1.4301, which is not resistant to NaCl-solutions.

The reactor tube has an inner diameter of 134.5 mm and is filled to a height of about 1.1 m, resulting in a height-to-width ratio of about 8 - the optimal range for airlift reactors. The full constructional drawing of the reactor skid is shown in Appendix 3. The side and top view of the drawing are depicted in Figure 19.

The red marked sides in the top view of the reactor skid in Figure 19 - the front and the lefthand side - indicate where the plant is accessible during operation. All manual valves (bypass valve, sampling valve, etc.) and probes are accessible from these two sides during operation. The rack has to be moved to reach the other sides. Furthermore, the reactor is placed asymmetrically on the rack, so that the gage glass can be reached more easily from the accessible front side. The switchboard is positioned below the handle of the rack on the righthand side and is marked by a bolt-symbol in the construction drawing.

All ports on the reactor are Tri-Clamp connections, except for the level switch port, which had to be a threaded connection by default. Tri-Clamps (see Figure 28) are simple, sterile connections that are detachable and commonly used in pharmaceutical industry, whereas threads are usually avoided there since they do not allow hygienic design.
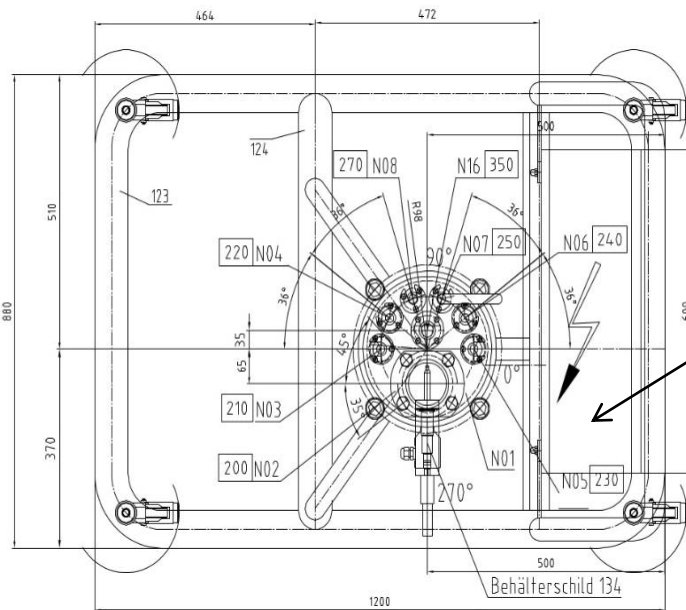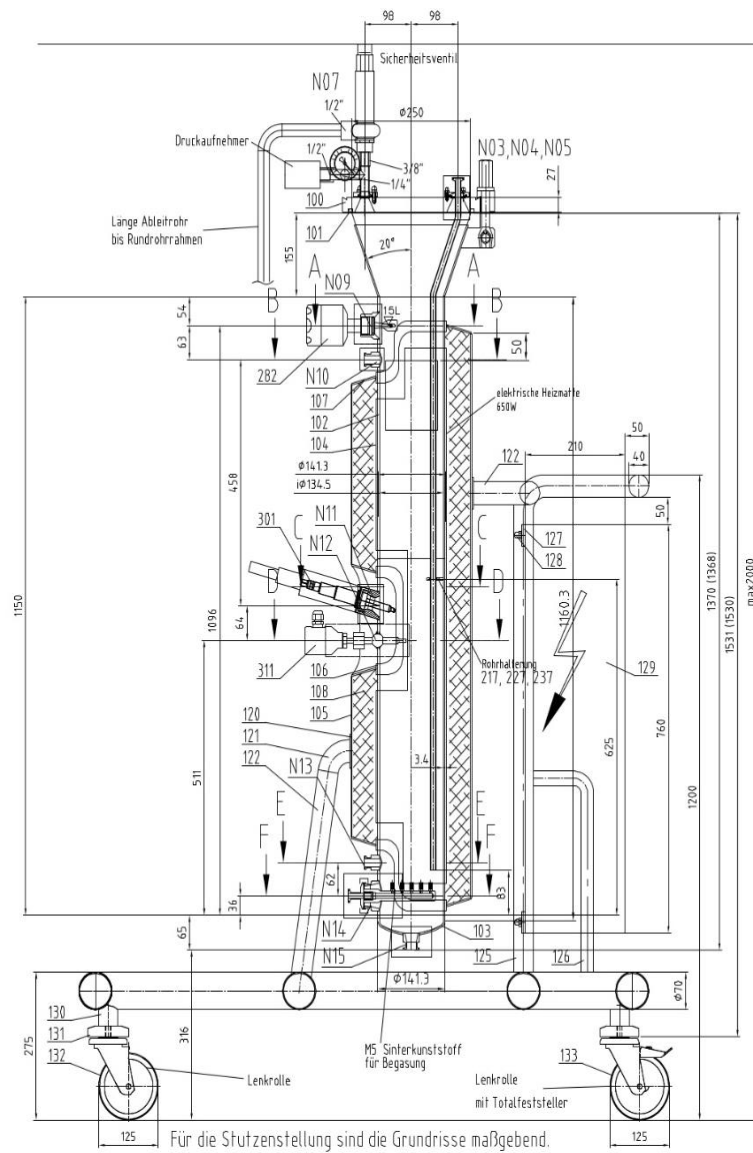
Figure 19: Design Drawing of the Airlift Reactor (Side and Top View)

The as-delivered reactor skid is shown in Figure 20 and the dismounted reactor lid is displayed in Figure 21. It is attached to the reactor vessel by four clamps.


Figure 20: As-delivered Reactor Skid

Figure 21: Reactor Lid (left) and Clamp (right)

The top view of the design drawing shows the reactor lid with its ports. Compared to the initial design of the connections on the lid in Chapter 3.5.2 and Table 5, several changes had to be made, mainly due to the lack of space. Firstly, a second, smaller gage glass had to be installed in the centre. Through it, the interior of the reactor can be illuminated, while the large main gage glass is used for actual inspection. Furthermore, due to lack of space, only six ports could be placed on the lid, whereas nine connections besides the gage glass are required according to Table 5. For this reason, a special fitting was constructed that houses the safety valve with its discharge line, the pressure sensor and the manometer, but only requires one port on the lid. This construction is depicted in Figure 22. However, due to the lack of space on the lid, the initially planned excess port for later supplement has to be used as the port for anti-foam addition as well.
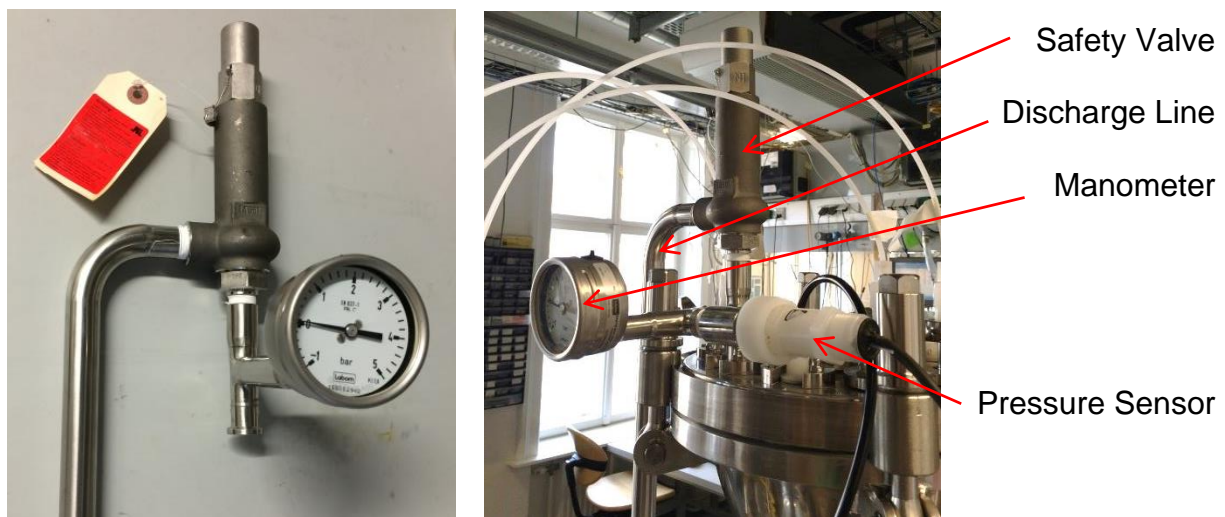
Figure 22: Fitting for Safety Valve with Discharge Line and Manometer

To provide better mixing, dosing pipes (see Figure 23) are installed on the ports for feed, acid and base addition. These tubes are mounted on the lid and protrude into the vessel. They end near the sparger and thus decrease the mixing time of the added substances in the reactor. One of these dosing pipes is shown built out in Figure 23. The dosing pipes are fixed by support plates welded to the inner surface of the reactor vessel, as shown in Figure 24.

Figure 23: Dosing Pipe

Figure 24: Top View inside the Reactor Vessel

Figure 24 also displays the sparger, the protective sleeve of the temperature sensor and the DO-sensor that all extend into the reactor vessel. The sparging tube is made of PTFE and is attached to the reactor at the bottom by a Tri-Clamp connection. Five interchangeable PE-sparging cartridges are screwed into the tube. The whole built out sparger is displayed in Figure 25:
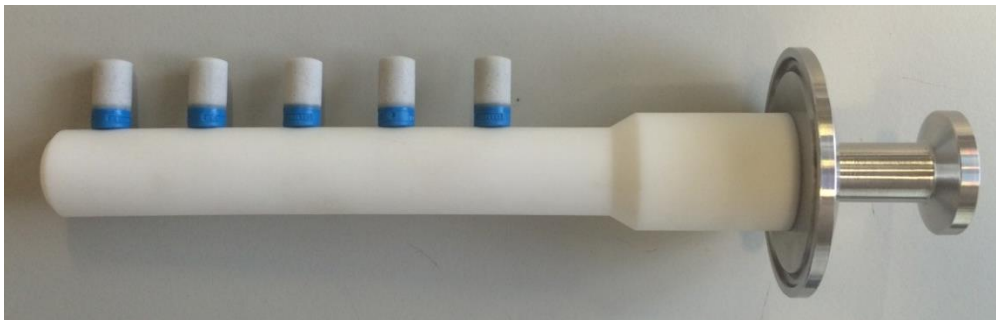
Figure 25: Sparger

4.1.2 Switchboard

The switchboard is mounted to the reactor rack. It powers the pilot plant and contains terminal blocks for the control signals as well as a temperature control unit for the heating pad. The interior of the switchboard in as-delivered condition is shown in Figure 60 and a full description of its functionality and all built-in components is given in Chapter 5.2.

4.2   Piping

The piping and fittings of the pilot plant are made of PVDF and PTFE components manufactured by the German company EM-Technik GmbH [32]. All tubes consist of PVDF and are translucent so that the flow can be visually observed. Depending on the medium and flow rates, different tube sizes are used, as Table 9 shows.

Table 9: Tubing Dimensions

External Tube Diameter [mm]	Inner Tube Diameter [mm]	Used for:
12	10	Cell retention loop tubing
6	4	Inlet air tubing, off-gas line
4	2	Feed-, acid-, base-, filtrate- and bleed lines

The tubes are connected by compression fittings, as shown in Figure 26. The fittings themselves are joined by threads (see Figure 29).
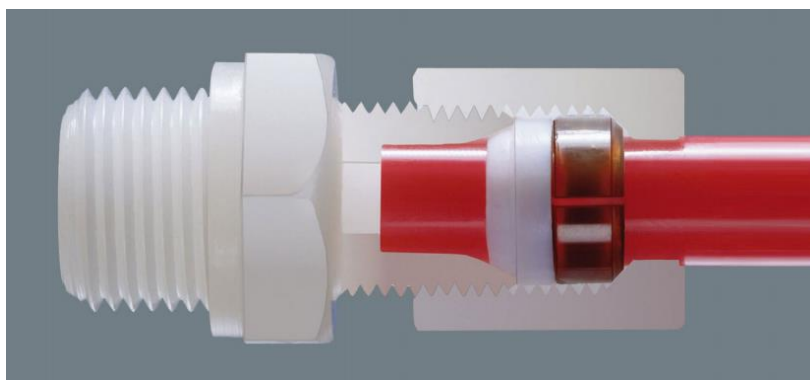
Figure 26: Cross Section of a Compression Fitting from EM-Technik GmbH [32]

The compression fittings from EM-Technik are available with various connection types (threaded, Tri-Clamps, etc.) and modifications (elbow pieces, T-pieces, etc.):
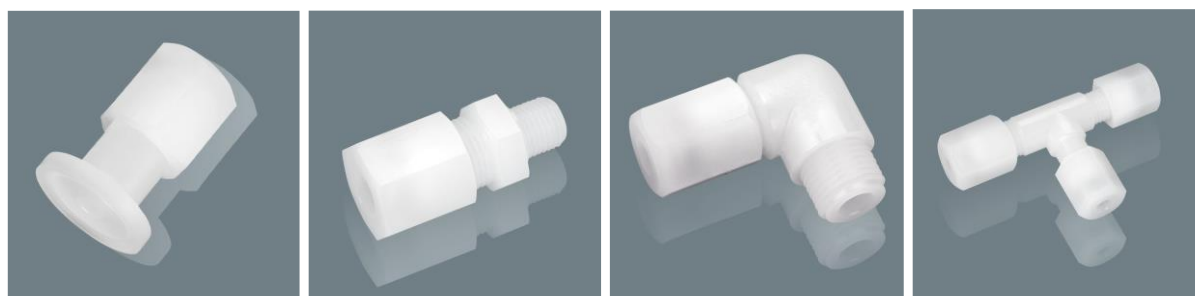
Figure 27: Compression Fitting Types from EM-Technik GmbH [32]

The piping is connected to the reactor vessel by compression fittings with Tri-Clamp connections (Figure 27, far left). The loop pump and the membrane module are connected to the tubes in the same way. Tri-Clamp connections (see Figure 28) are

flange like connections with a seal ring in between that are compressed by a clamp that is usually made of stainless steel.
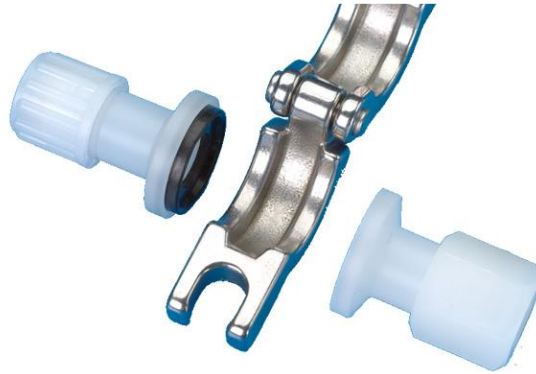
Figure 28: Tri-Clamp Connection from EM-Technik GmbH [32]

The valves and fittings are joined with the piping by threaded connections, mostly compression fittings with outside threading. The following picture shows the three different pipe connection types used for the loop:

Compression Fittings with Outside Threading

Compression Fittings with Tri-Clamp Connections

Double-sided Compression Fittings

Figure 29: EM-Technik GmbH Fittings in the Cell Retention Loop

A stocklist of all piping components can be found in Appendix 5. Furthermore, the limits of use for these parts are listed in it. The PVDF fittings have lower temperatur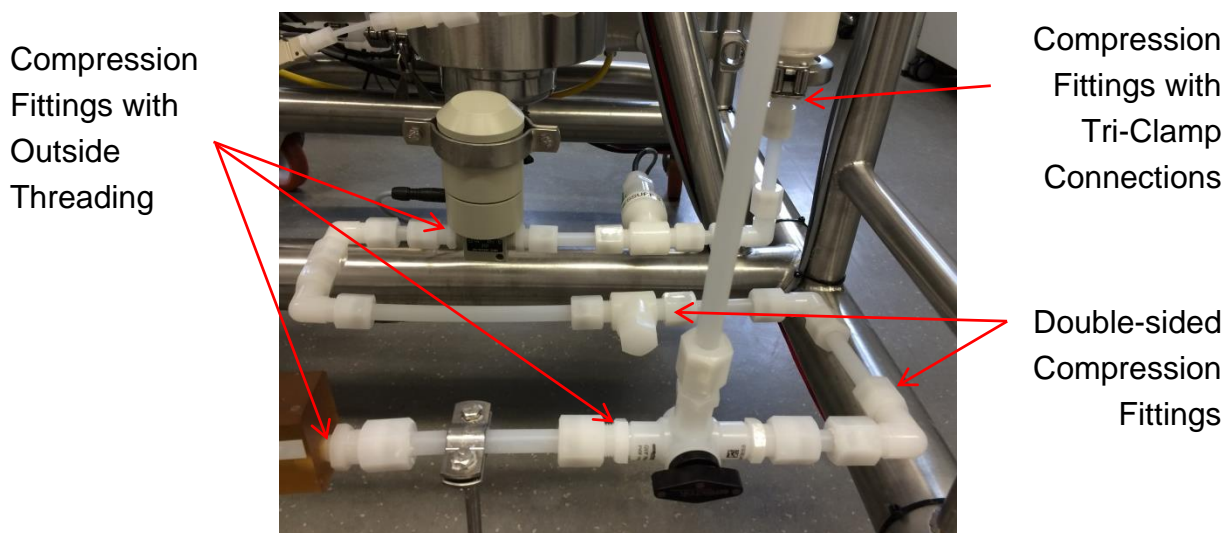e and pressure resistance than the PTFE ones. They can withstand pressure up to 3.6 barg at 50°C which is sufficient for application in the pilot process. All PVDF parts from EM-Technik are FDA-approved. However, the used compression and threaded connections are not in accordance with hygienic design because they have small crevices and are not free from dead spaces.

A manual for assembling the EM-Technik plastic fittings is given in Chapter 8.1.1.

4.2.1 Manual Valves

The manually actuated valves of the cell retention loop were bought from EM-Technik GmbH [32], too. For flow regulation, shut-off ball valves (V6, V8, V9, V14, V15) and a 3-way ball valve (V11) are used. Furthermore, a needle valve is utilized for sampling (V11). All these valves are made of PVDF and can resist pressure up to 6 barg at 50°C. Besides, a check valve (V2, Figure 30 bottom right) made of PVDF with a Hastelloy C-22 spring was bought. It is approved for pressures of up to 3.6 barg at 50°C. All manual valves are connected to the tubing by compression fittings with outside threading (Figure 27, second from left).

Figure 30: Valves from EM-Technik GmbH [32]

4.2.2 Flow Cells

Flow cells are flow-through armatures that allow the installation of sensors in tubing of smaller scale. They consist of a sealed probe housing and base body with a cavity. The sensor tip extends into the cavity, which is connected by two channels, through which the medium flows and can be analysed.

In the pilot plant, one of the DO-sensors (QIRC 011) as well as the pH-sensor (QIRC 009) have to be positioned in the loop tubing by means of flow cells. For that purpose, easyFlow 23 fittings from Mettler Toledo GmbH [33] were bought. They are made of the polymer polysulfone (PSU) and pressure-resistant up to 6.8 barg at 65°C. Like the manual valves, these flow cells are connected to the tubing by compression fittings with outside threading. The Mettler Toledo easyFlow 23 fitting is shown in Figure 31:
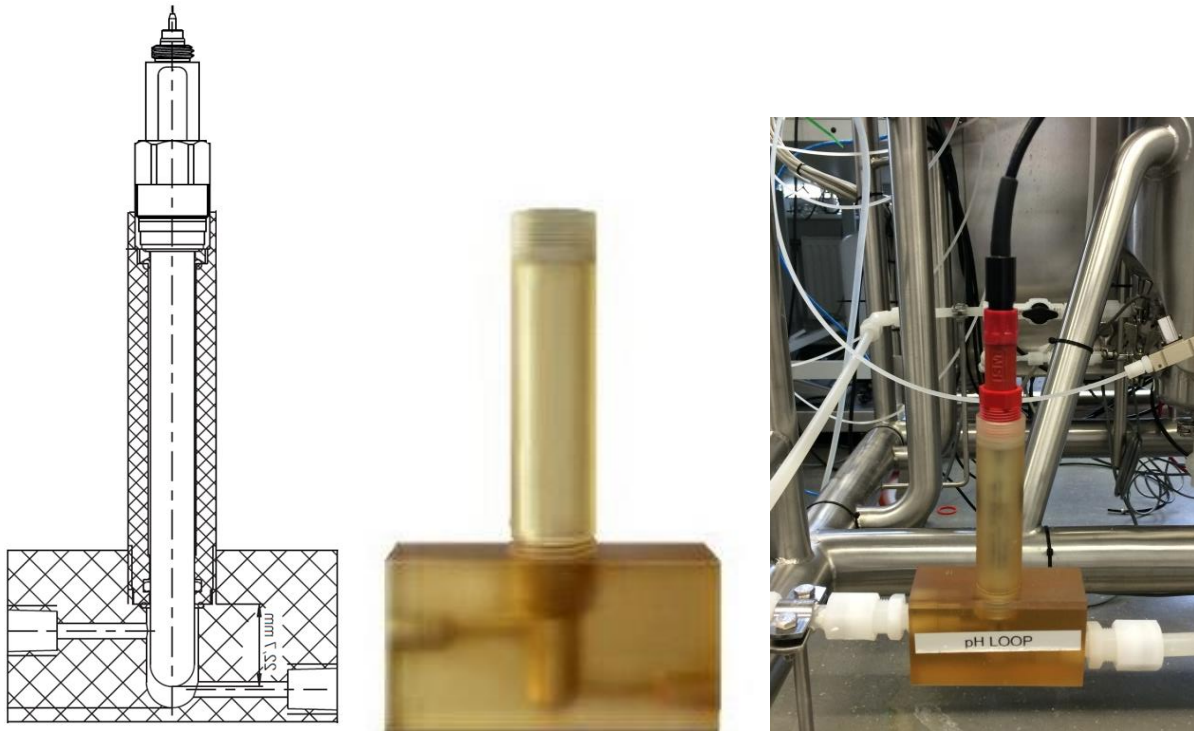
Figure 31: Flow Cells: Mettler Tolendo easyFlow 23 [34]

The flow through this flow cell has to be bottom-up (flow direction from right to left in Figure 31) for optimal measurement. This configuration leads the air bubbles in the tubing back into the reactor, but an additional drainage port has to be installed at the lowest part of the lower loop level.

4.3 Loop Pump (P4)

For circulating the broth through the cell retention loop, the Quattroflow 150SU 4-piston-diaphragm pump by ALMATEC Maschinenbau GmbH is used. This pump type was chosen because it is cell protecting due to very low shear rates, is not affected by bubbles and even allows dry running.
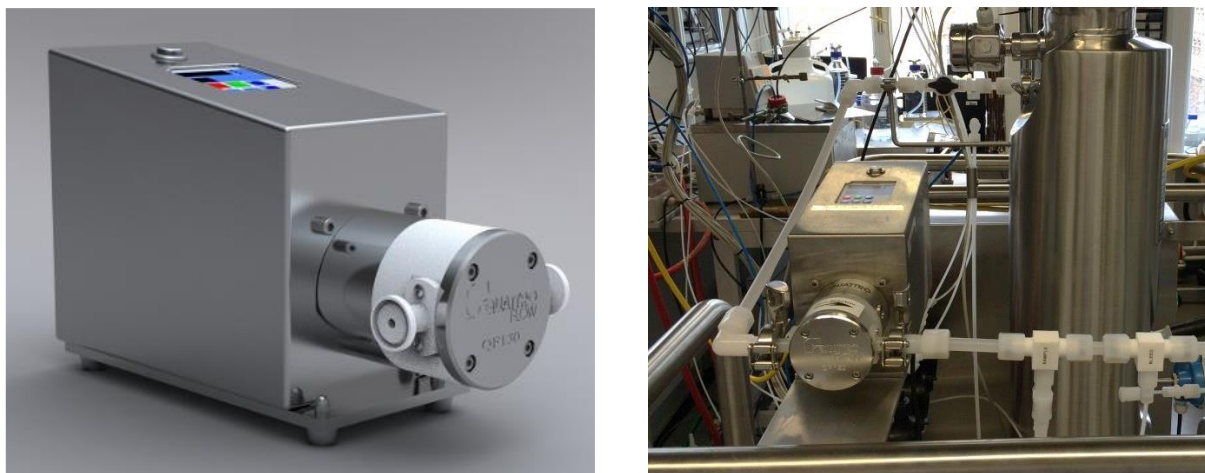
Figure 32: Quattroflow 150SU 4-Piston-Diaphragm Pump by ALMATEC [35]

The pump chamber of this pump is standardly made of the stainless steel alloy 1.4435, which is not corrosion resistant in NaCl-solution. Corrosion-proof Hastelloy C-22 pump chambers are available as well, but they are extremely expensive. For this reason, single use plastic pump chambers made of polypropylene are used instead. They are significantly cheaper, but have an operating life of only 200 h. Furthermore, the single use plastic pump chambers slightly reduce the capacity and decrease the allowable pressure of the pump.

The flow characteristics of the loop pump are given in Figure 33. The flow rate increases linearly with the engine speed and is slightly decreased with increasing pressure. At the maximum allowable pressure of 4 barg, the pump can convey approximately 190 L/h at full speed.
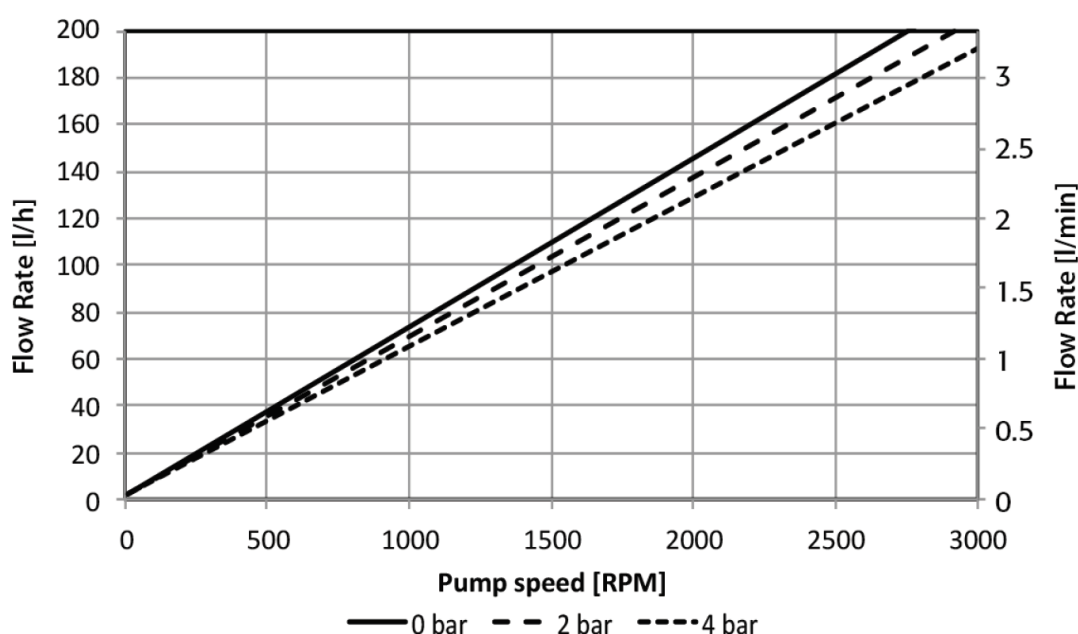
Figure 33: Quattroflow 150SU Performance Chart [35]

The PP-pump chamber is connected to the loop tubing by compression fittings with Tri-Clamp connections (Figure 27, far left). The pump is fixed to a platform at the upper level of the cell retention loop, just below the loop inlet, as shown on right side of Figure 32.

4.4   Dosing Pumps

The dosing pumps for feed, acid and base have to be able to handle the counterpressure from the reactor of up to 3 barg and to deliver an output as specified in Table 2. For that task, solenoid-diaphragm dosing pumps from Lutz-Jesco GmbH were chosen. The three pumps are placed on a platform that is welded to the rack and the dosing lines are directly connected to the pumps by 6 mm tube compressions.

Figure 34: Platform for Dosing Pumps

4.4.1 Feed Pump (P3)

The MAGDOS LA 4 dosing pump from Lutz-Jesco GmbH [36] is used for feed addition. The maximum flow rate decreases with increasing counter pressure, but at 16 barg it can still pump up to 3.4 L/h. Furthermore, the pump's capacity can be controlled by adjusting the stroke rate, either manually on the control unit of the pump or externally by an analogue input signal. The delivery characteristic curve of the MAGDOS LA 4 is marked in red in Figure 35:
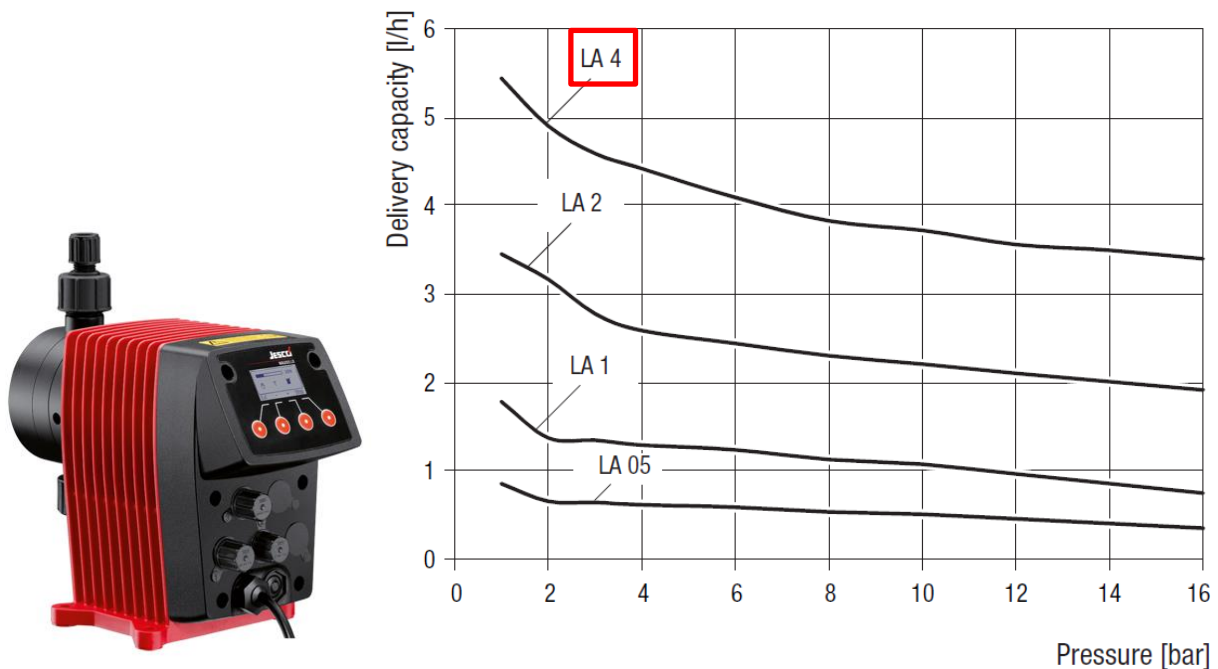
Figure 35: MAGDOS LA 4: Delivery Characteristic Curves [36]

Since the feed pump's delivery capacity is dependent on the counter pressure from the reactor, a back pressure valve was bought to increase the dosing accuracy. This valve generates a defined back pressure and hence the flow rate can be decoupled from the reactor pressure.

4.4.2 Acid and Base Pump (P1, P2)

For the addition of acid and base, the MAGDOS LB 1 dosing pumps from Lutz-Jesco GmbH [37] are used. They have a maximum flow rate of 0.76 L/h at 16 barg. During operation they are switched on and off by a relay, which in turn is controlled by the PCS. Their capacity can be controlled manually. The delivery characteristic curve of the MAGDOS LB 1 pump is marked in red in Figure 36:
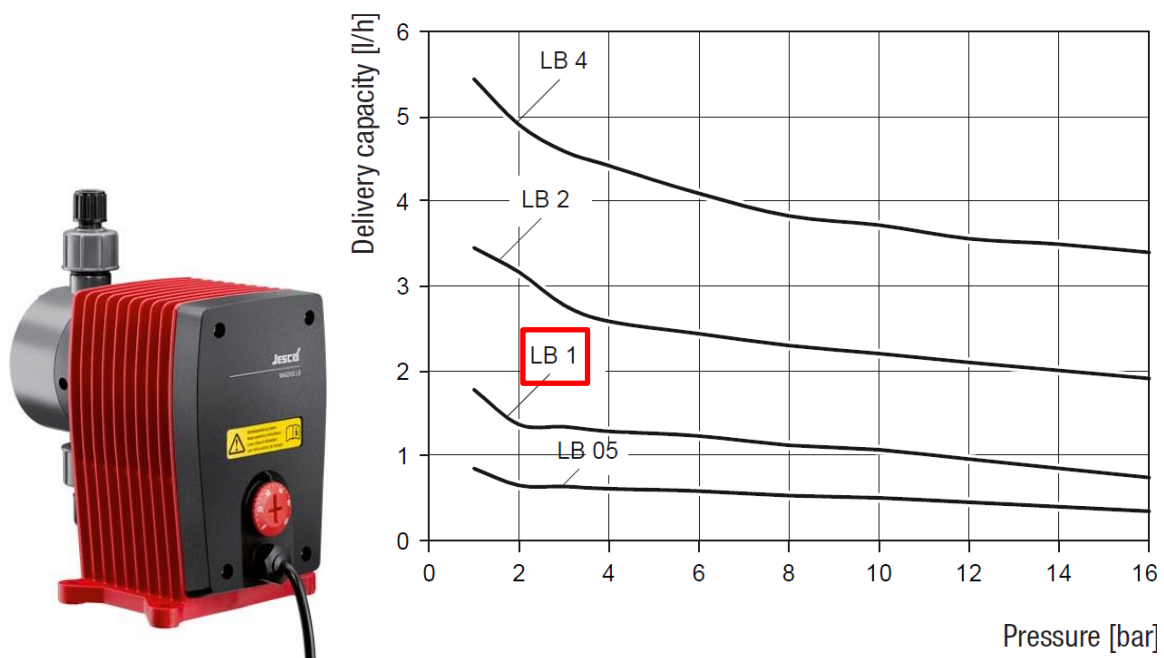
Figure 36: MAGDOS LB 1: Delivery Characteristic Curves [37]

4.5   Mass Flow Controller (FRC 019)

To control the flow of the inlet air for aeration, a GF40 series thermal mass flow controller by Brooks Instrument LLC [38] is used. It has an operating range of 0 to 30 L/min and resists pressure up to 10 barg. It is connected to the gassing line by two 6 mm tube compressions. For safety reasons, the device has to be placed well above the reactor to avoid contamination by backflow of fluid if the check valve fails.

Figure 37: GF40 Thermal Mass Flow Controller from Brooks Instrument LLC [38]

4.6   Membrane (F1)

For cell retention, a cross flow filtration cartridge type CFP-2-E-9A from GE Healthcare Life Sciences [39] was bought. It is made of polysulfone and has a membrane area of 8400 cm². The cartridge is pressure-resistant up to 5.2 barg and can even be autoclaved. The feed and retentate ports are Tri-Clamp connections, while tubing nipples are available on the permeate side. The EM-Technik GmbH compression fittings can be directly attached to these nipples. The cartridge is positioned vertically and the upper permeate port is closed, since no backflush-cleaning occurs in this application. A schematic representation and an actual picture of the membrane setup are shown in Figure 38:

Figure 38: Cross Flow Filtration Cartridge Setup [10]

4.7 Control Valves

4.7.1 Pressure Control Valve (V3)

The pressure control valve (V3) is installed in the off-gas line and adjusts the reactor pressure to the desired value by altering its aperture. For this task, a Type 2871 [40] solenoid control valve was bought from Bürkert Contromatic GmbH. It can be made of stainless steel because it does not come into contact with the corro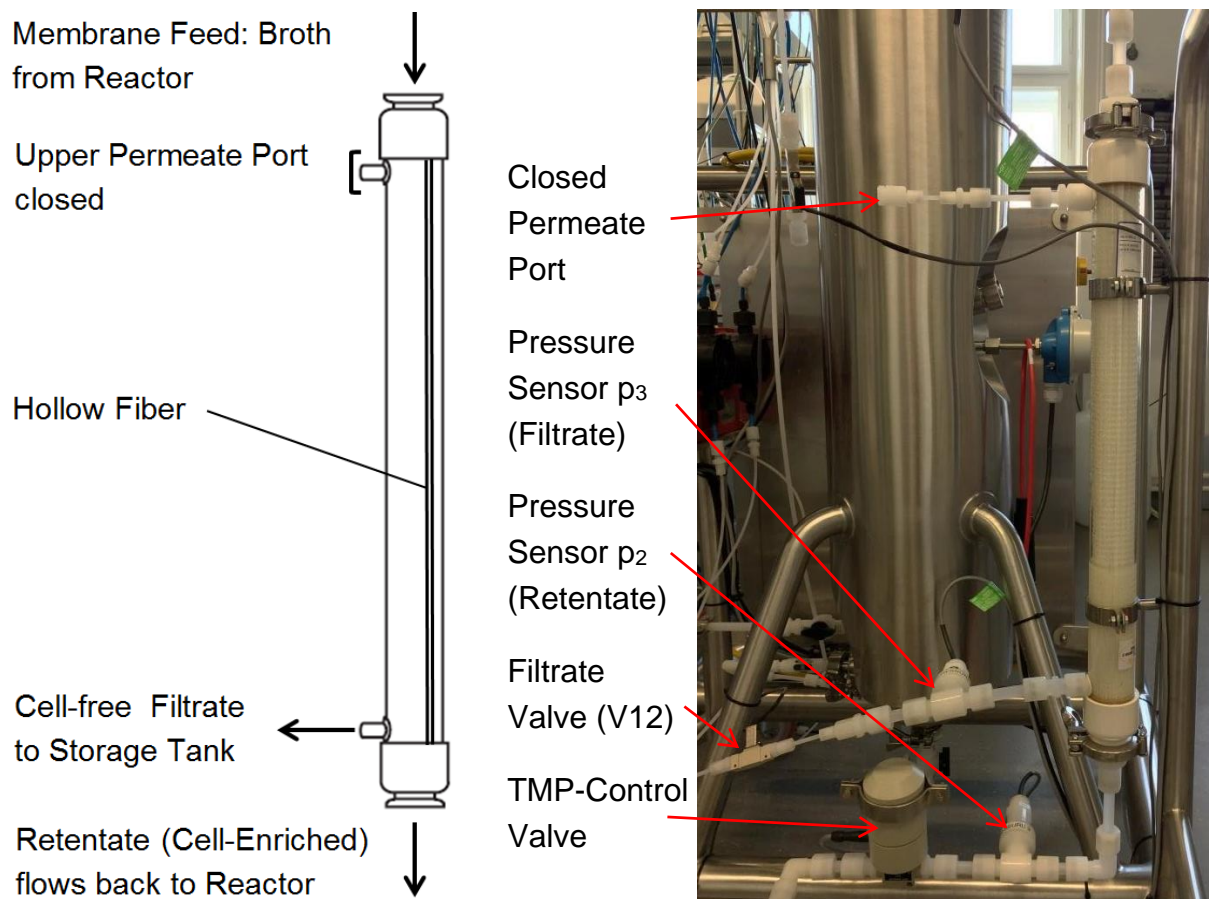sive medium. The proportional opening of the valve is achieved by pulse width modulation (PWM). For that purpose, an additional control unit is necessary (Bürkert Type 8605 [41]), which receives an analogue input signal from the PCS and adjusts the aperture via PWM. The control unit is installed in the switchboard. The pressure control valve is connected to the off-gas tubing by compression fittings with outside threading.

Figure 39: Bürkert GmbH Control Valve Type 2871 (left, middle) [40] and Control Electronics Type 8605 (right) [41]

4.7.2 TMP-Control Valve (V10)

The TMP-control valve is placed on the permeate side of the membrane module and is used to adjust the transmembrane pressure and hence the filtrate flow. For this task, the electrically actuated control valve Type 5E made of polypropylene was bought from EM-Technik GmbH [32]. The flow through the valve can be automatically regulated by the spindle rotation which alters the aperture. The flow rate can be adjusted between 10 and 100 L/h at 1 barg, as the red marked curve in Figure 40 shows. However, at higher pressures the flow rate increases proportionally and can be estimated by multiplying the valve's flow coefficient K_v with the pressure. The flow coefficient of this valve amounts to 100 L/h when fully opened. However, it has to be noted that by reducing the control valve's aperture, the local flow velocity and hence the shear rates increase, which could damage the cells. Like the manual valves, the TMP-control valve is connected to the tubing by compression fittings with outside threading (Figure 27, second from left).
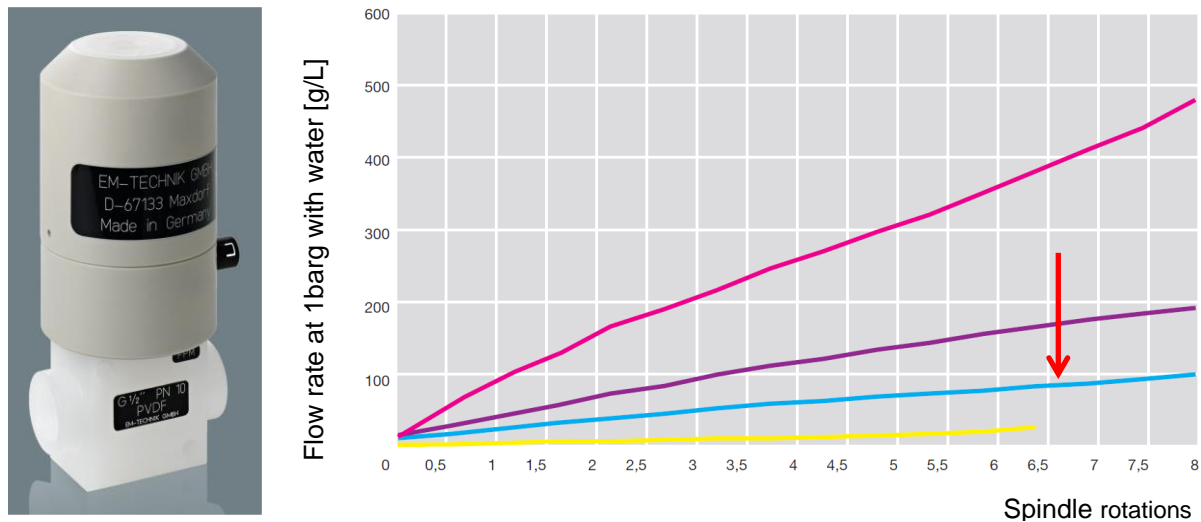
Figure 40: TMP-Control Valve: Flow Characteristic Curves [32]

4.7.3 Filtrate and Bleed Control Valves (V12, V13)

To achieve steady state, the flow rates of filtrate and bleed have to be controlled with high accuracy. The desired flow rate of bleed amounts to 0.48 L/h and to 1.44 L/h for filtrate. Since the flow rates of these streams are extremely small, standard control valves are not feasible. Instead, two solenoid membrane micro-valves were provided from Bürkert Contromatic GmbH. The type 6712 valve [42] has an aperture of only 0.4 mm and a flow coefficient K_v of 4 L/h. Its wetted parts are made of PEEK and it is electrically actuated. However, this micro-valve is not capable of continuous flow adjustment, but it can be switched open or closed very quickly. Hence, by altering the switching frequency, a quasi-continuous flow control is possible. That way, extremely low flow rates can be achieved by only opening the micro-valve for a short period of time. The actual flow rates through the valves at different pressures were measured in Chapter 6.1.2.2. The micro-valves are connected to the loop tubing by threads.
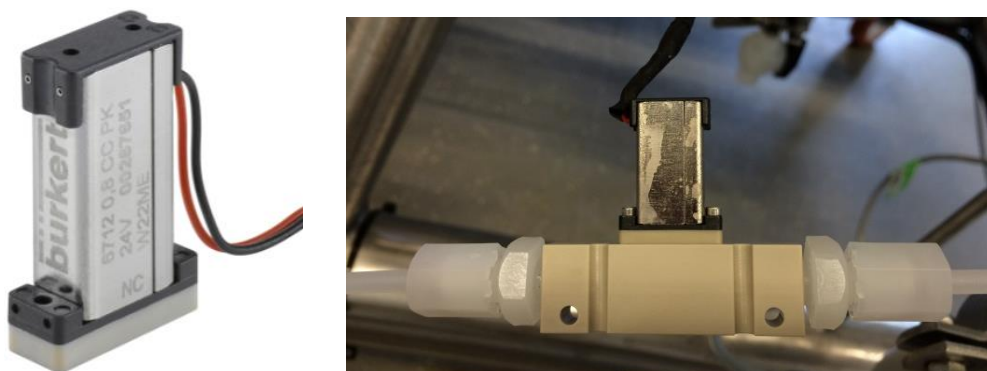
Figure 41: Bürkert GmbH Micro-Valve Types 6712 [42]

4.8   Sensors

4.8.1 Level Switch (LRC 001)

For level control, the Liquiphant M FTL50 level switch from Endress+Hauser GmbH [43] is used. The device consists of a vibrating fork that protrudes into the reactor vessel laterally, as Figure 42 shows. The fork and all other wetted parts of the sensor are made of Hastelloy C-22. In air, the sensor's fork vibrates at its intrinsic frequency, but this frequency is reduced when the fork is immersed in liquid. Such a change in frequency causes the level sensor's signal to switch.

Compared to other commercially used methods of level measurement (optical-, radar- or ultrasonic techniques as well as floats) that offer the possibility to continuously monitor the level, the chosen device is only capable of point level detection. However, these other devices would have had to be installed at the top of the reactor, which is impossible for the pilot reactor due to lack of space on the lid. By contrast, the vibrating fork sensor can be mounted laterally, too. Furthermore, the vibrating-fork method is especially advantageous for airlift reactors since its function is not affected by bubbles or foam.
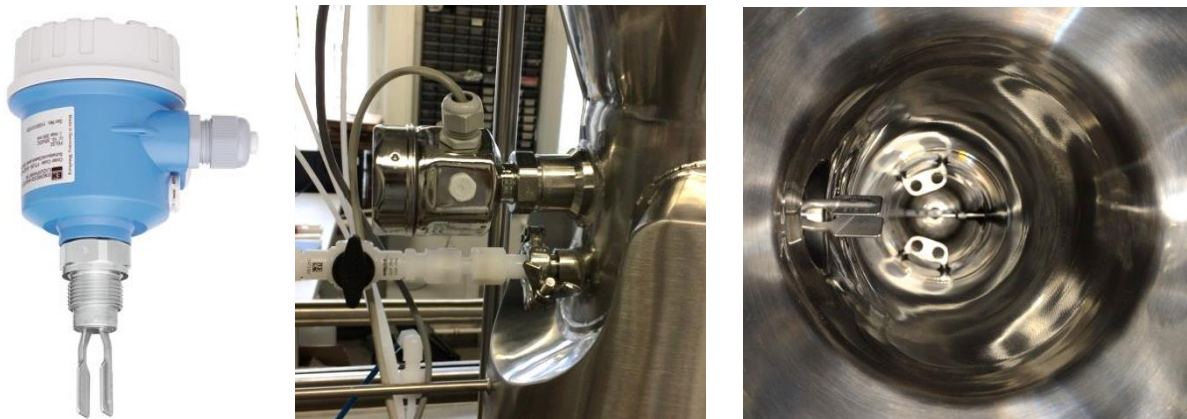
Figure 42: Liquiphant M FTL50 by Endress+Hauser GmbH [43]

The switch point of the Liquiphant M FTL50 level sensor lies approximately 4 mm above the centre plane of the fork when mounted from the side, as Figure 43 indicates:
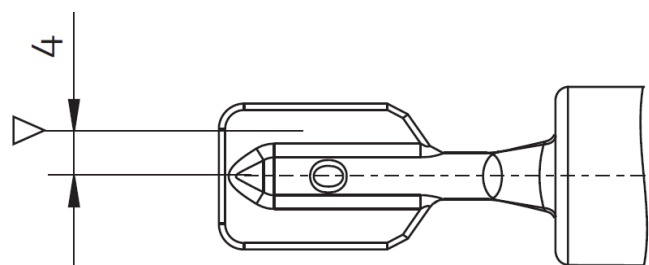
Figure 43: Switch Point of Level Switch [43]

The repeatability of the level switch is 0.1 mm. However, the switching hysteresis amounts to approximately 2 mm. This height difference corresponds to a fluid volume of 28.4 mL in the reactor tube, which is about 2‰ of the total reactor volume. Thus, the inherent inaccuracy is sufficiently small for the pilot process. Figure 44 shows the level sensor immersed in the broth during the test fermentation.

Figure 44: Level Switch in the Broth

4.8.2 Dissolved Oxygen Sensors (QIRC 002, QIRC 011)

To measure the dissolved oxygen concentration inside the reactor vessel as well as in the cell retention loop, two optical VisiFerm DO Arc-sensors were bought from Hamilton Bonaduz AG. Their measurement principle is oxygen dependent luminescence quenching. The interchangeable cap at the sensor tip (see Figure 45) contains the luminophore, the sensory element, which is slowly consumed during the probes operating life. An advantage of this sensor is that no external signal transmitter is required, since one is built into the probe.

Figure 45: VisiFerm DO Arc Sensor & ODO Cap from Hamilton AG [44]

Due to cost reasons, Hastelloy C-22 could not be used as sensor material. Instead, the probes had to be made of stainless steel, which is not fully corrosion resistant to NaCl-solutions. A Hamilton probe made of stainless steel type 1.4435 has been successfully used in halophilic bioprocessing at the department of bioprocess engineering for several years without severe signs of corrosion.

To determine the suitability of stainless steel DO-sensors, the corrosion resistance of two probes made of the alloys 1.4404 and 1.4435 was tested with culture medium for the halophiles-process, containing 20% salt. According to resistance tables [45], both materials are sufficiently resistant to uniform corrosion at low temperatures, but prone to pitting in NaCl-solutions. In the experiment, both probes were placed in flow cells (see Chapter 4.2.2) and then culture medium at 50°C steadily flew through the cells, wetting the sensor cap. After 3 days of exposure, the probes were removed and inspected for signs of corrosion. While pitting corrosion could be observed on the cap of the 1.4404 sensor (see red marks on the right side of Figure 46), no visible corrosion could be detected on the 1.4435 one. Therefore, a VisiFerm probe made of the stainless steel 1.4435 was chosen for the pilot plant. But it has to be minded that this probe could still be affected by pitting after longer exposure to the medium. However, since the sensor cap is interchangeable, slight corrosion is acceptable.
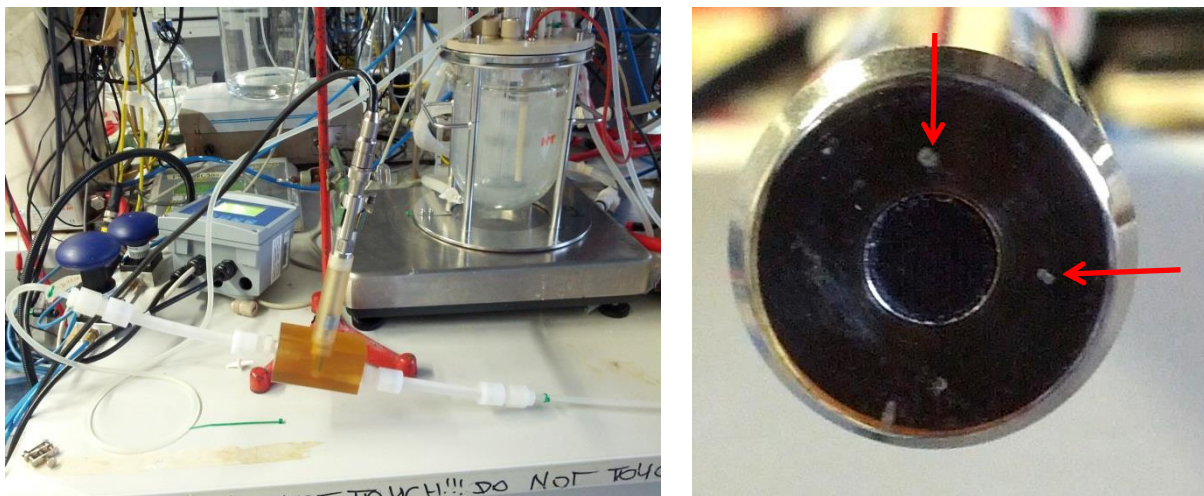
Figure 46: Corrosion Resistance Test for DO-Sensors

One DO-sensor (QIRC 002) is placed in a PVDF-insertion housing and connected to the reactor vessel by an Ingold-nozzle (see Figure 47, right). The second one is installed in the cell retention loop by a flow cell. To connect these DO-probes to the signal interface of the PCS, a Siemens S7-300 automation system (Siemens AG, Austria), two isolation amplifiers had to be bought because the internal pulse width modulation of the sensors interferes with the hardware. The isolation amplifiers are installed in the switchboard.

4.8.3 Temperature sensor (TIRC 003)

To measure the temperature of the broth inside the reactor vessel, the Omnigrad S TR88 resistance thermometer (PT-100) from Endress+Hauser GmbH is used [46]. It is already equipped with a transmitter and calibrated between 0 and 60°C by the manufacturer. The thermometer is placed in a measuring sleeve that protrudes into the reactor vessel laterally (inside view see Figure 24).
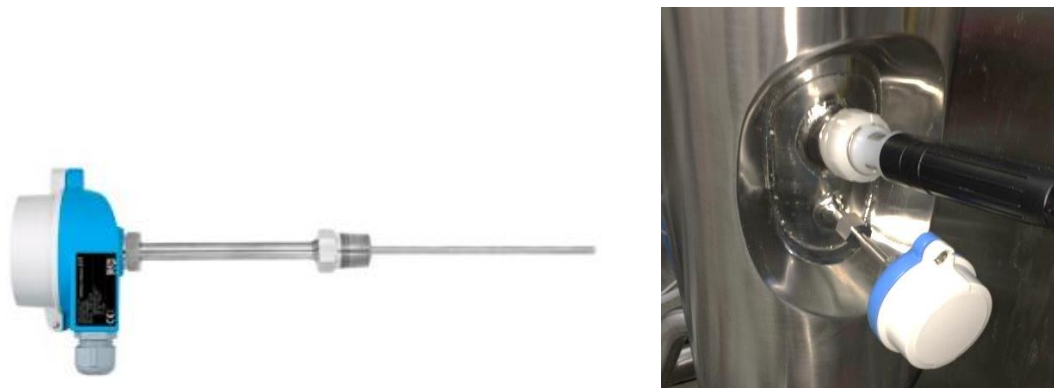
Figure 47: Omnigrad S TR88 Thermometer from Endress+Hauser GmbH [46]

4.8.4 Pressure Sensors (PIRC 005-008)

Four pressure sensors are required for the plant. One is installed on the reactor lid to measure the reactor pressure and the other three are placed in the loop for TMP-determination. Four Signet 2450 pressure sensors were bought from Georg Fischer Rohrleitungssysteme GmbH [47]. They have a PVDF body as well as a ceramic diaphragm for superior compatibility in corrosive liquids and are calibrated between 0 and 3.4 barg by the manufacturer. The sensors are connected to the plant by external threads. However, since the thread types of the pressure sensors are not compatible with EM-Technik GmbH tubing parts, custom made PVDF-adapter pieces had to be made.

Pressure Sensor

Adapter piece

T-pieces by EM-Technik
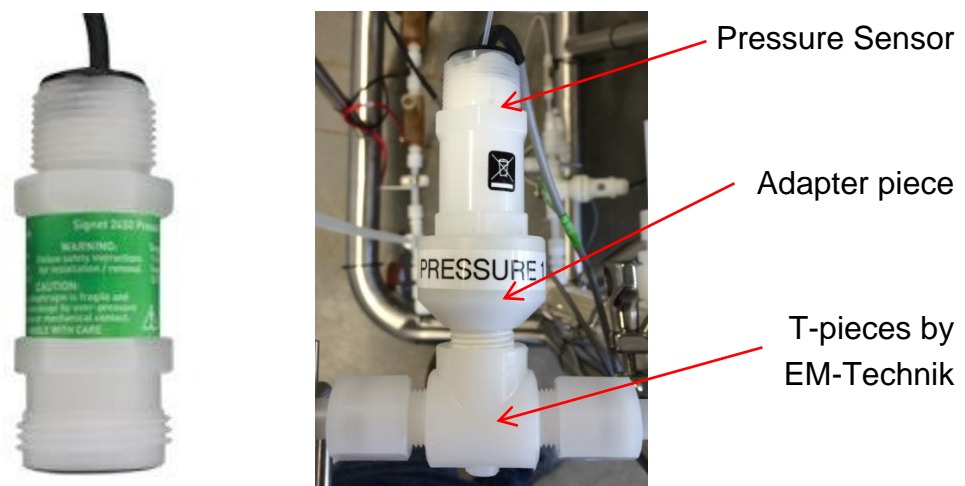
Figure 48: Signet 2450 Pressure Sensors by Georg Fischer GmbH [42]

4.8.5 pH-Probe (QIRC 009)

To measure the pH-value of the broth, an InPro3250i pH-electrode from Mettler Toledo GmbH is used [33]. It is a liquid electrolyte glass membrane electrode and is resistant to pressures up to 4 barg. Furthermore, this sensor can simultaneously measure the temperature of the fluid and is thus used to quantify the temperature in the loop (TIRC 010). To create proportional pH- and temperature signals for the process control system, a transmitter is necessary. For this purpose, a Mettler Toledo M400 multi-parameter transmitter is used. The pH-probe is placed in the cell retention loop by a flow cell and the transmitter is integrated into the switchboard on the reactor rack. In addition, the transmitter unit displays the current pH- and temperature values, as Figure 49 shows.

Figure 49: pH-Probe in Loop and pH-Transmitter in Switchboard

4.9   Off-gas Cooler (W2)

Offers for an off-gas cooler according to the requirements stated in Chapter 3.5.5 were obtained. The most promising quote was a PVDF tube bundle condenser from the German company Polytetra GmbH. A picture of plastic heat exchangers from Polytetra is shown in Figure 50. However, due to the high costs of such a device, it was decided to operate the pilot plant without an off-gas cooler first and measure the actual humidity of the gas. Thereby, the calculated heat transfer area of 0.135 m² calculated in Chapter 3.5.5 could possibly be further reduced if the off-gas is less humid than estimated. That way, a smaller and hence cheaper cooler would be feasible.

Figure 50: Plastic Tube Bundle Heat Exchanger from Polytetra GmbH [48]

4.10   Storage Tanks

As described in Chapter 3.5.1, the preliminarily planned storage tank volume for feed and filtrate (B3, B4) was enlarged from 50 to 200 L so that the plant can be operated autonomously for up to 4 days. Yet, for initial operation of the pilot plant, two 50 L bottles made of PP (see Figure 52) were bought for storage of feed and filtrate. Once a stable bioprocess is achieved, they will be replaced by 200 L tanks, for example by KAISER+KRAFT GmbH. One of the 50 L bottles can then be utilized as bleed storage tank (B5). Glass bottles from the equipment stock of the department of bioprocess engineering are used for the smaller acid and base tanks.

Figure 51: 200 L Storage Tank by KAISER+KRAFT GmbH [49]

4.11   Balances

To measure the weight of the feed and filtrate tanks (WIRC 012, WIRC 015), two balances with a maximum load of 300 kg were bought from the Austrian company Bloderer GmbH. They are large enough to house the 200 L storage tanks from KAISER+KRAFT GmbH (see Figure 51). However, compared to smaller laboratory scale balances, which usually have an accuracy of ±0.1 g, the highest possible readability of balances that size is ±2 g. Due to cost reasons, the accuracy of the selected balances from Bloderer GmbH was even reduced to ±10 g. This lower measurement resolution affects the flow control by increasing its response time. All

other balances required for the pilot plant (for acid, base and bleed) are taken from the equipment stock of the department of bioprocess engineering at Vienna University of Technology.

Figure 52: 300 kg Balances for Feed and Filtrate with 50 L Bottles

4.12   Mixing Tank

To produce 200 L culture medium at once, a separate mixing tank made of polyethylene was bought from Schwarzer Rührtechnik GmbH [50]. It is equipped with a PE-agitator and placed on a wheeled rack. In the mixing tank the medium can be blended, rolled to the 200 L feed tank and then transferred into it by a peristaltic pump.

Figure 53: Mixing Tank for Feed by Schwarzer Rührtechnik GmbH [50]

5 Installation Phase

After all components had been bought, the pilot plant was assembled and prepared for the subsequent integrity and functionality test of the equipment. First, the pumps and the membrane cartridge were installed. Next, the tubing of the cell retention loop was put together from the EM-Technik GmbH parts. Then, supports for the piping were welded to the frame of the rack (see Figure 56). Finally, the electronic devices (sensors, pumps, control valves) were connected to the switchboard for power supply and control signal transmission. From there, the control signals were connected to the process control system of the department of bioprocess engineering at Vienna University of Technology.

5.1 Assemblage

The pilot plant consists of two main parts, the reactor skid and the media skid. The reactor skid - the wheeled rack - contains the airlift reactor, cell retention loop, the pumps, membrane module and probes as well as the switchboard. The media skid is stationary and consists of a table on which the storage tanks for all media (feed, filtrate, bleed, acid and base) and the corresponding balances are placed.

5.1.1 Reactor Skid

The fully assembled reactor skid is depicted in Figure 54. The left side shows the accessible front view of the plant. From this side, the control buttons on the switchboard can be operated and the reactor interior can be inspected via the gage glass on the lid. The right side of Figure 54 shows the back view of the plant, which is not accessible during operation. From this side, the dosing pumps for feed, acid and base can be manually controlled, which should not be necessary at normal use. Figure 55 shows the top view of the reactor lid and the assignment of the ports.

Figure 54: Reactor Skid: Front View (left) and Back View (right)
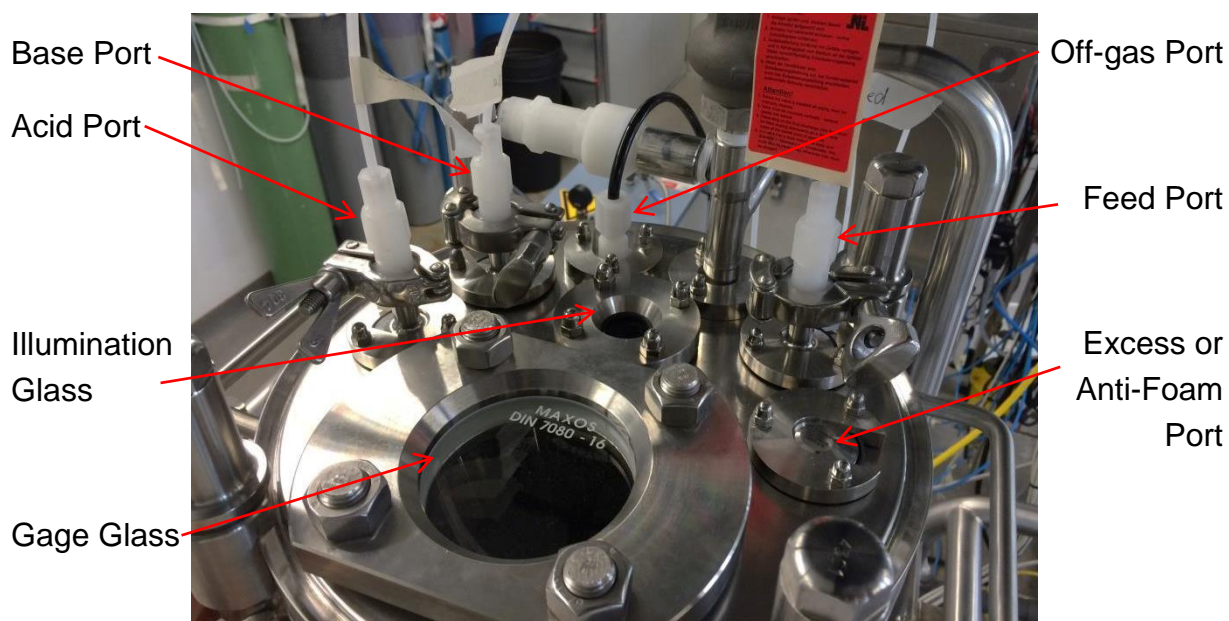
Figure 55: Reactor Skid: Top view (left) and Assignment of the Ports

5.1.1.1 Assemblage of the Cell Retention Loop

The fully assembled tubing of the cell retention loop is depicted in Figure 56. All manual valves in the loop (sampling-, bypass- and shut-off valves) as well as the loop pump are accessible from the lefthand side of the plant. The cell retention loop runs on two levels that are separated by the vertically installed membrane cartridge. For drainage, both levels of the loop are slightly inclined. The upper level is tilted downwards, but the lower had to be inclined upwards because of the flow cells. For this reason, an additional drainage port had to be installed at the lowest point of the loop tubing. However, due to the upward inclination of the lower level of the loop, gas bubbles are forced to leave the loop tubing and cannot accumulate at bottlenecks. This is beneficial because air pads inside the flow cells could interfere with the measurement.
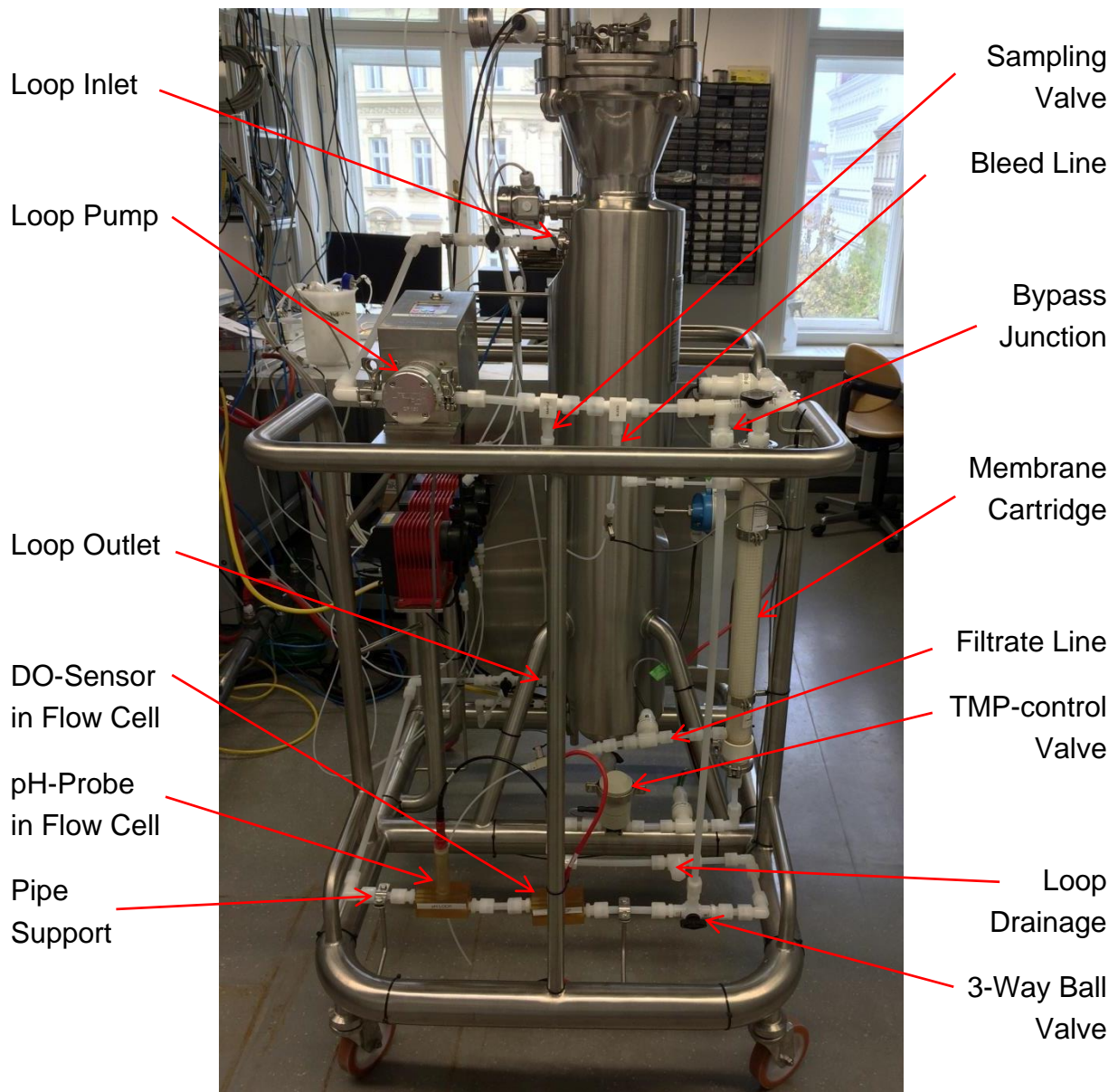
Figure 56: Reactor Skid: Lefthand View with Cell Retention Tubing

5.1.2 Media Skid

The media skid is stationary and contains all storage tanks and corresponding balances. For this purpose a laboratory table is used. On the tabletop, the smaller balances and tanks for acid, base and bleed are placed (Figure 57, left), while the large 300 kg scales and tanks for feed and filtrate are positioned below the table (Figure 57, right).
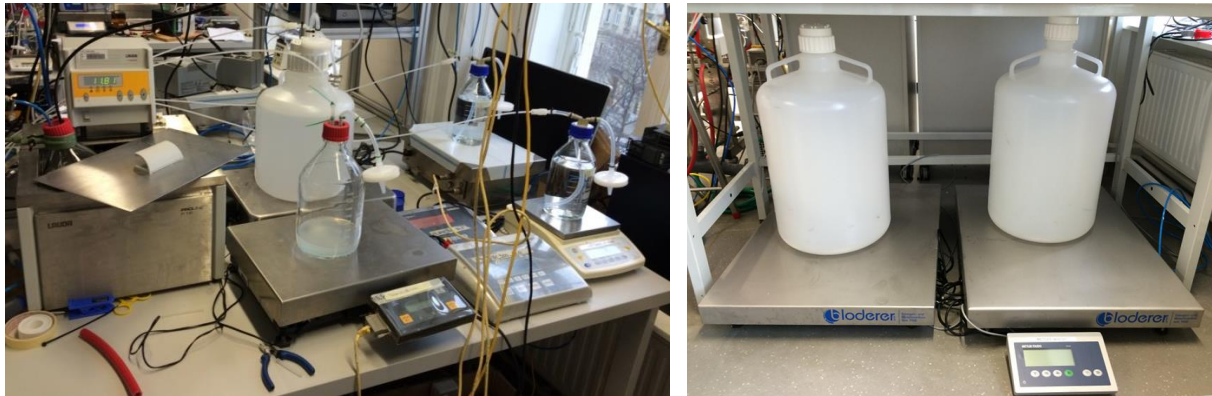
Figure 57: Media Skid: Upper Level (left) and Lower Level (right)

5.2 Electrical Installation

The last step of the installation phase was the electrical connection of the equipment. All electronic devices on the reactor skid (sensors, pumps, control valves) were connected to the switchboard for power supply and control signal transmission while the balances (media skid) were externally powered and connected to the PCS.
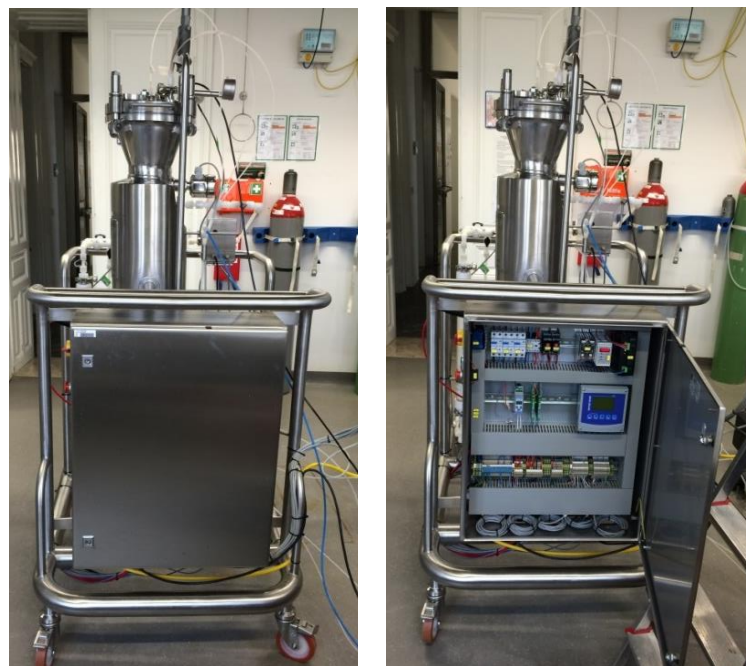
Figure 58: Position of the Switchboard on the Reactor Skid (Righthand view)

The switchboard itself is powered by connection to a 230 V AC electric socket and is positioned on the righthand side of the reactor skid (Figure 58), which is not accessible during operation for safety reasons. Therefore, the switches and buttons of the switchboard are placed on its side, the front side of the plant. The switchboard has a main and a kill switch for power supply of the linked equipment as well as buttons for activating/deactivating the internal 230 V AC power supply. Their arrangement is indicated in Figure 59. The interior of the switchboard in as-delivered condition is shown on the left side of Figure 60. The right side illustrates the cable installation in progress.

Figure 59: Switches and Buttons and the Switchboard
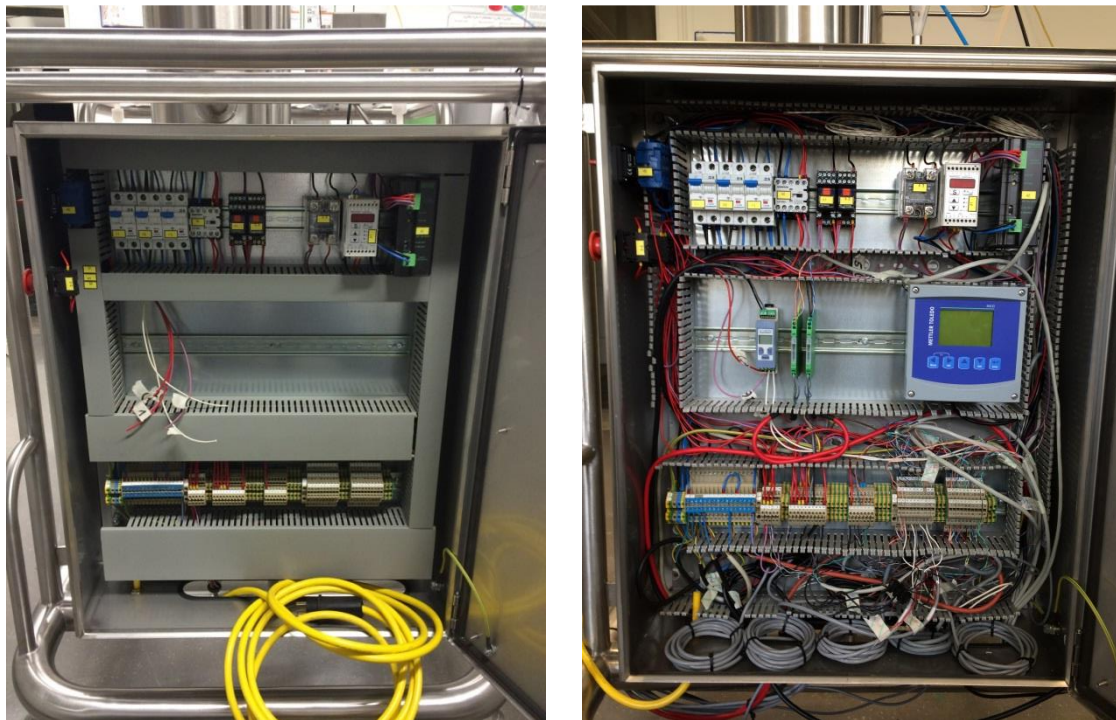
Figure 60: Switchboard: As-delivered (left) and in Progress (right)

Inside the switchboard, the electronic devices are connected to either the 230 V AC (pumps, heating pad) or the 24 V DC (sensors, control valves) internal power supply. Furthermore, all control signal lines are collected in terminal blocks. From there, the control signals are connected to the signal interfaces of the process control system. The department of bioprocess engineering uses the process control system Lucullus with the Siemens S7-300 automation system (Siemens AG, Austria) as well as terminal blocks from WAGO (WAGO Kontakttechnik GmbH, Austria) as signal interfaces (hardware).

The following four signal types are used for process automation:

- **Analogue Inputs:** (4-20 mA, 0-10 V) are utilized to retrieve the measuring signals of the sensors (DO, temperature, pressure and pH).
- **Analogue Outputs:** (4-20 mA, 0-10 V) are used to control the capacities of the loop and feed pump as well as the aperture of the control valves (TMP-control valve and pressure control valve). Furthermore, the MFC and heating pad are regulated by analogue outputs.
- **Digital Inputs:** are utilized for retrieving the signal of the level switch.
- **Digital Outputs:** are used to switch the acid and base pumps on/off when needed as well as to open or close the intermittent filtrate and bleed valves for flow control.

The housing of the switchboard has three top-hat rails onto which the electronic parts are attached. The upper rail contains the fuses, relays, the temperature control unit and the voltage converter for the internal 24 V DC power supply. The middle level is used for installation of external components, in this case, the control electronics for the pressure control valve, the isolation amplifiers for the DO-sensors as well as the transmitter for the pH-probe. The lowest top-hat rail contains the terminal blocks for the 230 V AC supply, 24 V DC supply as well as for the control signals.

The temperature control unit, which was implemented by the plant manufacturer, was originally decoupled from the process control system. It receives an analogue signal and adjusts the reactor temperature to the target value by controlling the heating pad. The setpoint can only be entered manually on the unit's interface. In the as-delivered configuration of the plant, the signal of a temperature probe positioned in the heating jacket was used as input for the control unit. However, since the temperature inside the jacket does not correspond to the actual temperature of the broth but is about 4 to 5°C higher, this setup had to be modified. For the new approach, the temperature control unit was connected to the PCS instead of the sensor inside the heating mantle. The PCS sends an analogue output signal, which equals the reactor temperature measured by the sensor TIRC 003 in the vessel, to the control unit that in turn regulates the heating pad. That way, the actual temperature of the fluid inside the reactor can be adjusted to the set value, which has to be entered manually on the

unit's interface. However, when using this method, the plant cannot be operated without the PCS. Also a system failure or an unexpected breakdown of the PCS-connection can cause a malfunction of the temperature control.

The fully assembled interior of the switchboard with description of all built-in components is shown in Figure 61.
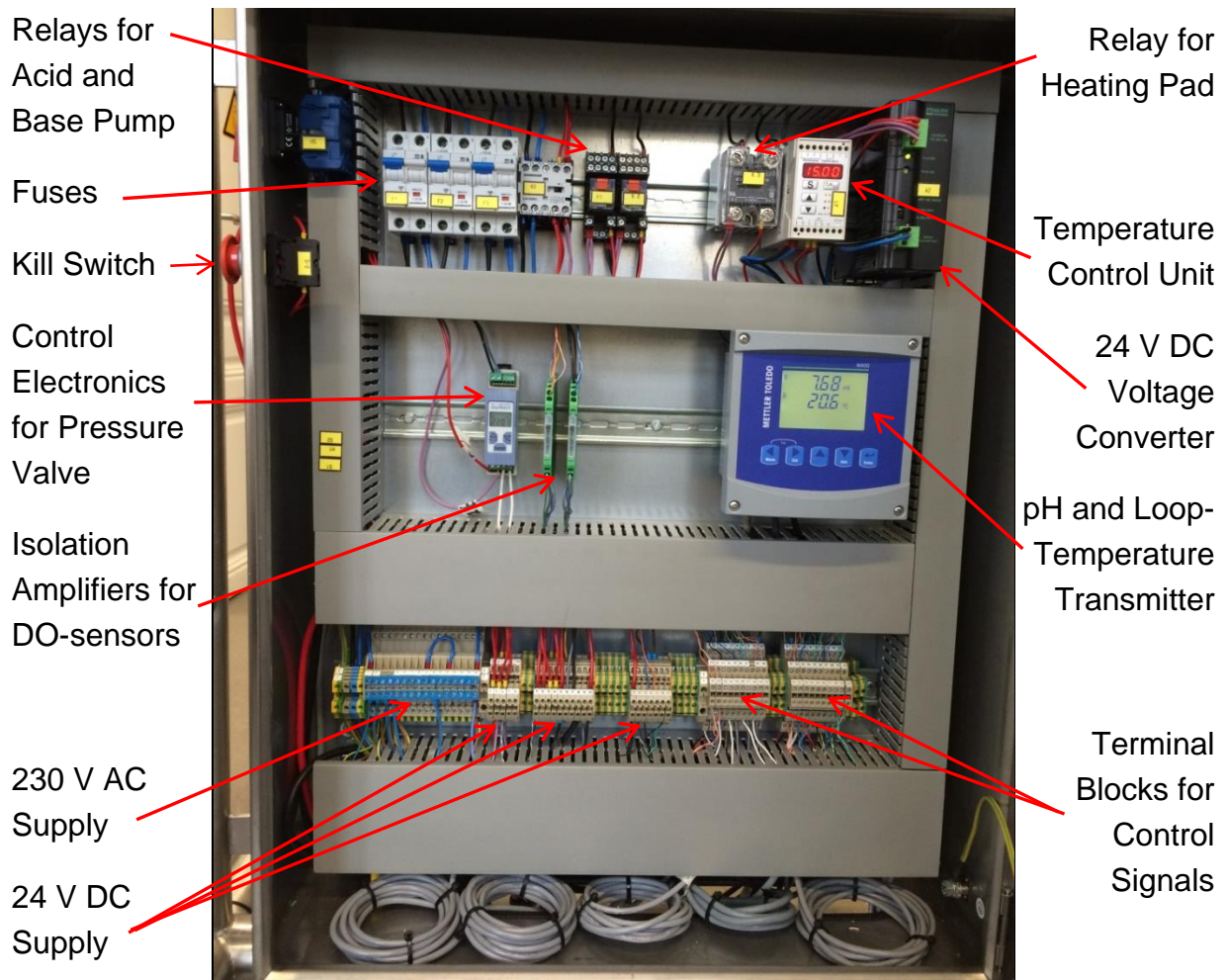
Figure 61: Interior of the Switchboard

The circuit diagram of the switchboard can be found in Appendix 6. It contains a detailed construction drawing of the fully assembled switchboard as well as the plug-in positions of the power and signal lines in the terminal blocks of the switchboard. The corresponding plug-in positions in the signal interfaces (Siemens and WAGO boxes) as well as channel assignment in Lucullus are listed in a folder in the laboratory of the department of bioprocess engineering.

6 Test Phase

After the system had been completely assembled, several tests were performed to show the operability of the whole installation and that the components could withstand the conditions occurring during operation, especially the pressure and the salinity of the media. For this purpose, integrity and functionality tests as well as test fermentations in batch and continuous mode were executed.

6.1 Methods

6.1.1 Integrity Tests

During the integrity tests, the pressure resistance and the tightness of the connections were examined at the plant's maximum allowable pressure of 3 barg and maximum temperature of 50°C. The reactor and the loop were filled with water via the excess port on the lid. Then, the loop pump (P4) was switched on and adjusted to maximum power. Next, the reactor was gassed with compressed air. To increase the pressure in the system, the proportional opening of the pressure control valve (V3) was reduced until the maximum pressure of 3 barg was indicated at the manometer on the reactor lid (PI 004). Then, the tightness of the connections was examined after 2 h of exposure to the maximum operating conditions.

6.1.2 Functionality Tests

After the integrity tests, three functionality tests were performed on the completely assembled plant. These experiments were necessary to obtain control characteristics for the subsequent test fermentations. The tests were performed with tap water and the loop setup according to the PFD in Appendix 2.

6.1.2.1 Control Characteristics of the Pressure Control Valve

To test the functionality of the pressure control valve and to demonstrate that the reactor pressure can be adjusted to a requested value, the course of the reactor pressure at decreasing valve aperture was measured at a constant gassing rate of 5 L/min.

6.1.2.2 Flow Rate Calculation of the Bleed/Filtrate Valves

This test was used to determine the flow rate through the intermittent valves for bleed and filtrate at different pressures and to find out if the micro-valves are feasible to control the small flow rates of the bleed (0.48 L/h) and filtrate stream (1.44 L/h) by intermittent opening. The valve was mounted at the lower level of the loop, resulting in a hydrostatic pressure of approximately 0.12 bar when the reactor was filled to the 15 L mark. The flow rate through the valve was measured gravimetrically at three different pressure setpoints.

6.1.2.3 Membrane Test

To test the operability of the membrane module and the suitability of the Bürkert GmbH micro-valves for filtrate flow control, the TMP and the flux rate were determined at different filtrate valve setups. The test was executed at a gassing rate 5 L/min, resulting in a reactor pressure 0.166 barg, as well as with a loop pump capacity of 40% (about 85 L/h). The transmembrane pressure was calculated from the measured pressures in the loop according to Eq. 9. The filtrate's flow rate was measured gravimetrically. Furthermore, the volume of the cell retention loop was measured to determine the total working volume of the plant.

6.1.3 Test Fermentations

The target of these experiments was to demonstrate the operability of the plant by cultivating a halophilic microorganism in the reactor and to show the functionality of the corresponding control devices. First, a batch fermentation was executed to quickly generate biomass. Then, the grown culture was utilized in a continuous fermentation with cell retention to increase the biomass concentration.

The halophilic organism *Halomonas sp.* (MA-C) was chosen for the test runs. The cultivation conditions for this strain are specified in Table 10:

Table 10: Cultivation Conditions for *Halomonas sp.* (MA-C)

Strain	*Halomonas sp.* MA-C (DSM No. 7328) [51]
pH-Value	7
Temperature	30°C
Medium	Defined, composition see Table 11

For the test fermentations, the whole setup as shown in the PFD in Appendix 2 was used, except for the TMP-control valve (V10). Balances with an accuracy of 0.1 g were used to monitor the flows of feed, acid, base, filtrate and bleed.

Furthermore, since the off-gas cooler had not been chosen at the time of the experiments, an improvised cooler (Figure 62, left) was used instead. To simulate the functionality of a Liebig-cooler, the off-gas was passed through a 2 L Schott-bottle which lay in a water bath cooled down to 10°C. This setup also provided an additional safety barrier against flooding and contamination of the off-gas analyser by foam. During fermentation, foam that accidentally passed through the off-gas line could be separated in the bottle. Another advantage of this setup was the possibility to quantize the condensate separated in the bottle gravimetrically.

Two different control approaches were programmed in Lucullus for the two fermentations. They mainly differ in the level control and are presented in Chapters 6.1.3.6 and 6.1.3.7. Both are simplified versions of the full control approach introduced in Chapter 3.4.3.
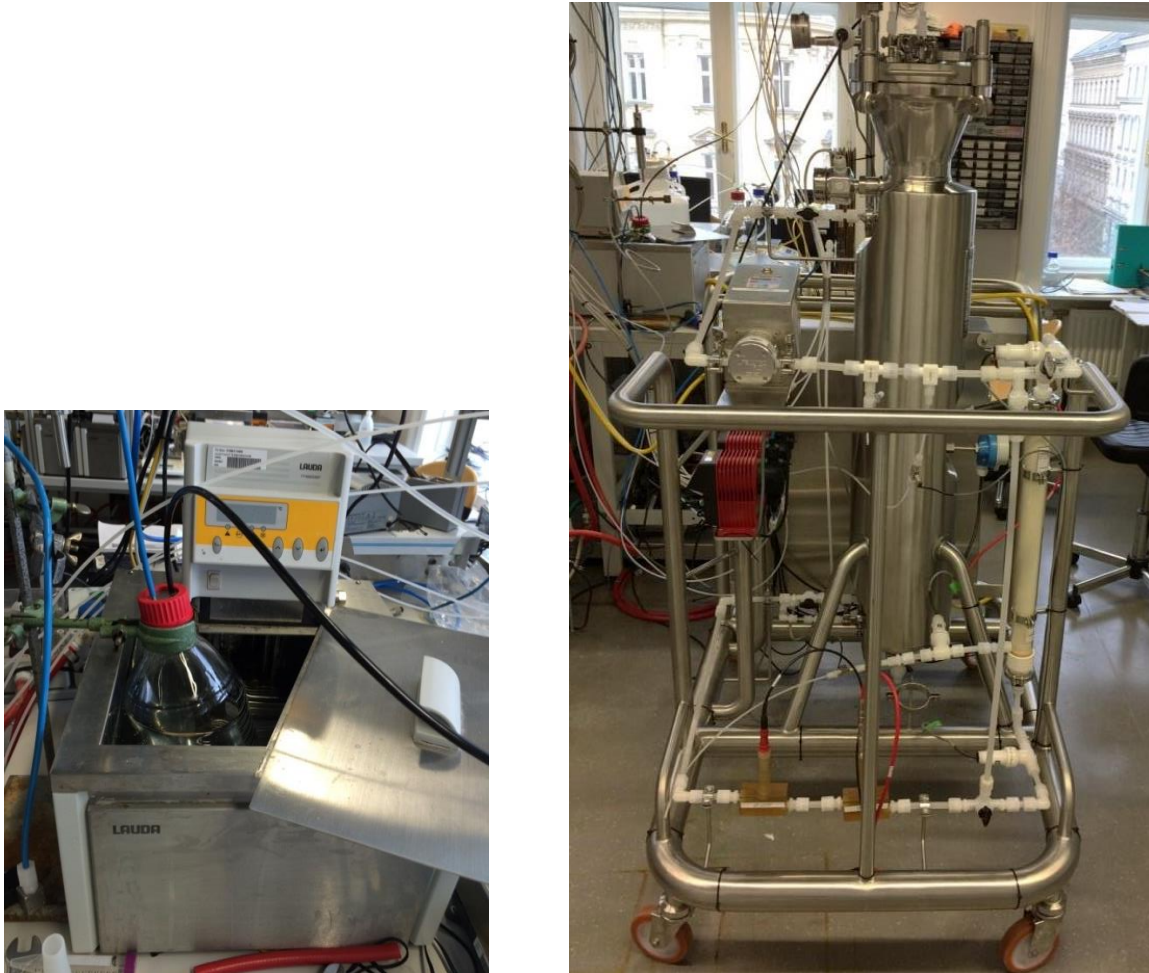
Figure 62: Improvised Off-gas Cooler (left) and Test Fermentation Setup (right)

6.1.3.1 Media Preparation

The composition as indicated in Table 11 was used as culture medium in the batch process and as feed in the continuous fermentation. Moreover, it was utilized for level control in both experiments to maintain a constant liquid level. By adding hydrochloric acid after dissolving all the ingredients in demineralized water, the pH-value of the medium was set to 7. The composition of the trace elements stock solution that was added to the culture medium is shown in Table 12. For pH-control, each 1 L of 0.5 molar hydrochloric acid and sodium hydroxide were prepared. The media had not been autoclaved before use.

Table 11: Defined Media Composition

Substance	Concentration in Demineralized Water
NaCl	100 g/L
NH_4Cl	1.5 g/L
Na_2HPO_4	0.5 g/L
$MgCl_2$ x 6 H_2O	10 g/L
KCl	1 g/L
Na_2SO_4	0.5 g/L
$Na(CH_3COO)$	5.6 g/L
Trace Elements	2.5 mL/L

Table 12: Trace Elements Stock Solution Composition

Substance	Concentration in Demineralized Water
$CoCl_2$ x 6 H_2O	0.5 g/L
$MnCl_2$ x 4 H_2O	3 g/L
$CuCl_2$ x 2 H_2O	0.24 g/L
H_3BO_3	0.6 g/L
Na_2MoO_4 x 2 H_2O	0.5 g/L

6.1.3.2 Inoculum

To prepare the inoculum for the test runs, approximately 100 mL of the bleed of an ongoing continuous fermentation of *Halomonas sp.* (MA-C) was harvested one day before the start of the experiment. It was transferred into the lab-scale bioreactor for halophiles, filled up to 1 L with complex media (composition see Table 13) and cultivated in a batch process, using the conditions shown in Table 10.

Table 13: Complex Medium Composition

Substance	Concentration in Demineralized Water
NaCl	100 g/L
$MgCl_2$ x 6 H_2O	10 g/L
KCl	1 g/L
Na_2SO_4	0.5 g/L
Yeast extract	5 g/L
Tryptone	2.5 mL/L

Although a mistake was made during the preparation of the complex medium by only adding 10 g/L NaCl instead of the prescribed 100 g/L according to Table 13, the biomass concentration of the preculture rose to 4 g/L overnight. This was possible because *Halomonas sp.* (MA-C) is a halotolerant, and not solely halophilic, organism. Figure 63 shows the 1 L lab-scale bioreactor used for the cultivation of the preculture:

Figure 63: Cultivation of the Inoculum in the 1L Lab-scale Bioreactor

6.1.3.3 Sanitization

Although a sterile environment is not necessary for the used halophilic strain, the reactor had to be cleaned and sanitized before usage, e.g. of dust and other contaminants from fabrication. As the reactor is not capable of being autoclaved, it was sanitized by flushing with hot sodium hydroxide solution instead. Since the membrane is allowed to be washed with maximally 0.5 molar NaOH-solution at 50°C, these two parameters were used for sanitization. The limits of use for all equipment parts can be found in the stock list in Appendix 4.

First, the reactor vessel and loop tubing were rinsed with tap water. Then, both were filled with cold 0.5 molar sodium hydroxide solution and the loop pump was started to achieve liquid circulation through the piping and the membrane cartridge. Then, the temperature of the cleaning agent was increased by means of the reactor's heating pad, which is regulated by the control unit in the switchboard. Once the set temperature of 50°C had been reached, the system was flushed for one hour. In the meantime, the three dosing pumps were sanitized with NaOH-solution, too. After one hour of exposure, the whole system was drained from the base and flushed twice with demineralized water to remove the last residues of the base. The dosing pumps were rinsed with it as well.

6.1.3.4 Calibration of the Sensors

To ensure the comparability of the measurement results, the DO-sensors, pH-probe and the off-gas analyser had to be calibrated before starting the operation. The temperature and pressure probes were already pre-calibrated by their manufacturers.

- **pH-Probe:** was calibrated with two reference solutions with defined pH-values of 4 and 7 using the transmitter inside the switchboard.
- **DO-Sensors:** were calibrated in the culture medium by gassing the reactor with nitrogen (0% DO) and air (100% DO). The calibration was performed at 30°C reactor temperature and 0.5 barg pressure for both gases. The gassing rate of the compressed air was 7.5 L/min (0.5 vvm)
- **Off-gas Analyser:** (Blue Sens GA 4, DASGIP AG, Germany) was calibrated with air and a reference gas with defined composition, consisting of N_2 with an O_2-content of 16% and a CO_2-concentration of 9%.

6.1.3.5 Offline-Sampling

During fermentation samples of 5 mL were taken every 3 hours during the workday, none overnight. Two assays were performed:

- **Biomass Concentration:** was determined by triple measurement of the samples' optical density (OD) at a wavelength of 600 nm. The mean value was then converted to a biomass concentration in g/L by using the following empirical equation:

$$x\ [g/L] = 0.6399 * OD \qquad \text{Eq. 17}$$

- **Substrate Concentration:** was measured by HPLC-analysis of the acetate concentration of the offline-samples, the feed as well as the filtrate from the continuous fermentation. The biomass had to be removed from the samples. After separation in a refrigerated centrifuge (10 min, 14.000 rpm), the supernatant was filtered and filled in HPLC-measuring cups for analysis. The samples were stored at 4°C until analysis.

6.1.3.6 Batch Fermentation

The targets of the batch fermentation were as follows:

1. Increasing the biomass concentration in the reactor.
2. Testing the pH- and temperature control as well as optimizing them until a temperature deviation of ±0.2°C and a pH-deviation of ±0.05 from the setpoints can be achieved. These values are specified in Table 3.
3. Investigating the effect on the dissolved oxygen concentration by pressurizing the reactor and if the oxygen is limited in the loop.
4. Testing the level control approach for batch mode.

5. Testing the improvised off-gas cooler and measuring the humidity of the off-gas by weighing the separated water to find out if a gas cooler is needed.

Setup

The simplified process flow diagram for this test run is illustrated in Figure 64. The cell retention system was not used. For that, the membrane was bypassed by adjusting the shut-off valves (V8, V9) and the 3-way ball valve (V11). The improvised off-gas cooler and balances for monitoring the weight of the feed, bleed, acid and base storage tanks were set up on the media skid. This setup is depicted in Figure 65. Due to the low gassing rate, the whole off-gas could be passed through the off-gas analyser and the two needle-valves (V4, V5; see Appendix 2) for splitting the flow were not needed.
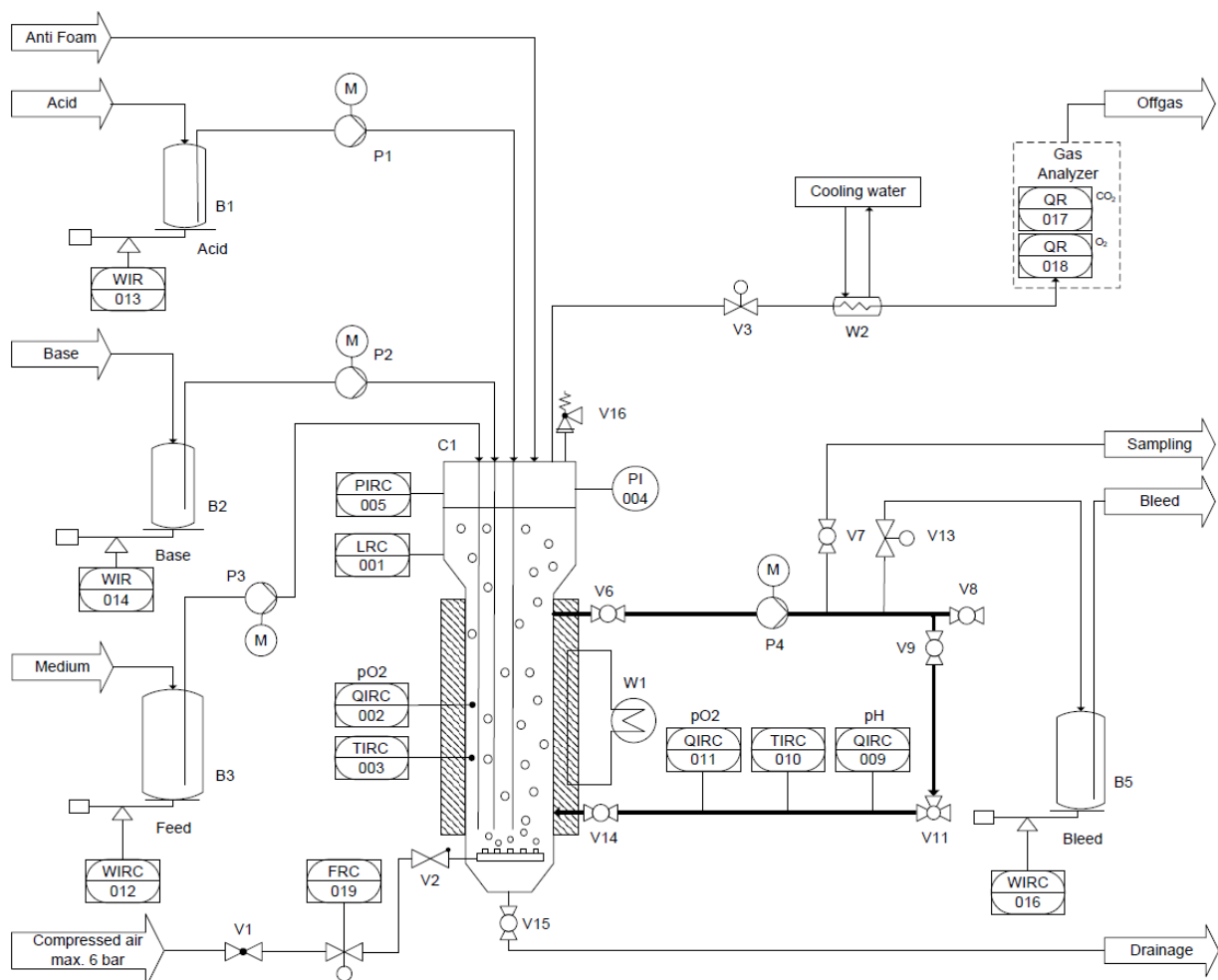
Figure 64: PFD of the Test Fermentation in Batch mode
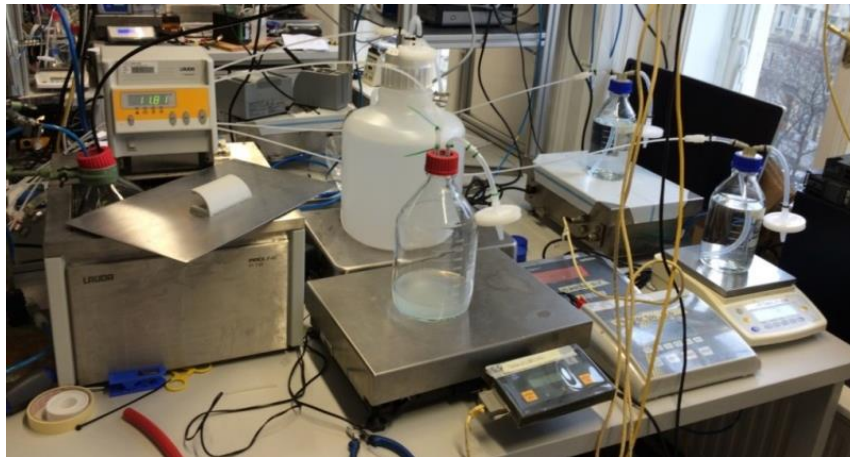
Figure 65: Off-gas Cooler and Media Skid for the Batch Fermentation

Control Approach

For process control, a simplified version of the control approach introduced in Chapter 3.4.3 was programmed in Lucullus. It consists of the following four main control loops:

- **Temperature Control:** was performed by the temperature control unit of the heating pad in the switchboard, which received a proportional 4-20 mA signal from the PCS that corresponded to the temperature signal from the probe (TIRC 003) inside the reactor. The setpoint was entered manually on the controller unit, which was configured as a PID-controller with a single input value. In addition to that, a protection against overtemperature was implemented, which shut down the plant if the reactor temperature exceeded a certain input value, in this test run 50°C.

- **Overpressure Protection:** a protection against unacceptable high pressure was implemented, which fully opened the pressure control valve if the reactor pressure was higher than 2.5 barg.

- **pH-Control:** this circuit consisted of two separate 2-point-control loops, an acid and a base control. Depending on the pH-value, measured by the pH-sensor in the loop, the acid and base dosing pumps were switched on and off at predefined thresholds.

- **Level Control:** was used to keep the liquid level of the broth at constant height, equalling a working volume of 15 L, and thus preventing the reactor and the off-gas tubing from flooding. This circuit consisted of two control loops, namely "level too high" and "level too low". The level was maintained constant by either removing liquid from the system through the bleed valve, or by supplying new medium via the feed pump. Therefore, a timer was

implemented in order to check if the digital signal from the level switch was either on ("level too high" → open bleed valve) or off ("level too low" → start feed pump) after a certain period of time and to start the corresponding countermeasure until the level signal switched again. For this test, a relatively short time interval of 30 min was chosen due to safety reasons. To avoid overshoots of the liquid level, the pump's capacity was adjusted to just 10%.

Operating Conditions

The operating conditions for this test run are listed in Table 14. The aeration rate was set to 0.1 vvm or 1.5 L/min. This rate was chosen because it equals the rate which has been usually used for the current experiments in the 1 L lab-scale reactor. Due to comparability to the small scale process and for safety reasons, the test run was launched without applying overpressure.

Table 14: Batch Fermentation: Operating Conditions

Loop flow	85 L/h (40%)
Aeration rate	1.5 L/min (0,1 vvm)
Pressure	0 barg (initial)
Temperature	30°C
pH-value	7

Procedure

After the reactor had been sanitized, it was filled with approximately 13 L of the culture medium. Then, 1 L inoculum with a biomass concentration of 4 g/L was added. Afterwards, medium was fed until the level switch and thus the nominal reactor volume of 15 L had been reached. Then, the dosing pumps for feed, acid and base were activated and vented. Next, the setpoint of 30°C was entered on the temperature control unit and when the desired temperature had been reached, the control application for the batch process was activated in Lucullus. The measured data was recorded from then on. During the Fermentation, anti-foam (Struktol J671-3) was periodically added via the excess port on the lid.

Once the batch had ended and all substrate had been consumed, the Lucullus operation was stopped and the next experiment, the continuous fermentation, was started several hours later after to the setup had been modified. The grown culture from the batch test was directly used for the continuous fermentation.

6.1.3.7 Continuous Fermentation

The targets of the continuous fermentation were as follows:

- Increasing the biomass concentration in the system by cell retention.
- Testing the flow controllers as well as achieving constant flow rates of feed and filtrate, thus steady state.
- Testing the level control approach for continuous mode.
- Determination of the mass balance as well as calculation of the water loss from the mass balance gap to determine the off-gas humidity and thereby find out if an off-gas cooler is necessary for the process.
- Calculation of the TMP during fermentation and investigation of membrane fouling effects.

Setup

During the continuous fermentation, the microfiltration membrane (F1) was used for cell retention. For this operation mode, the bypass had to be closed with the shut-off valve V9 as well as the 3-way ball valve (V11) so that the whole fluid flew through the filter. The process flow diagram for this test run is illustrated in Figure 66.
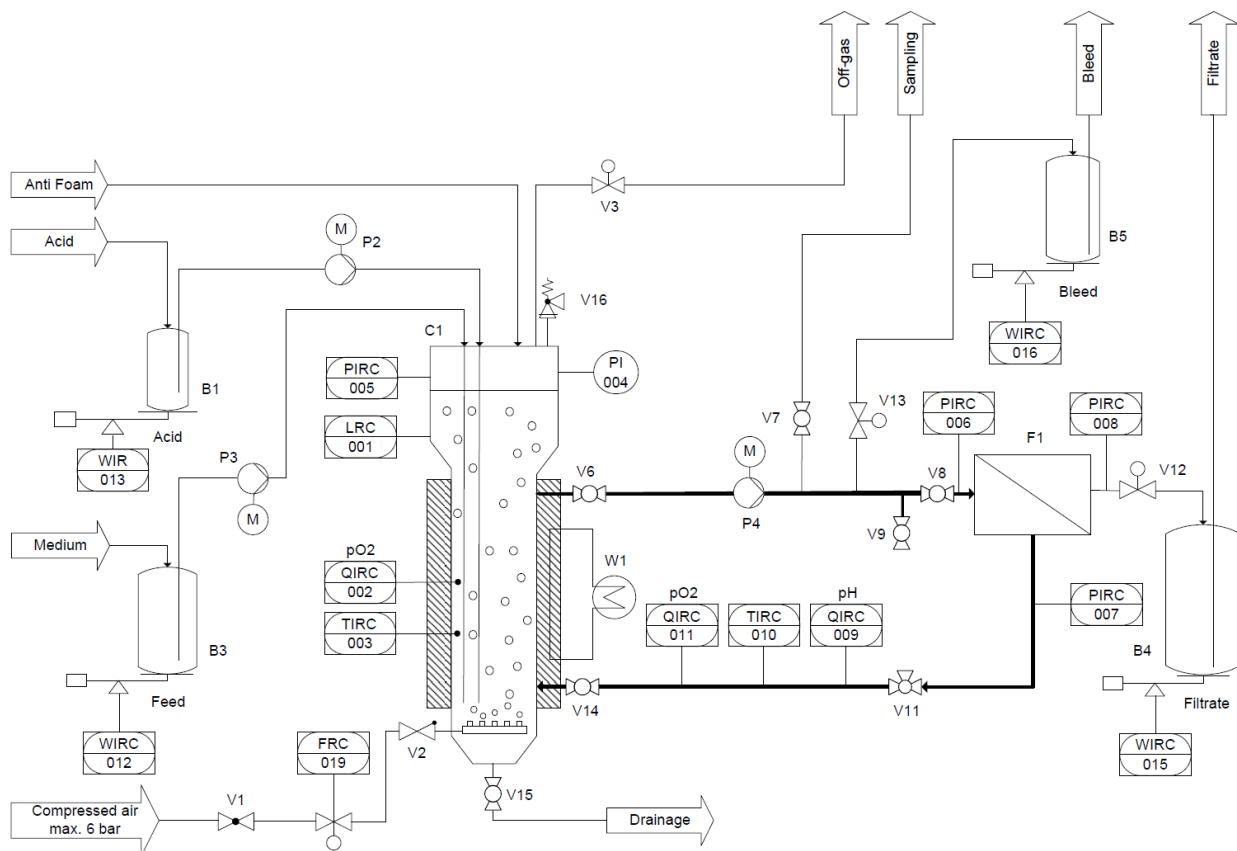
Figure 66: PFD of the Test Fermentation in Continuous Mode

In this test, the weight signals of the feed, acid, bleed and filtrate storage tanks were monitored. Base was not provided since none had been needed during the batch fermentation. The improvised off-gas cooler (see Figure 62) was not used for this test.
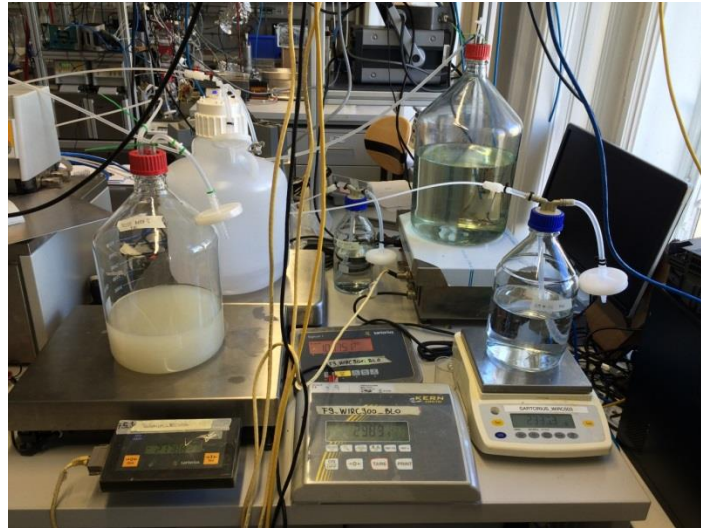
Figure 67: Media Skid for the Continuous Fermentation

Control Approach

For this test, the previously described control approach for the batch fermentation (Chapter 6.1.3.6) was enhanced. In order to achieve constant flows of feed and filtrate, flow controllers were programmed in Lucullus. Furthermore, the level control program was adapted:

- **Flow Control:** was used to calculate the flow rates of feed and filtrate by using the balance signals and to adjust them to the desired value by means of PID-controllers. Two different flow controllers were programmed: the feed flow was regulated by adjusting the dosing pump's capacity, whereas the filtrate flow was controlled by defining the opening time of the intermittent filtrate valve within a certain period, in these experiments 10 s. For example, if the PID-controller adjusted the flow to 30% and the chosen period was 10 s, then the filtrate was only opened for 3 s. The remaining 7 s of the period time it remained closed. That way, the filtrate flow could be quasi-continuously controlled.

- **Continuous Level Control:** Compared to the level control for the batch process, only the control loop "level too low" was altered. This had to be done because during the continuous operation, the feed was flowing constantly, as opposed to the batch fermentation, where it was only used for the level control to increase the level inside the reactor. For this approach, the liquid level had to decrease steadily. This was achieved by setting a slightly larger filtrate than

feed flow. Whenever the level sensor detected the state "level too low" after the level controller's timer interval of 30 min, the capacity of the feed pump was temporarily increased to 25% (1.4 L/h, see Figure 35) until the level signal switched. In this preliminary version of the continuous level control, the filtrate flow was stopped for safety reasons whenever the state "level too low" was detected and the feed flow was increased.

Operating Conditions

Compared to the batch test, all operating parameters were kept the same, expect for the gassing rate, which was increased from 1.5 L/h to 5 L/h (0.33 vvm) to maintain a sufficient DO-concentration in the reactor broth. The feed flow was set to 500 g/h and the filtrate flow to 520 g/h so that the liquid level would slowly decrease during operation. The operating conditions for the continuous fermentation test run are listed in Table 15:

Table 15: Continuous Fermentation: Operating Conditions

Loop Flow	85 L/h
Aeration Rate	5 L/min (0.33 vvm)
Feed Flow	500 g/h
Filtrate Flow	520 g/h
Pressure	0 barg
Temperature	30°C
pH-Value	7

Fermentation Procedure

After the setup had been adjusted and the advanced control program had been implemented, the continuous fermentation was started by activating the feed and filtrate flows. At the start of the operation the flow controllers were optimized. Once relatively constant filtrate and feed flows were achieved, a steady state process with cell retention was executed for approximately 13 h. Only this time period was used for process evaluation.

Finally, the whole system was drained and sanitized by flushing with hot sodium hydroxide solution for final cleaning.

Determination of the Mass Balance Gap to Calculate the Water Loss

In a steady state, the mass balance gap should ideally be zero, meaning that the mass flows entering (feed, acid, base) and leaving (filtrate, bleed, samples, off-gas humidity) the reactor are equal. The in- and outflowing liquid streams of the pilot plant are depicted in Figure 68.
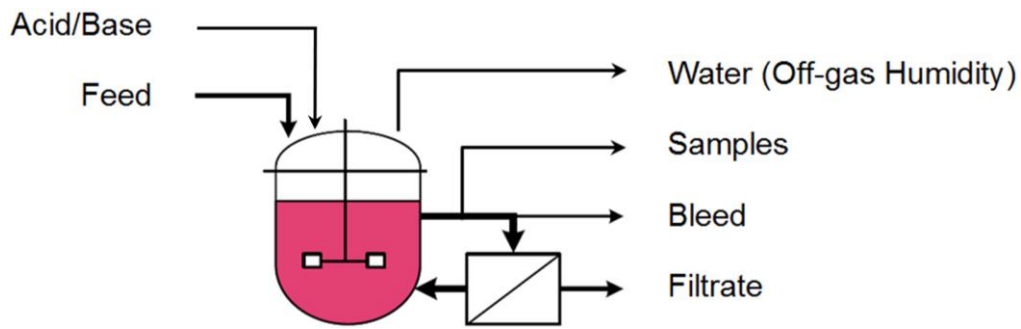
Figure 68: Mass Balance for the Pilot Reactor

The mass balance gap of the in- and outflowing streams can be calculated by Eq. 18:

$$\Delta m_{ges} = \sum_i \Delta m_i \ [g]$$

Eq. 18

$$\Delta m_{ges} = \Delta m_{Feed} + \Delta m_{Acid/Base} + \Delta m_{Bleed} + \Delta m_{Filtrate} + \Delta m_{Samples} [g]$$

The change in mass Δm_i for each component i is calculated from the weight difference of the storage tanks between end and start of the examined period:

$$\Delta m_i = m_{i,End} - m_{i,Start} \ [g]$$

Eq. 19

The calculated mass balance gap equals the water loss through the off-gas plus the inaccuracy of the level control and flow controllers. The largest control inaccuracy results from the 2 mm switching hysteresis of the level sensor. This height difference corresponds to a fluid volume of approximately 28.4 mL. By conversing with the measured density of the brine of 1.023 kg/L, the mass difference due to the measurement error of the level switch is 29.1 g. Hence, by subtracting this value from the calculated mass balance gap, the water loss can be estimated. The humidity of the off-gas can then be derived from the water loss during a certain period and the gassing rate.

6.2   Results

6.2.1 Results of the Integrity Test

The tightness and pressure resistance of the plant's connections were examined at the maximum operating conditions of 3 barg at 50°C. While the Tri-Clamp connections and the nozzles on the reactor were completely tight up to 3 barg, several plastic screw connections had started leaking at 0.5 barg, especially the ones of the adapter pieces of the pressure sensors and on the flow cell, see Figure 69. In order to seal them properly, the system was depressurized and the loop was drained. Next, the leaky plastic screw connections were tightened and the transition pieces of the pressure sensors were sealed again with thread seal tape. Afterwards, the system was pressurized again and the previously described procedure was repeated

until all connections were tight at the maximum pressure of 3 barg. Then, the system was exposed to the maximum pressure for 2 h. During that time, no visible leaking was observed. Hence, the pressure resistance of the setup at the maximum operating conditions could be demonstrated.
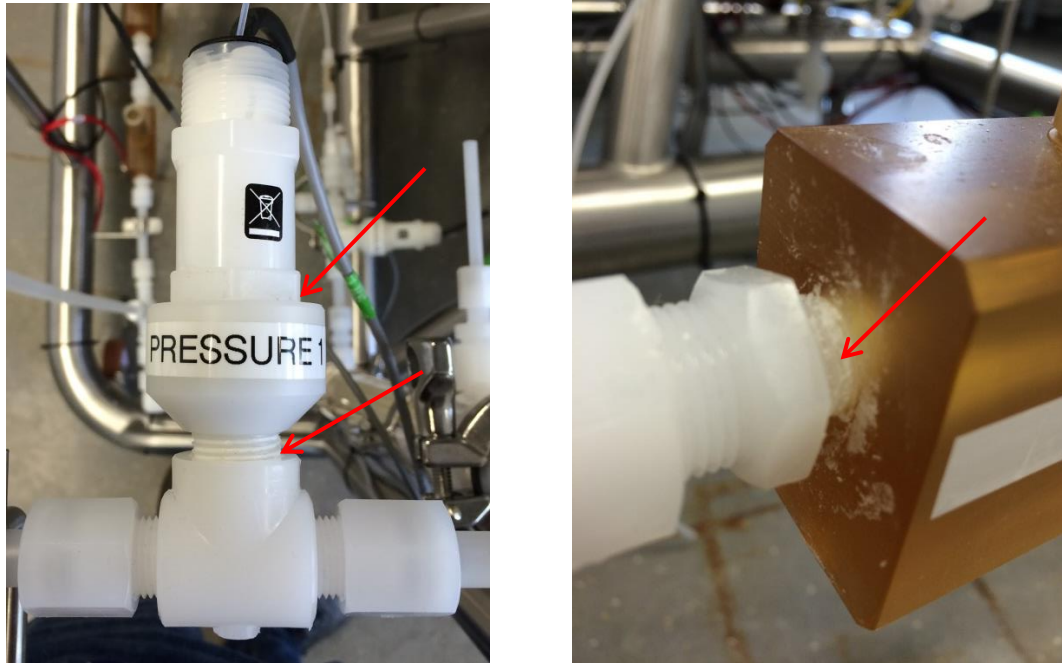
Figure 69: Leaky Screw Connections

6.2.2 Results of the Functionality Tests

6.2.2.1 Control Characteristics of the Pressure Control Valve

The characteristic curve of the reactor pressure as a function of the pressure control valve's aperture (or input signal) was measured twice at a constant gassing rate of 5 L/min. The results are listed in Table 16:

Table 16: Reactor Pressure as Function of the Pressure Control Valve's Aperture

Valve Opening [%]	Pressure [barg]		
	First Run	Second Run	Deviation [%]
100	0.173	0.176	2
80	0.249	0.261	5
60	1.483	1.319	12
50	1.503	1.338	12
45	1.562	2.200	41

Table 16 shows that the pressure could be increased by decreasing the pressure control valve's aperture. The correlation between pressure and valve opening is not linear but rather stepped. The maximum allowable pressure of 3 barg had been exceeded at 40% valve opening, which is why 45% aperture is the minimum limit for

the control valve at a gassing rate of 5 L/min. Although constant pressure levels could be achieved at each setting after an equilibration phase of at least 5 min, the pressure values of the first and second test run differ from each other at the same valve opening. The measured deviations increase with the pressure and reach 12% at 50% valve aperture.

In addition to this inaccuracy, the pressure depends on the previous state of the valve. Depending on whether the aperture is increased or reduced, the pressure values after equilibration significantly differ from each other. This can be seen at the last measuring point with 45% valve opening. In the first run, the aperture had been initially reduced from 50 to 40%. But since the maximum allowable pressure had been reached at this setting, the opening was increased again to 45%. However, in the second run, the opening was directly decreased to 45 from 50% and the resulting pressure was over 40% higher than in the first run. This means that the adjusted pressure is different if a setpoint is approached from above or below.

In addition, it was found that the reactor could not be completely depressurized back to the initial pressure at 100% opening of about 0.176 barg by fully opening the control valve. Instead, the pressure remained at about 0.26 barg. In order to fully depressurize the system, the pressure control valve had to be temporarily dismounted. After reinstallation, the control characteristics according to Table 16 could be achieved again.

6.2.2.2 Flow Rate Calculation of the Bleed/Filtrate Valves

The flow rate through the fully opened micro-valve from Bürkert GmbH was measured gravimetrically at three different settings. First, the flow rate caused by the hydrostatic pressure (height difference 1.2 m) was determined. Next, the loop pump was activated with a capacity of 40% (85 L/h) and the flow rate through the micro-valve was measured at 0 and 3 barg reactor pressure. The resulting flow rates at the three tested settings are listed in Table 17.

Table 17: Flow Rate through the Bleed/Filtrate Valves depending on the Pressure

Pressure [barg]	Flow Rate [L/h]
0.12	1.36
0.16	1.40
3.00	8.20

Table 17 shows that the flow rates through the micro-valve with an aperture of 0.4 mm are larger than the designed bleed flow of 0.48 L/h (see Table 2), regardless of the pressure. Even the flow caused by the hydrostatic pressure of the system (first row in Table 17) is approximately three times larger than the desired bleed flow. This makes the flow control by intermittently opening the valve possible. For example, the

bleed valve has to be opened for approximately a 17th part of the process time to achieve the desired bleed flow of 0.48 g/h at the maximum reactor pressure of 3 barg. Moreover, Table 17 indicates that a pressure of slightly above 0.16 barg in the loop is necessary to achieve the required filtrate flow rate of 1.44 L/h through the micro-valve.

6.2.2.3 Membrane Test

In this experiment the TMP as well as the flux rate of the membrane cartridge were determined with and without the filtrate valve. The TMP-control valve was fully opened during the test. The results of this calculation are listed in Table 18. In it, p_1 is the liquid pressure before the membrane, p_2 the pressure on the retentate side and p_3 equals the pressure on the permeate side of the membrane.

Table 18: Membrane Test: TMP and Flux Rate Determination

	Without Filtrate Valve		With Filtrate Valve	
	Filtrate Port closed	Filtrate Port open	Filtrate Port closed	Filtrate Port open
p_1 [barg]	0.810	0.599	0.834	0.763
p_2 [barg]	0.857	0.650	0.872	0.808
p_3 [barg]	0.843	0.627	0.870	0.799
TMP [barg]	-	-0.003	-	-0.017
Flux Rate [L/h]	-	20.9	-	3.3

Table 18 shows that the flux rate is significantly reduced by the installation of the filtrate valve, but is still more than twice as large as the desired flow rate of 1.44 L/h. This makes the chosen filtrate valve feasible for the designed process.

Moreover, the three measured pressure values in the loop are close together. When the filtrate port is closed, a pressure of about 0.85 barg is applied to the membrane. This means that the loop pressure is about 0.7 barg higher than the reactor pressure itself. This rise is created by the loop pump when the TMP-control valve is fully opened and can be further increased by reducing the valve's opening.

Furthermore, the pressures on the retentate (p_2) and the filtrate side (p_3) are larger than on the membrane's feed side. Usually the fluid pressure decreases from in- to outlet of a membrane module due to the flow resistance. However, with the used vertically mounted cross flow filtration cartridge (Figure 70), the contrary is the case. This means that the hydrostatic pressure, caused by a height difference of about 0.8 m between membrane in- and outlet, is larger than the pressure drop over the membrane.

When the filtrate port or the filtrate valve is opened, the pressure on the membrane's permeate side (p_3) is reduced by only about 0.2 barg or 0.07 barg respectively. However, when open, the pressure in the filtrate line p_3 is supposed to sink to almost ambient level.

Due to the two aforementioned facts, the resulting transmembrane pressure according to Eq. 9 is very small and negative. Hence, the used equation for the TMP is not feasible for this application.

Lastly, the volume of the cell retention loop was measured to determine the total working volume of the plant. It was found that the liquid in the loop had a volume of 760 mL. However, as the red mark in Figure 70 shows, this value is most dependent on the level of liquid in the membrane, which in turn is depending on other process parameters, most of all the reactor pressure and the filtrate valve setting. At the end of this experiment, the membrane housing was filled to approximately 60%. When the membrane is fully filled, the loop volume is estimated to 1 L, adding up the total working volume in the system to 16 L.

Figure 70: Membrane Cartridge during Operation

6.2.3 Results of the Test Fermentations

6.2.3.1 Measuring Results of the Offline Analysis

Biomass Concentration

The biomass concentration of the offline samples was calculated from the measured OD-values by Eq. 17. Figure 71 and Figure 75 show the biomass trend for both test fermentations.

Substrate Concentration

All samples that were taken from the reactor were contaminated and thus only the feed and filtrate sample could be analysed by HPLC. The results of the analysis were that the desired acetate concentration of 4 g/L could be detected in the feed and the concentration in the filtrate of the continuous fermentation was below the detection limit of the analyser.

6.2.3.2 Results of the Batch Fermentation

Biomass Growth

In the first phase of the batch fermentation, an exponential growth of the cells was observed by the OD-measurement and the off-gas analysis. Figure 71 shows the off-gas composition, the O_2- and CO_2-concentration in %, as well as the biomass concentration in the first 19 h of the batch fermentation.
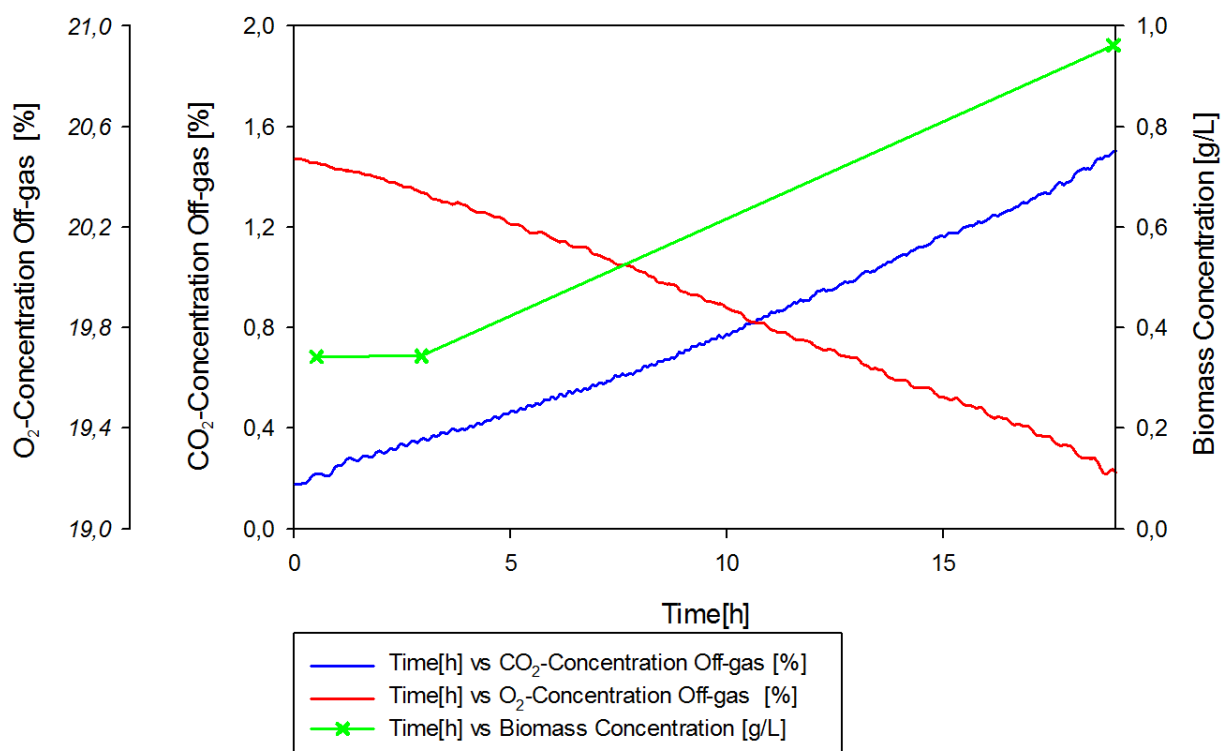
Figure 71: Batch Fermentation: Off-gas Composition and Biomass Concentration

The batch phase lasted for about 37.5 h. Figure 75 shows the overall progress of biomass concentration during the batch (0 to 37.5 h) and subsequent continuous fermentation. Starting with about 0.35 g/L after inoculation, the biomass concentration increased almost exponentially to about 1.5 g/L for the first 27 h of the batch phase. Afterwards, the biomass concentration slightly decreased because of dilution by a control error. The end of the batch was indicated by the sudden rise of the dissolved oxygen concentration in Figure 72 when the whole substrate had been consumed. At this point, the biomass concentration had reached about 1.5 g/L again.

Study of the Dissolved Oxygen Concentration

Figure 72 shows the trend of the DO-concentrations in the reactor vessel and loop as well as the reactor pressure. The DO-signals were very noisy due to the presence of bubbles in the measuring sections. Therefore, the curves in Figure 72 were smoothed by averaging.
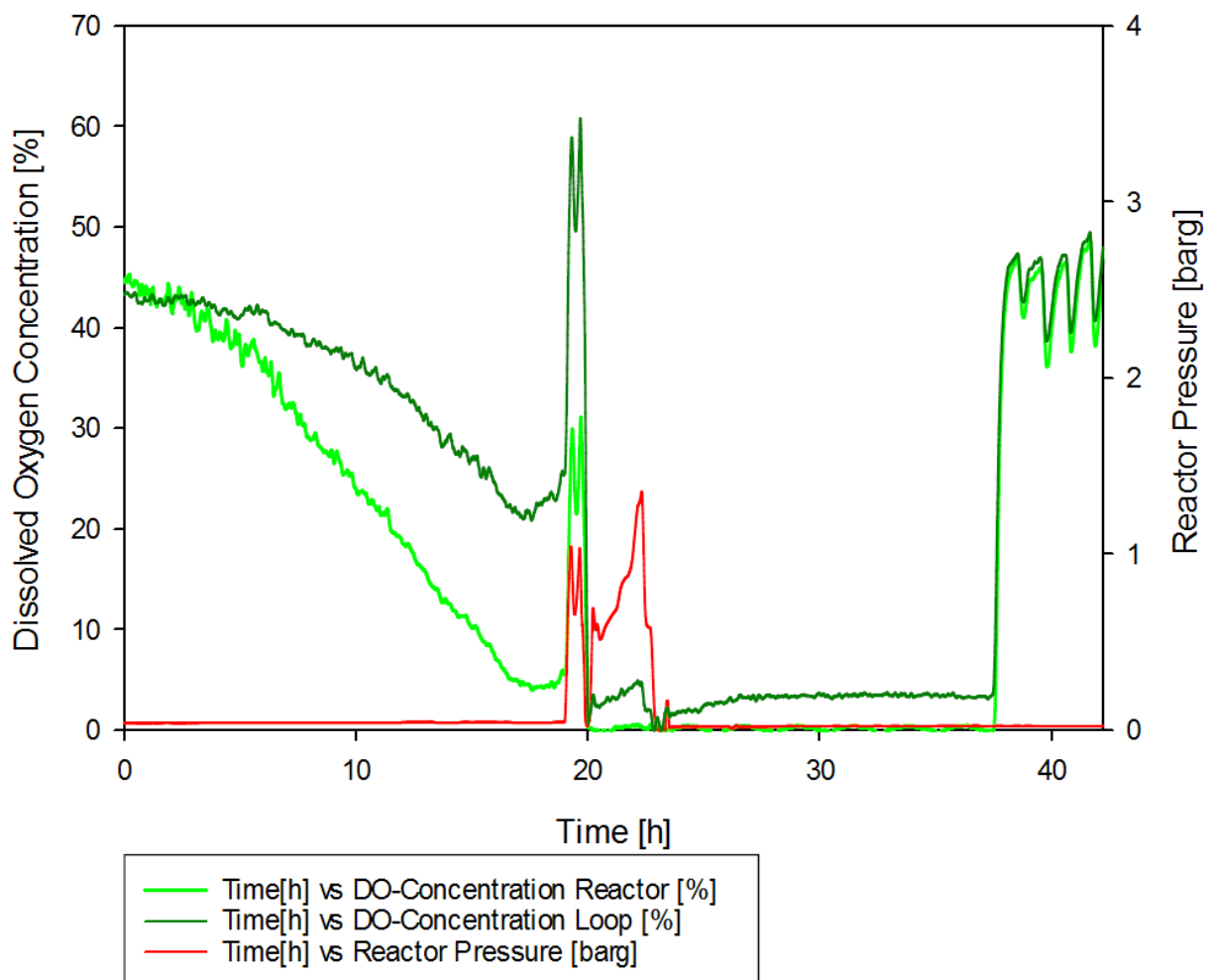
Figure 72: Batch Fermentation: DO-signals and Reactor Pressure

The most notable fact about this chart is that the DO-concentration in the loop was significantly higher than in the reactor itself, especially at low dissolved oxygen concentrations. This is presumably caused by air bubbles from gassing that are

carried into the loop tubing. While passing through the piping, there is significantly more time for oxygen mass transfer than in the reactor vessel. Thus higher dissolved oxygen concentrations can be reached in the loop.

Hereinafter, the qualitative course of the DO-curves is examined. During the first hours of fermentation, an exponential growth of the cells was achieved and the dissolved oxygen concentrations decreased exponentially as well. After 19 hours, the DO-concentration in the reactor had sunk to 4% and in order to increase it, the reactor pressure was raised to approximately 1 barg by reducing the aperture of the pressure control valve (V3) to 60%. Immediately after pressurizing, the DO jumped to 30%, therefore proving that pressure and measured DO-concentration are directly proportional.

However, due to the increased pressure, foam was continuously pressed through the off-gas line and the pressure control valve. It was then separated in the Schott-bottle of the improvised off-gas cooler. Pressure deviations of up to 0.5 barg occurred afterwards. After 20h, the reactor was temporary depressurized for anti-foam addition. The reactor pressure continuously rose to approximately 1.5 barg in the following hours. Even when the aperture of valve was completely opened, the pressure still increased. The only explanation for that was that the pressure control valve had been partially blocked by the overflowing foam. In order to restore a safe operation mode, the improper functioning valve was removed after 23 h. Hence, no operation at increased pressures was possible from that point on.

Moreover, the DO-concentration in the reactor decreased to almost 0% after anti-foam addition at 20 h. The reason for this was that the anti-foam agent (Struktol J673-1) decreased the oxygen mass transfer. This phenomenon had also been observed in previous experiments with the lab-scale bioreactor. In the loop a slightly higher DO-concentration of approximately 4% was achieved due to longer possible mass transfer inside the tubes. The dissolved oxygen concentrations in reactor and loop stayed at these low levels until the end of the batch, which was reached after 37.5 h. During that period, an oxygen limitation occurred and the cells grew more slowly, as the biomass trend in Figure 75 shows. However, the measured DO-concentrations did not increase to 100% but only to 55% after the end of the batch. This is because the DO-probes were calibrated with a higher aeration rate of 7.5 L/min and a pressure of 0.5 barg (see Chapter 6.1.3.4), instead of the operating conditions of 1.5 L/min at 0 barg. Afterwards, several small peaks occurred periodically, because small amounts of new substrate were added every time the level control pumped feed into the reactor to maintain the level.

Test of the Temperature Control

In this experiment, the temperature control of the pilot plant was tested and monitored. The progress of the temperatures in reactor and loop as well as of the pH-value in the first half of the batch fermentation is shown in Figure 73.

The temperature control unit in the switchboard was configured as a PID-controller with a single input value. Before operation, an automatic optimization program for the control parameters according to Ziegler and Nichols was executed by the control unit. Deviations of +0.5°C and -0.1°C from the setpoint of 30°C were observed during the test. These were sufficient for the test runs, but have to be reduced for future operations so that the desired temperature deviation of ±0.2°C can be achieved.

The two temperature graphs in Figure 73 show that the temperature in the loop was about 1°C lower than in the reactor since the tubing of the loop was not insulated. The pointed course of both graphs shows that the heating pad was periodically turned on for a very short time and afterwards the temperature slowly decreased again due to heat loss to the environment. The increasing periodic time of the heating intervals from approximately 20 to 40 min indicated that the cooling phases lasted longer because of the increasing heat production by the cells' metabolism.
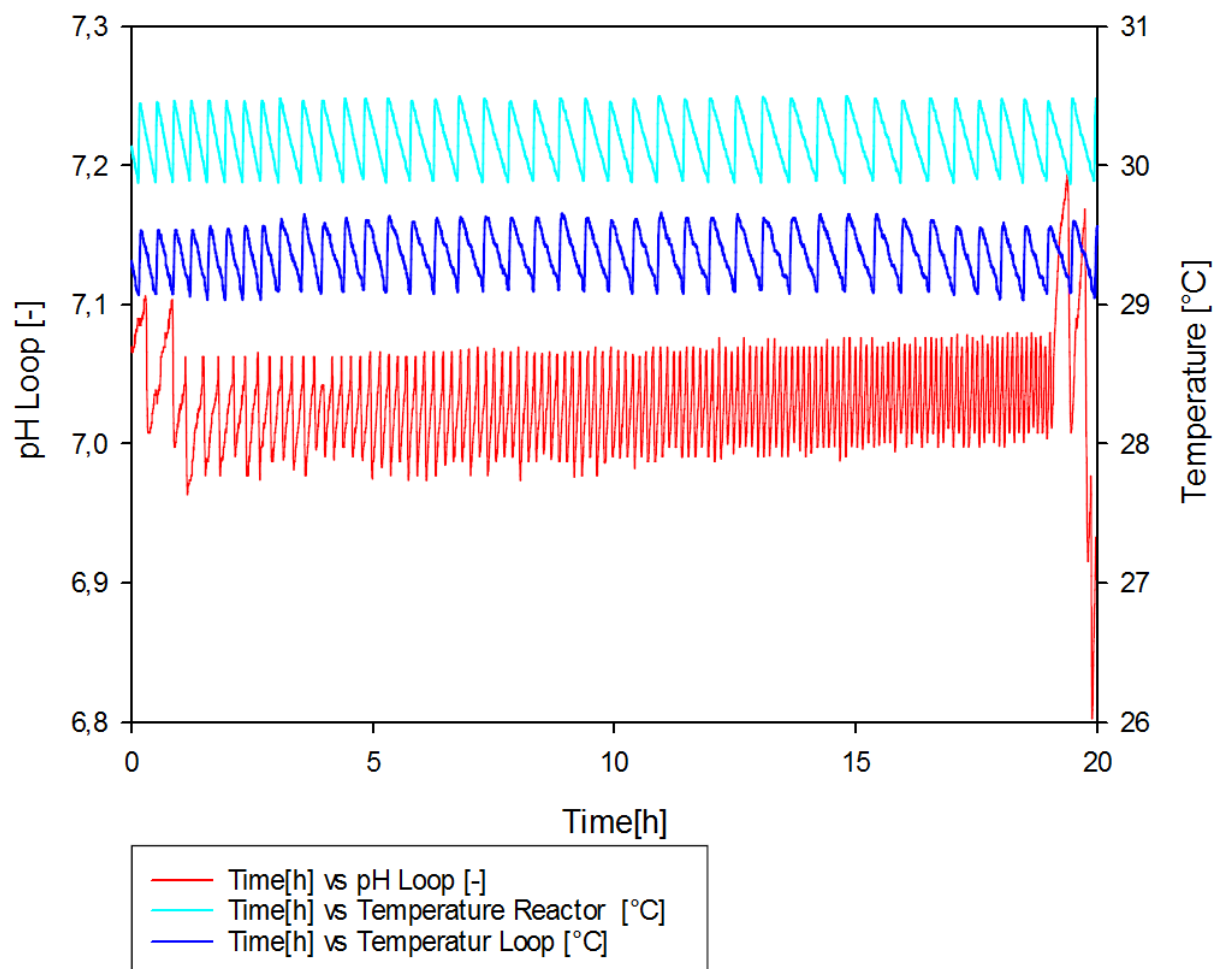
Figure 73: Batch Fermentation: Temperature and pH-Signals

Test and Optimization of the pH-Control

In this experiment, the pH-control of the pilot plant was tested and optimized so that sufficiently small deviations from the setpoints were reached. The progress of the pH-value in the first half of the batch fermentation is indicated in Figure 73. The pH-control consists of two separate 2-point-control loops that switch the acid- and base dosing pumps on and off, depending on the measured pH-value. At the start of the experiment, these thresholds for both 2-point-controls were adjusted until an acceptable total deviation was achieved. During this test, only acid was added to keep the pH-value constant. However, it became apparent that it took approximately 2 min before the pH-value began to drop after the pH-control had started adding acid to the reactor. This high inertia of the system can be explained by the arrangement of the pH-probe in the loop. Once the pH started changing after adding acid, 0.5 molar HCl, a sudden drop of approximately 0.1 occurred. Since the pH-value of the system responded very slowly to the dosage of acid or base, the threshold interval had to be narrowed down significantly. Additionally, the flow rates of the dosing pumps were reduced to their lowest possible setting of 5% to reduce the pH-drop due to the lagged measurement in the loop. The adjustment of the limit values can be seen at the beginning of the pH-graph in Figure 73. In the end, periodic deviations of approximately +0.07 and -0.03 from the pH-setpoint were achieved with 0.5 M HCl. Hence, the desired total deviation of ±0.05 specified in the URS could be reached by shifting the setpoint by 0.02. During the test, the period of the pH-jumps declined from about 20 to 6 min. This indicated an increased cell metabolism.

Moreover, the 0.5 molar acid was replaced by a 1 molar one in order to reduce the consumption of acid. However, it was found that the pH-drop after the 2 min delay doubled from 0.1 to 0.2, thus falling below the threshold for the start of the base-control. As a result, the pH-value and the consumption of acid and base escalated. Therefore, the acid was diluted to a molarity of 0.5 again. This modification showed that the pH-control could be improved by further diluting acid and base. Furthermore, it showed that the thresholds of the 2-point-pH-control have to be adjusted to the used concentration of acid or base.

At the end of the pH-graph at approximately 19 h, large peaks occurred after the reactor pressure had been increased because the dosing pumps had stopped working above 0.6 barg. At elevated pressure, gas was pressed back into the dosing lines and the dosing pumps were filled with air. To make the pumps operational again, the reactor pressure had to be decreased and they had to be vented.

Test of the Level Control

Figure 74 shows the signals of the feed, acid, base and bleed balances as well as the state of the level sensor in the first 19 h of the batch fermentation. It indicates that the consumption of acid increased exponentially, corresponding to the exponential growth phase during that period. Since the pH-value rose during fermentation, almost no base was used. The weight curves of feed and bleed are stepped because of the level control, which was activated every 30 min. However, these signals were noisy, especially the first third of the feed curve. Furthermore, additional small steps in the bleed curve occurred although the bleed valve had not been opened at these times. These deviations were probably caused by interference, because the supply lines touched each other and the weighed tanks during operation.
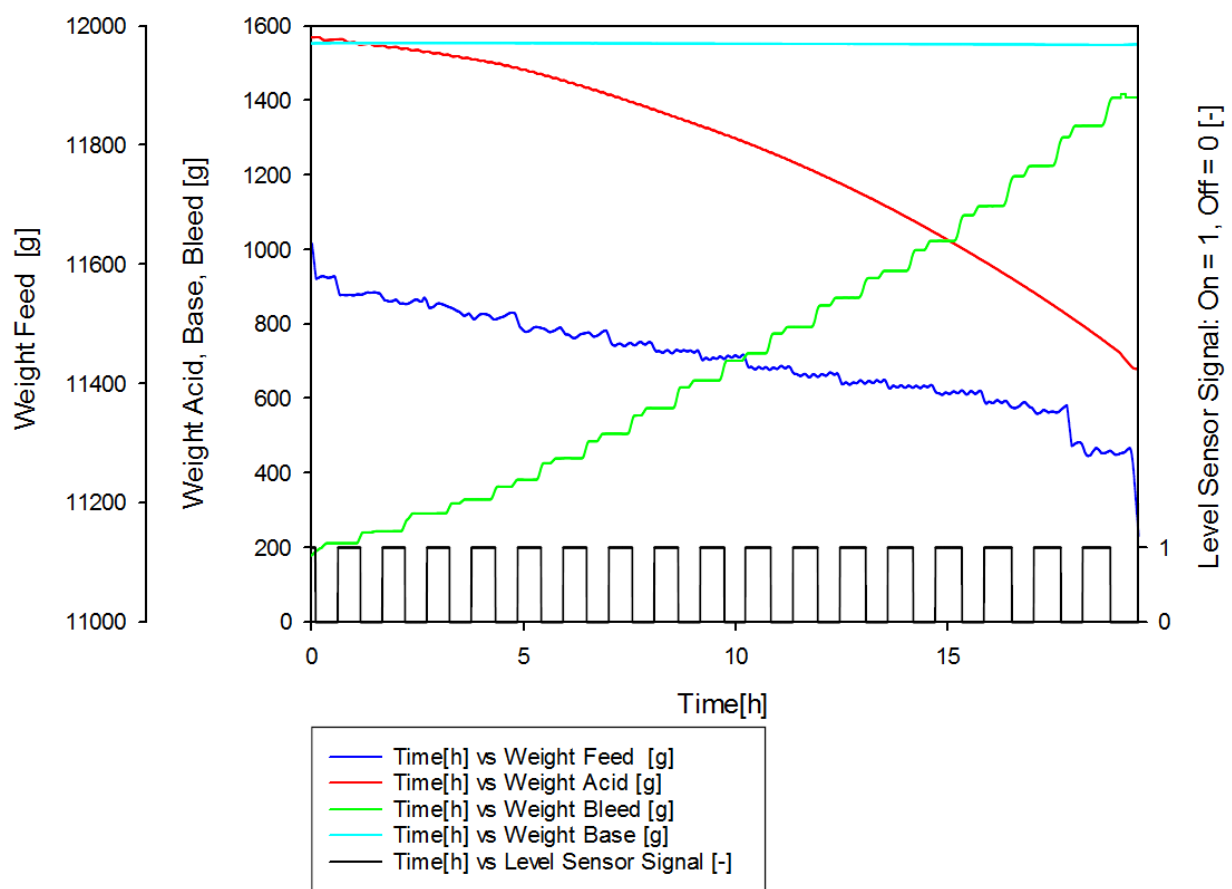
Figure 74: Batch Fermentation: Balance Signals

Furthermore, the digital signal of the level sensor is depicted in Figure 74, using the number 1 for the state "On" and 0 for "Off". Whenever the vibrating fork of the level sensor was immersed in the liquid (see Figure 44), its digital signal switched to "On". When the level decreased and the sensor was exposed to air, the signal switched to "Off". This is depicted in the stepped curve of the level sensor in Figure 74.

For this test run, the timer for the level control (see Chapter 6.1.3.6) was set to 30 min. Therefore, after every half an hour the state of the level switch was bound to change. This is indicated by the start or end of a block of the level signal in Figure 74. Hence, every change of the level signal is correlated with an increase of the bleed weight or a decrease of the feed weight.

Since only acid was added in significant amounts during the batch fermentation, ideally only this volume, approximately 900 mL, would have had to be removed from the reactor in order to keep the level inside the reactor constant when neglecting the water loss through the off-gas and sampling. However, Figure 74 shows that approximately 1200 mL of broth were discharged via the bleed valve. The difference between these two volumes results from the fact that every time the level control was activated, the measurement hysteresis of 2 mm had to be exceeded and therefore slightly too much fluid was added or removed.

Test of the Improvised Off-gas Cooler
The batch test showed that almost no water could be separated in the improvised off-gas cooler (see Figure 62). This could either be due to the fact that, most likely, the off-gas was not very humid or that the heat transfer area of the cooler, the inner surface of the 2L-Schott-bottle, was too small and the gas couldn't be cooled sufficiently for condensation.

The weight of the separated water could not be measured since foam and reactor broth were pressed through the off-gas line and into the glass bottle when the reactor was pressurized during operation.

6.2.3.3 Results of the Continuous Fermentation

Compared to the batch mode, the aeration rate during the continuous fermentation was increased from 1.5 to 5 L/min to enhance the DO-concentration in the broth and avoid oxygen limitation like in the previous experiment. Even though anti-foam agent was added beforehand, shortly after raising the gas flow, foam was pressed through the off-gas line and blocked the pressure control valve. This lead to an unintended increase of the reactor pressure and the pressure control valve had to be removed from the system. But still, foam flew constantly from the off-gas line throughout the whole continuous fermentation. Hence, additional measures for foam control have to be taken for future operations, especially when the plant has to be operated at high gassing rates or elevated pressures.

Biomass Concentration

Figure 75 shows the overall progress of biomass concentration during both batch (0 to 37.5 h) and continuous fermentation (42 to 66.5 h). At the end of the batch fermentation, a biomass concentration of about 1.5 g/L had been reached. The continuous fermentation began at 42 h, when new substrate was added by the feed flow. Initially, this flow had a variable rate because the flow controller was still being adjusted. At 53.6 h the desired constant feed flow of 500 g/h was reached and at the same time 520 g/h filtrate was removed from the system. From 53.6 to 66.5 h, a continuous process with constant feed and filtrate flows was accomplished. The recorded data from this period is shown in Figure 76 and Figure 77. During that time, the biomass concentration slightly increased to 1.73 g/L at first and then remained relatively constant until the end of the experiment. This means that the concentration could be maintained in the reactor, but the desired significant increase of the biomass concentration by means of cell retention could not be achieved yet.
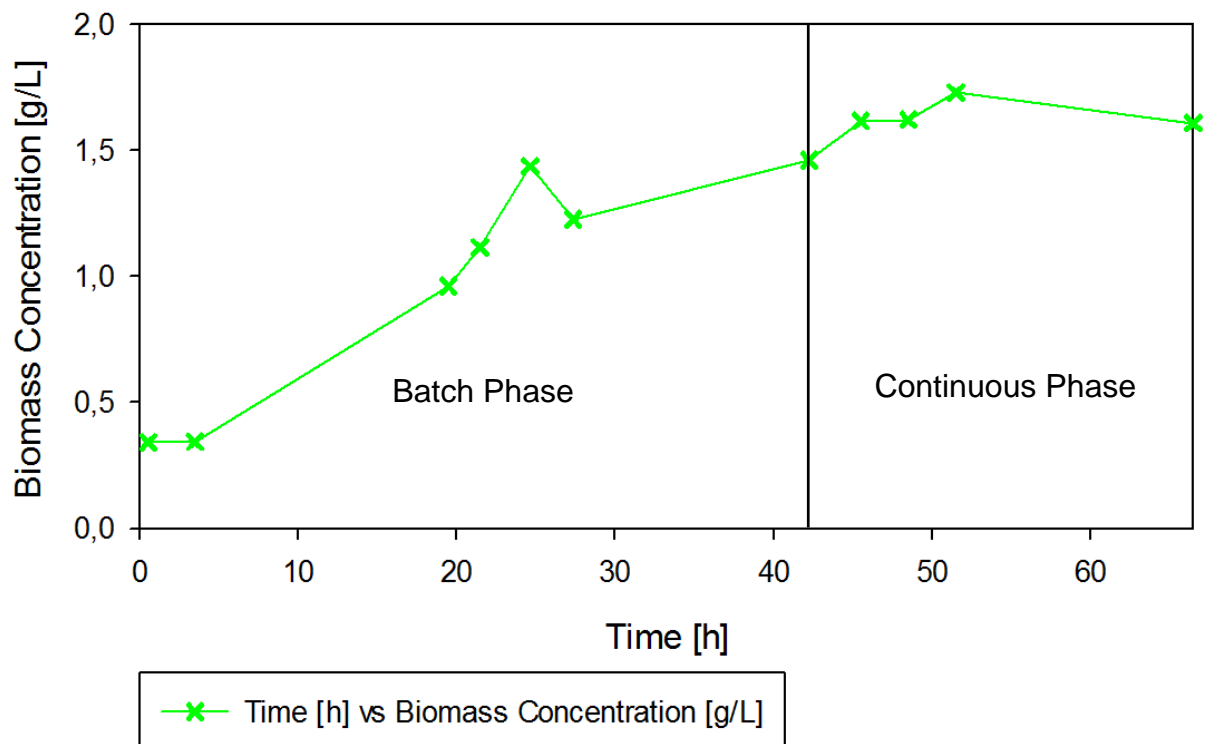
Figure 75: Biomass Trend for Batch and Continuous Fermentation

Study of the Flow Controllers for Feed and Filtrate

Figure 76 indicates the flow rates of feed and filtrate as well as the level signal during the continuous process:
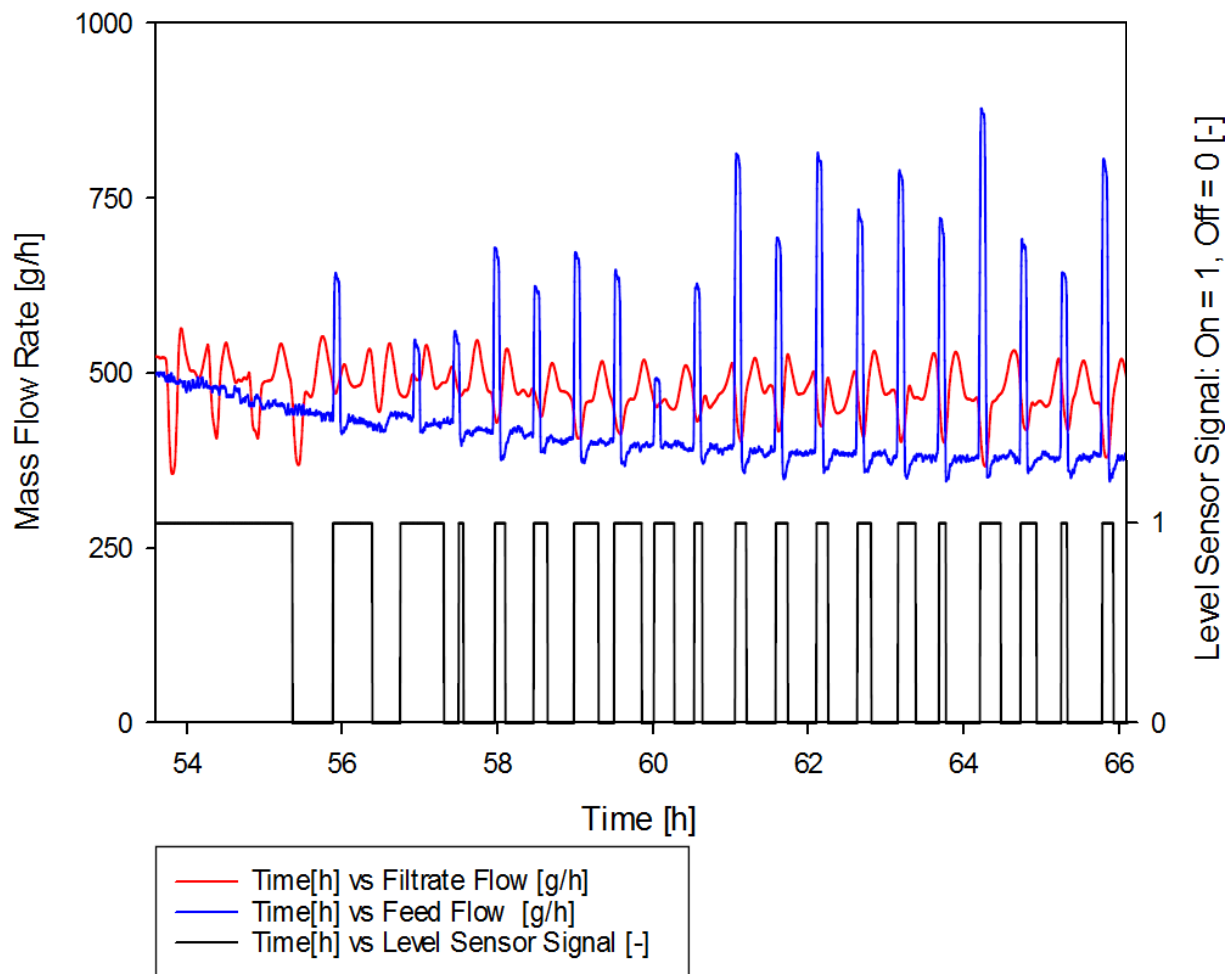
Figure 76: Continuous Fermentation: Flow Signals and Level Sensor

Figure 76 shows that both flow rates fluctuate significantly, especially the filtrate flow. The feed flow is less noisy, but large periodic peaks occur in its curve, which result from the level control. In addition, the mean values of both streams had a large offset from the setpoints, as Table 19 shows:

Table 19: Mean Feed and Filtrate Flows

	Set Flow [g/h]	Mean Flow [g/h]
Filtrate	520	477
Feed	500	422

Both flows fell distinctly below their target values. Beside of measurement inaccuracies, this was presumably caused by the fact that the feed flow was also used for level control. Whenever the state "level too low" was detected and the reactor was filled up by temporarily increasing the capacity of the feed pump, the filtrate flow was stopped during that process. Thus, the overall filtrate flow was

reduced. However, the feed and filtrate flows didn't escalate but instead, over time, a settled, stable operating state was formed, though with lower flow rates than desired.

The functionality of the flow controllers is also confirmed by Figure 77. It shows the weight signals of the feed, acid, filtrate and bleed balances as well as the temporary deviation from the mass balance. The weight signals of feed and filtrate both have a linear progress although their flow rates were fluctuating strongly, as Figure 76 indicates. Thus, on average, constant flow rates could be achieved.
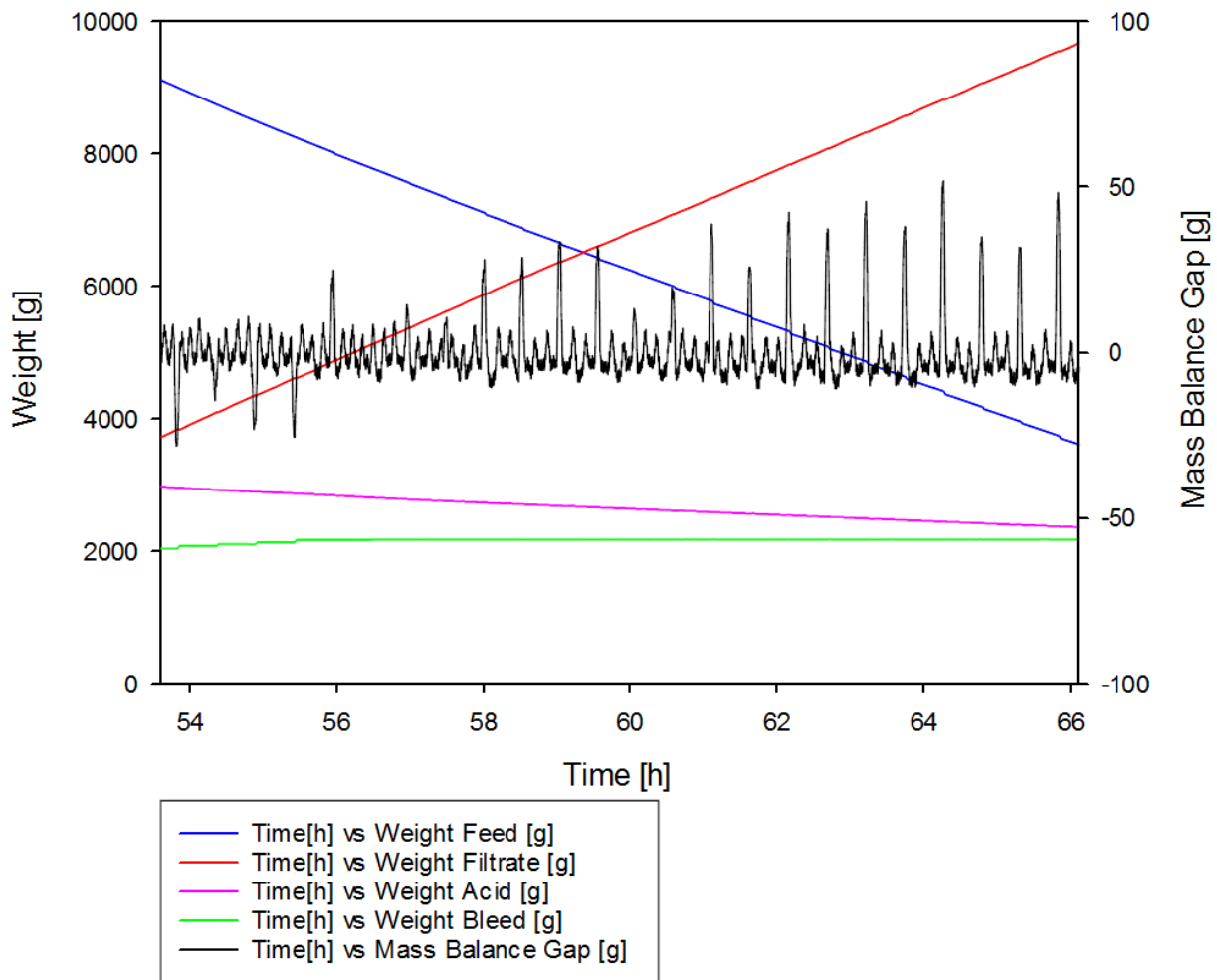
Figure 77: Continuous Fermentation: Balance Signals

Study of the Level Control in Continuous Mode

The course of the filtrate flow in Figure 76 also proves the functionality of the tested level control approach in continuous mode. Since the filtrate flow was slightly larger than the feed flow, the liquid level in the reactor slowly decreased. Every 30 min, the level control was activated and temporarily increased the feed pump's capacity to 25% when the level was below the level switch (Signal "Off"). The course of the level sensor's signal in Figure 76 indicates that the sensor was only activated for a short period after the periodic feed flow peaks caused by the level control.

Study of the Mass Balance and the Water Loss

The local mass balance gap according to Eq. 18 was determined within a 3 min interval and is depicted in Figure 77. It fluctuates mainly between +10 g and -10 g and therefore the measured deviation is on average less than half as small as the maximum error of the level sensor. However, every 30 min large deviations of up to +50 g occurred. These periodic peaks were caused by the level control and were compensated quickly, as the total mass balance showed. Overall, the local mass balance graph shows that a steady state with an accuracy below the level sensor's measuring error had been reached during the whole fermentation.

Then, the total mass balance gap for the continuous fermentation was calculated according to Eq. 18. The result was then used to determine the water loss through the off-gas. The change in mass of each component during the investigated period of 10.62 h is listed in Table 20. No samples were taken during that period. The start and end times were chosen at the end of the first and last level signal block in Figure 76, when the signal switched from "On" to "Off". That way, it was ensured that the level was exactly the same at both states.

Table 20: Mass Balance for Continuous Fermentation

	Time [h]	Weight Feed [g]	Weight Acid [g]	Weight Bleed [g]	Weight Filtrate [g]	Total Weight [g]
Start time	55.45	8254.5	2873.3	2170.7	4619.5	17918.0
End time	66.07	3625.5	2363.2	2178.5	9674.1	17841.3
Difference	10.62	-4628.9	-510.1	7.8	5054.6	76.7

According to Table 20, the total mass balance gap during the examined period amounts to 76.7 g. The main part of this difference was presumably caused by the loss of water through off-gas humidity and the rest mostly resulted from the 2 mm switching hysteresis of the level sensor, which equals a mass of 29.1 g. This means that water loss per day minimally amounts to 107.6 g, when the maximum level sensor error is considered, and maximally to 173.3 g without level switch inaccuracy. The former value equals a loss of 0.67% of the reactor volume per day and the latter 1.09%. The corresponding calculated water loads Y of the off-gas are 0.012 and 0.02 kg water per kg gas. Both values are very small and indicate that the humidity of the exhaust gas is very low.

Study of the TMP and Membrane Fouling

To investigate membrane fouling, the progress of the transmembrane pressure is generally used. But since it was found in Chapter 6.2.2.3 that the used equation for the TMP according to Eq. 9 is not feasible for this application because it would result in a negative TMP, the course of the three pressures for TMP-determination was investigated instead. Figure 78 shows the progress of the reactor pressure, p_1 (membrane feed pressure), p_2 (retentate pressure) and p_3 (permeate pressure) during the whole continuous fermentation. It can be seen that the offset between the three pressures as well as to the reactor pressures is constant regardless of the total pressure. This proves again that the pressures in the membrane setup are mainly determined by the hydrostatic pressure and not by the drag of the filter. Moreover, during the examined time period no fouling could be detected as the pressures did not decrease over time.
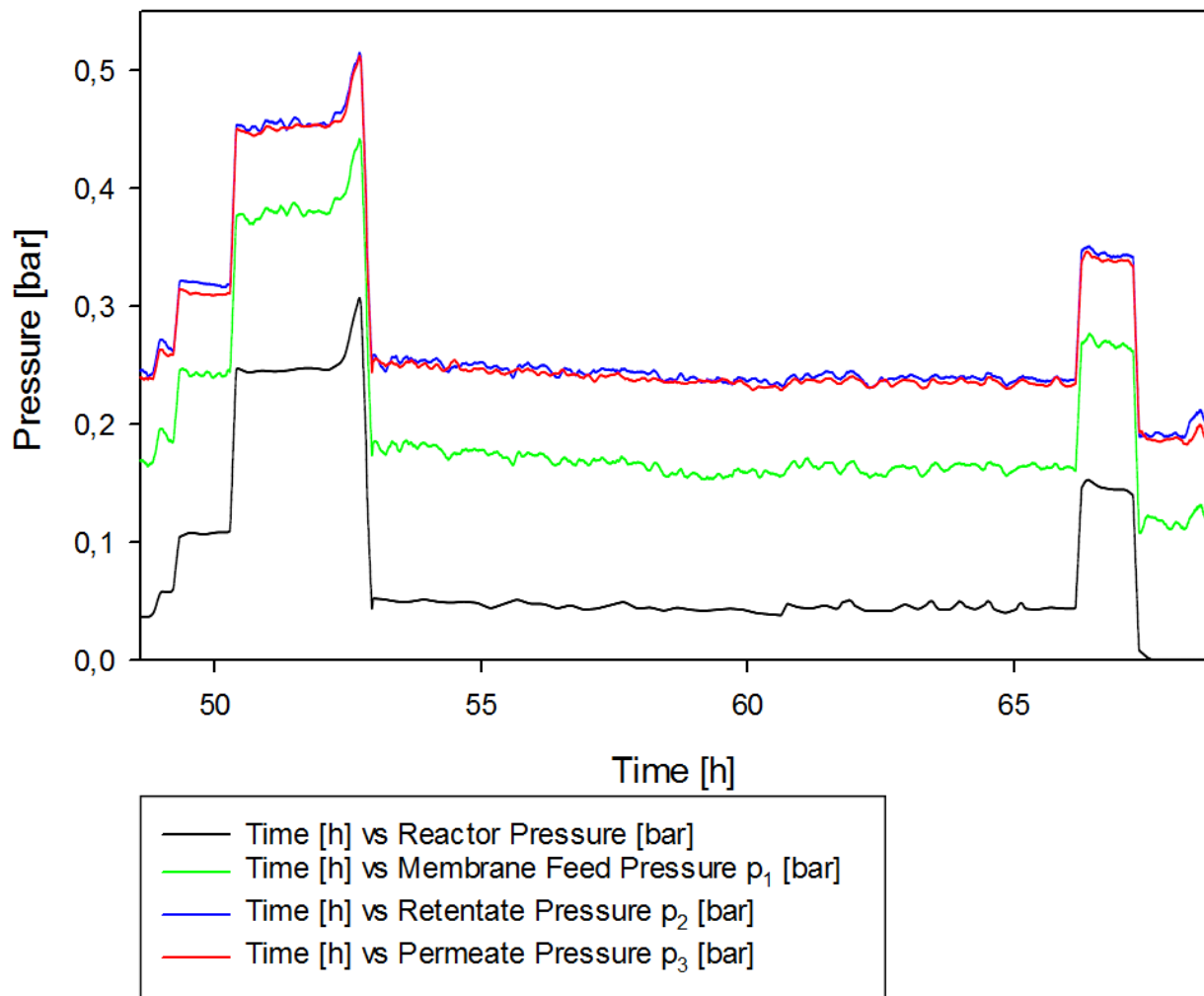
Figure 78: Continuous Fermentation: Pressures Signals

6.3   Discussion of the Tests

6.3.1 Discussion of the Integrity Test

The integrity test showed that all components could withstand the maximum operating conditions of 3 barg and 50°C and were tight. However, in the subsequent test fermentations with brine that were performed mostly pressureless, crusts of salt were detected on several plastic screw connections (Figure 69) which indicated leaks. These were probably caused by the long lasting exposure to the vibrations of the reactor-rack, caused by the pumps. Placing the pumps on underlayments made of rubber could damper the vibrations and increase the tightness of the connections.

6.3.2 Discussion of the Functionality Tests

6.3.2.1 Discussion of the Control Characteristics of the Pressure Control Valve

The functionality test of the pressure control valve showed that it is able to set the reactor pressure to a certain value and to maintain a constant pressure in the system. In the experiment, a control accuracy of 12% was achieved in the range from full to 50% valve opening. However, the adjusted pressure is different if a setpoint is approached from above or below. Hence, at the tested configuration, the device is not capable to control quickly changing pressures. For a reproducible pressure control with this setup, the pressure can only be increased. When the pressure level has to be decreased, the system has to be depressurized first and then increased again to the new value. This procedure is suitable for the pilot plant since maintaining a constant pressure is usually sufficient and changes rarely occur in the continuous process. Nevertheless, a control strategy adapted to the pressure control valve's special behaviour has to be implemented.

6.3.2.2 Discussion of the Flow Rate Calculation of the Bleed/Filtrate Valves

The test showed that the flow rates through the Bürkert GmbH micro-valve with an aperture of 0.4 mm are larger than the designed bleed flow of 0.48 L/h, regardless of the pressure. However, a pressure of slightly above 0.16 barg in the loop is necessary to achieve the required filtrate flow rate of 1.44 L/h. Considering that during operation the filtrate has to pass the membrane as well, this pressure threshold has to be further increased. However, in the subsequent membrane test it was found that the pressure in the loop increases to approximately 0.8 barg when the TMP-control valve is installed and fully opened, which is high enough to produce the desired filtrate flow. The obtained results make the flow control by intermittently

opening the valve possible. This control approach could be successfully demonstrated during the test fermentation in continuous mode (Chapter 6.2.3.2).

Furthermore, it was found that the water flowing out of the micro-valve foamed up intensively at a pressure of 3 barg. This indicates high shear forces and turbulence while the fluid passes through the valve's small aperture of 0.4 mm and could presumably stress or even damage cells.

6.3.2.3 Discussion of the Membrane Test

The membrane test showed that the pressures on the retentate and the filtrate side are larger than on the membrane's feed side. This means that the hydrostatic pressure difference between membrane in- and outlet is larger than the pressure drop over the membrane. Furthermore, it was found that the pressure on the filtrate port does not sink to ambient level when opened but is only slightly reduced. Due to these facts, the resulting transmembrane pressure according to Eq. 9 is very small and negative. But since filtrate is produced, a negative TMP is physically impossible. Hence, the used equation for the TMP is not feasible for this application, because the pressure differences at the three measuring points are mainly determined by the hydrostatic pressure and not by the drag. Therefore, an alternative characteristic value to describe the flux rate has to be found. This could possibly be the pressure difference between permeate and filtrate ($p_2 - p_3$). As Table 18 shows, this difference is always positive and the hydrostatic pressure is insignificant since these two ports are almost mounted at the same height (see Figure 38). However, an actual correlation between this parameter and the flux rate has to be developed.

Another possible solution to achieve a positive TMP would be to install the currently vertically mounted cross flow cartridge horizontally. That way, it is assumed that the general equation for the TMP would be feasible again, but the reactor skid would have to be redesigned for that purpose.

However, the experiment showed that even at low reactor pressure, medium loop flow and fully opened TMP-control valve, a filtrate flow that is almost twice as large as the maximum specified flow could be achieved. Hence, TMP-control by a control valve may not be necessary. Instead, the filtrate flow, which is in any case larger than needed, could be solely controlled by the opening time of the intermittent filtrate valve.

6.3.3 Discussion of the Test Fermentations

6.3.3.1 Discussion of the Batch Fermentation

Biomass Growth

During the batch fermentation, an exponential growth of the cells could be achieved. Thereby it was demonstrated that a halophilic strain, in this case *Halomonas sp.* (MA C), could be cultivated at non-sterile conditions with the setup. This confirms that this technology could be used for non-biotechnological industries and shows the overall robustness of the strain, because during the test huge deviations from the cultivation conditions occurred, for example of the pH-value and the salinity of the inoculum.

Study of the Dissolved Oxygen Concentration

It was found that the DO-concentration in the loop was significantly higher than in the reactor itself. This contradicts the initial assumption that was made during the design of the system that a temporary oxygen limitation could occur while the cell suspension runs through the loop, for which reason a second DO-sensor was installed in the loop. The explanation for this is that air bubbles from the gassing are carried off in the loop by the recirculation pump. While the broth runs through the loop tubing, there is sufficient time for the mass transfer of the oxygen from the bubbles to the broth and a quasi-equilibrium state is reached. By contrast, the contact time of the bubbles with the broth is significantly shorter in the reactor. This means that the loop acts as a downstream tubular reactor, which increases the oxygen mass transfer and thus higher dissolved oxygen concentrations are reached in the loop.

Furthermore, as expected, it was found that the oxygen mass transfer is lower in the 15 L pilot reactor than in the 1 L lab-scale reactor since significantly lower DO-concentrations were reached at the same volume specific aeration rate. While the air flow in the stirred tank reactor is used for oxygenation only, the gas flow is also needed for stirring in the airlift reactor. Hence, the airlift reactor achieves lower mixing quality and OTRs at the same volume specific aeration rate.

In addition, it could be demonstrated that the reactor pressure and measured DO-concentration in the broth are directly proportional. However, at increased pressures, foam formation was enhanced as well. After pressurization, foam was immediately pressed through the off-gas line and blocked the pressure control valve. Hence, an efficient method for foam control has to be implemented in order to operate the plant at elevated pressure.

Test of the Temperature Control

The temperature control unit in the switchboard, which was configured as a PID-controller with a single input value, achieved deviations of +0.5°C and -0.1°C from the setpoint. Hence, the desired temperature deviation of ±0.2°C specified in the URS were not reached. A reduction of these fluctuations from the target temperature could be accomplished by further optimizing the parameters of the temperature control unit. These parameters were automatically adjusted by the unit before the test by an optimization program according to Ziegler and Nichols. Another possibility would be to change the controller type to a 2-point-control and to adjust the thresholds manually.

During the test fermentation with a set temperature of 30°C, the temperature in the loop was about 1°C lower than in the reactor vessel because the tubing of the loop was not insulated. Hence, in order to minimize the heat losses of the system, the tubing of the loop should be insulated once the final loop setup is implemented. However, the currently occurring temperature drop of 1°C is probably small enough to not affect the cells negatively.

Test and Optimization of the pH-Control

After optimization of the thresholds of both 2-point-controls for acid and base addition, it was possible to keep the pH within in a 0.1 interval. When 0.5 molar HCl was added, periodic deviations of approximately +0.07 and -0.03 from the pH-setpoint were achieved. Hence, the required deviation of ±0.05, specified in the URS, could be reached with this setup by shifting the setpoint by 0.02.

However, the pH-value changed very slowly and abruptly. After the pH-control started adding acid to the reactor, it took approximately 2 min before the measured pH started to change. Then a sudden pH-drop occurred, for instance of 0.1 when 0.5 molar HCl was used. This lag can be explained by the arrangement of the pH probe in the loop. The size of this drop was found to be relatively independent of the limits of the 2-point-control but proportional to the concentration of the acid or base. For example, the drop was doubled to 0.2 when 1 molar acid HCl was used. Hence, the pH-drop can be reduced by further diluting these solutions. However, this results in significantly higher consumptions of these two solutions and thereby in higher dilution of the medium.

In conclusion, the accuracy of the pH control is mainly determined by the high measuring inertia of the system and not by the actual control parameters. Hence, the pH-control could be improved by increasing the loop flow rate to decrease the response time of the measurement. However, sudden changes of the pH-value occur that can potentially escalate the pH-control if the thresholds of the 2-point-controls are not adjusted to a specific concentration of acid or base.

Furthermore, it was found that the dosing pumps for acid and base were not functional at increased pressures. When they were inactive at elevated pressures, the liquid in their dosing lines was slowly pressed back into the storage tanks. Thereby, the tubing and the dosing pumps were filled with air and the pumps were no longer able to convey liquid. They had to be vented, before they were operational again. A possible solution to prevent this backflow of liquid and hence allow operation at increased pressure would be to install check valves in the dosing lines between the vessel and the pumps.

Test of the Level Control

The functionality of the level control approach in batch mode (see Chapter 6.1.3.6) could be demonstrated. The liquid level in the reactor was maintained at a constant level by periodically either adding culture medium or removing broth through the bleed line, depending on the state of the level switch. For this test run, a relatively short time interval of 30 min was chosen for the level control to be on the safe side and prevent a flooding of the reactor at all costs. However, due to the level sensor's measurement hysteresis of 2 mm, slightly too much fluid was added or removed whenever the controller was activated. This lead to a higher consumption of compensation fluid (culture medium) and a higher bleed flow than necessary. Especially the minimization of the bleed flow is essential since biomass is removed by it. Therefore, the interval of the level control timer has to be extended. For future operations with a fully developed continuous process, the period can be significantly larger (e.g. 2 h) as no significant level changes occur in batch mode.

Moreover, a problem of the usage of feed for level control in batch mode is that it contains substrate and thereby complicates the subsequent process evaluation. This can be seen in the small periodic peaks at the end of the DO-curves in Figure 72. They occurred periodically, wherever feed - and thus new substrate - was added to the reactor to keep the level constant. Hence, instead of feed, the utilization of substrate free culture medium for level compensation in batch mode would be advantageous.

Test of the Improvised Off-gas Cooler

For the batch fermentation, an improvised off-gas cooler was used to simulate the functionality of a Liebig-cooler. However, during the test, almost no water could be separated with it. The reasons for that could have been that the off-gas was not very humid or, less likely, that the heat transfer surface of the cooler was too small for condensation. Hence, additional experiments were required to find out whether or not an off-gas cooler was required for the pilot process. It was decided to operate the continuous fermentation without the improvised cooler and to measure the water loss and hence the humidity of the off-gas by the mass balance gap throughout the fermentation.

6.3.3.2 Discussion of the Continuous Fermentation

Biomass Concentration

Although the biomass concentration could be quadrupled in the batch fermentation, no significant increase could be achieved in continuous mode by using the cell retention membrane. During the continuous fermentation, which lasted for 24.5 h, the biomass slightly increased from 1.5 to 1.73 g/L at first and remained relatively constant afterwards. This means that the concentration could be maintained in the reactor, but the desired significant increase of the biomass concentration by means of the microfiltration membrane could not be achieved yet. There are several possible reasons for that. First, the used feed rate could have been too low, since it was only set at about a third of the designed flow (see Table 2). The HPLC-analysis of the filtrate confirmed that the feed flow was less or equal than the maximum dilution rate since the substrate concentration in the filtrate was below the detection limit. Second, the process time in continuous mode could have been too short and lastly, the cells may have been stressed due to the previous, fluctuating operation conditions. Thus, further long-term experiments are necessary to determine the operability of the cell retention system.

Study of the Flow Controllers for Feed and Filtrate

During the continuous fermentation, the flow controllers of feed and filtrate were able to create a stable operating state and relatively constant flows over time, as the linear progress of the weight signals in Figure 77 indicated. However, both flows fell distinctly below their target values and the actual local flow rates were fluctuating strongly, especially the filtrate flow that was adjusted by intermittently opening the Bürkert GmbH micro-valve for a controlled period. The feed flow controller was significantly more precise. The large deviations from the set value of the feed flow resulted from the level control, which increased the flow periodically. In the preliminary version of the continuous level control that was used for the test, the filtrate flow was stopped for safety reasons whenever the feed flow was increased for level compensation. This affected the filtrate flow controller negatively and is presumably the reason why the measured flow rates of feed and filtrate were below their set values. Hence, in the final control program, the feed and filtrate flow should be decoupled when the level control is active and therefore be able to run at the same time.

Furthermore, it has to be minded that smaller balances with an accuracy of 0.1 g were used to calculate the flow rates in the test run instead of the designed ones with a precision of only 10 g. Thus, the flows will respond slower in future operation when the designed balances with larger measuring range are utilized. Therefore, the control parameters of the PID-flow-controllers will have to be adjusted to achieve sufficient response times of the flow controllers.

Study of the Level Control in Continuous Mode

Compared to the designed level control approach from Chapter 3.4.3.6, a different method for level control in continuous mode was used for the test run. This simplified approach is described in Chapter 6.1.3.7. Its functionality could be demonstrated during the experiment. Thereby, the filtrate flow was set slightly larger than the feed flow so that the liquid level in the reactor slowly decreased. That way, the liquid level was slightly below the level switch during most of the operation time - the desired state to avoid flooding. Then, the level control was activated periodically and increased the feed pump's capacity to increase the liquid level to the 15 L mark. Despite the fact that the flow rates of filtrate and feed were varying and not nearly of the same size at the start of the test run, the level control was functional and achieved safe operation.

The initially designed level control approach from Chapter 3.4.3.6 works by varying the filtrate flow and keeping the feed flow constant. This method is advantageous regarding cell physiology and simplifies process evaluation, but the control program is more complicated. However, this superior approach has to be implemented and tested before it can be used for future operations.

Lastly, it has to be noted that the impact of changing gassing rates and thus different gas holdups on the level control has not been tested yet. The response of the level control to variable aeration rates has to be investigated for safe processing.

Study of the Mass Balance and the Water Loss

The local mass balance showed that a steady state with an accuracy ±10 g, which is smaller than the measuring error of the level sensor, had been achieved. Thus, it was demonstrated that the system is capable of executing a safe and robust continuous process, even with not fully developed flow controllers.

The total mass balance of the continuous fermentation was calculated to determine the water loss through off-gas humidity. The resulting mass balance gap was caused by the water loss as well as by the control inaccuracies, especially the switching hysteresis of the level sensor. It was found that the water loss per day minimally amounts to 107.6 g, when the maximum level sensor error is used, and maximally to 173.3 g without level switch inaccuracy. The former value equals a loss of 0.67% of the reactor volume per day and the latter 1.09%. The corresponding calculated water loads of the off-gas are 0.012 and 0.02 kg water per kg air. Both values are very small and indicate that the humidity of the exhaust gas is very low. The off-gas is not saturated by far and the calculated water load is only slightly larger than the target load of 0.01 that was used for off-gas cooler dimensioning in Chapter 3.5.5.

Hence, the experiments showed that the water loss through the off-gas at a reactor temperature of 30°C and without overpressure is acceptably small. Therefore, the

use of an off-gas cooler is not necessary when these process parameters are used. However, at different operating conditions, especially at higher temperatures, that may no longer be the case. When operating the plant without an off-gas cooler, the water loss is compensated by the level control. But since the compensation medium contains salt, a slight increase of the salt concentration in the broth will occur over time.

Study of the TMP and Membrane Fouling

Like the functionality test of the membrane module (Chapter 6.1.2.3), this experiment showed that the general equation for the TMP according to Eq. 9 is not feasible for this application since it results in a negative TMP. Furthermore, it could be confirmed that the membrane pressures p_1 (membrane feed pressure), p_2 (retentate pressure) and p_3 (filtrate pressure) are mainly determined by the hydrostatic pressure and not by the pressure loss over the filter since the offset between the three pressures as well as to the reactor pressure is constant regardless of the total pressure.

Moreover, no fouling could be detected during the examined time period of 24.5 h as the pressures did not decrease over time. However, further long term experiments are required to show the fouling behaviour of the membrane.

7 Suggested Improvements

Perceptions for improvement and optimization of pilot plant's setup as well as process control were gained during the test phase. These improvements are presented in the following.

7.1 Improvements of the Setup

Anti-Foam Addition

A new method for adding the anti-foam agent has to be developed. It was manually and periodically added through the excess port on the lid during the test runs. But the gassing has to be stopped and the reactor has to be depressurized in order to safely open this port. This procedure is time-consuming, complex and could even affect cell growth. Therefore, anti-foam should be continuously added by a dosing pump. Another, even simpler method would be to directly add the agent to the feed.

Foam Control

It was found that the foam formation during fermentation significantly increases with the reactor pressure and the gassing rate. Even though anti-foam was added periodically during the tests, foam was immediately pressed through the off-gas line when the reactor pressure was increased. Moreover, the overflowing foam blocked and disabled the pressure control valve. Hence, an efficient method for foam control has to be implemented in order to operate the plant at elevated pressure.

Foam reduction by anti-foam agents might not be sufficient for that purpose, as negative effects of anti-foams upon oxygen transfer by reduction of the mass transfer coefficient and gas hold up have been reported [52]. This phenomenon could be observed during the batch experiment when the DO-concentration in the reactor decreased to almost 0% for several hours after anti-foam (Struktol J673-1) had been added. However, since anti-foams are also reported to increase the k_La-value [52], tests with other agents may be necessary. If the foam cannot be sufficiently reduced by an anti-foam agent, a mechanical foam separator has to be installed in the off-gas line.

Hygienic Loop Piping

The implemented loop tubing layout does not provide total drainability. Instead of being inclined downwards, so that the cells automatically flow back into the reactor, the lower part of the loop piping was inclined upwards. That way, air bubbles are forced to leave the piping and therefore gas cannot accumulate inside the tubing, where it could potentially distort the signals of the pressure-, pH- and DO-probes.

The experiments showed that no accumulation of air bubbles occurred in the loop. Furthermore, the lower part of the loop tubing was examined after the test fermentations to find out if biomass had been deposited in corners and crevices of the plastic fittings, but no residues could be found. However, the experiment lasted only about 3 days and relatively low biomass concentrations were reached. Therefore, for future long lasting processes, the loop layout has to be redesigned to achieve total drainability.

Furthermore, the loop tubing is not designed hygienically since the used plastic screw connections have treads and small crevices on the inside. These parts were chosen to ensure a flexible layout of the piping and allow subsequent changes to the setup. However, once the process is fully developed, the plastic pipes with screw connections should be replaced with more robust, welded metal tubes with Tri-Clamp connections for a more hygienic installation that is easier to clean.

Salt Removal

A system to remove salt from the off-gas should be implemented in order to protect the off-gas analyser from deposition of salt crusts, which could damage it. The simplest method to achieve that would be to filter the gas.

7.2   Improvements of the Process Control

Optimization of the Control Parameters

As already discussed in Chapter 6.3, the performance of the temperature-, pH-, pressure-, flow- and level control loops could probably be significantly improved by optimizing their control parameters. This requires further experiments.

Determination of the Characteristic Curves of all Valves and Pumps

In order to achieve steady state, the flow rates have to be kept constant, even when the operation parameters change, especially the reactor pressure. Therefore, the characteristic curves of all valves and pumps at different pressures have to be measured and the gained data has to be implemented into the process control. This is most important to guarantee a continuous process with variable reactor pressures.

Temperature Control

The temperature control has to be improved for safety reasons. At the moment, the signal from the temperature probe in the reactor is sent to the temperature control unit in the switchboard by the process control system.

However, when using this method, the plant cannot be operated without the PCS. Also a system failure or an unexpected breakdown of the PCS-connection can cause a malfunction of the temperature control. Then, the temperature controller does not receive a signal anymore, assumes that the temperature is too low and activates the heating pad which will heat until it gets destroyed. Therefore, in order to prevent the

reactor from overheating, a second temperature sensor inside the heating jacket has to be connected to the temperature control unit in the switchboard. Another possibility would be to implement a system that activates the kill switch of the plant if the process control system fails or is shut down. This second measure would further increase the overall safety of the system.

Improvement of Analytics

To increase process monitoring and process understanding, two new probes are planned to be installed in the loop and integrated into the process control: a turbidity probe to measure the biomass concentration and a specific probe for the product, for example the optical estimation of the bacterioruberin concentration by Raman spectroscopy [53].

8   Documentation

The last phase of this master thesis was the documentation of the setup for subsequent usage by new operators. It included the creation of the following documents:

- **Stocklist:** the stocklist of all process components can be found in Appendix 4. It contains the limits of use for each equipment part as well as the plug-in positions in the switchboard for each electronic device. Furthermore, a special stocklist for the tubing parts from EM-Technik GmbH was created, which is given in Appendix 5.

- **Equipment Documentation:** the manuals, offers and other relevant documents of the equipment parts were collected and put together in folders, which can be found in the archives of the department of bioprocess engineering. Besides, a digital copy was stored on the network drive of the department.

- **Circuit Diagram:** The circuit diagram of the switchboard, which was originally created by the manufacturer of the reactor skid, was adapted. The modified, as-built diagram can be found in Chapter 9.5. It contains a detailed construction drawing of the fully assembled switchboard as well as the plug-in positions of the power and signal lines on the terminal blocks of the switchboard.

- **As-Built Process Flow Diagram:** the initial PFD by Nicole Mahler was adapted and extended. The as-built process flow diagram is given in Appendix 2.

- **Operating Instructions**: for the use of the reactor skid were created. These can be found in the following Chapter 8.1.

8.1   Operating Instructions

The following operating manual only covers the reactor skid, but not the media skid and the control program for automation. Since this thesis was submitted in June 2016, future changes to soft- and hardware have to be considered before using this manual. The labelling corresponds to the abbreviations in the process flow diagram in Appendix 2.

1. Electrical Connection

1.1.   Open the hatch of the switchboard with the designated key.

1.2.   Plug the yellow power cable into a 230V AC socket.

1.3.   Check if the kill switch is pressed and deactivate it if so.

1.4.   Turn the main switch to "On". Then, the 24 V DC power supply of the switchboard and thus all sensors and control valves are activated.

1.5.   Press the green button to activate the 230V AC power supply of the switchboard and the heating pad. Be careful because the heating pad immediately starts heating after the green button has been pressed. To prevent it from overheating, enter a temperature setpoint below ambient temperature (e.g. 10°C) on the temperature control unit in the switchboard. In order to do that, press the "S"-button of the device (Figure 79) and adjust the set value with the arrow buttons afterwards. To confirm the input, press the "S"-button again.

1.6.   Close the switchboard's hatch.

Figure 79: Control Panel of the Temperature Control Unit

2. Preparation of the Setup

2.1. Position the rack and fix the rollers on the rack.

2.2. Connect the lines of the three dosing pumps to the ports on the lid with the Tri-Clamps.

2.3. Place a DO-sensor (QIRC 011) and the pH-probe (QIRC 009) in the flow cells in the loop as well as the other DO-sensor (QIRC 002) in the insertion housing on the side of the reactor. The DO-sensors must not be turned left during insertion or else of their measuring caps could be unscrewed. Connect the probes with their corresponding cables (red for DO, black for pH).

2.4. Before the reactor is filled with liquid, check if the system is tight. The loop piping has to be assembled and all lateral ports and nozzles on the reactor (gassing port, loop inlet, loop outlet, DO-port, level sensor nozzle) and the drain valve on the bottom have to be closed.

3. Start-up of the Loop Pump (P4)

3.1. Before activating the loop pump, it has to be checked if its outlet line is open. If a shut-off valve in the loop is closed, the plastic single-use pump heads are destroyed due to overpressure when the pump is started. Hence, always either the bypass- or membrane line of the loop has to be open when the circulation pump is running. Furthermore, the valve positions, especially of the 3-way ball valve (V11), must not be changed while the pump is activated. Whenever the valve setting is adjusted, the loop pump has to be shut down beforehand.

3.2. To start up the pump, press the green button on its top (see Figure 80), labelled with "RUN". Then, it is ready to receive a capacity-setpoint from the process control system (PCS). The magnitude can be entered in Lucullus or at the Siemens-box. When a capacity larger than 0 is set, the pump starts running. To stop it again, enter a flow of 0. The pump allows dry running.

3.3. To shut down the pump, press the red "STOP"-button on its top. Then, it will not react to changes of the setpoint anymore until the green "RUN"-button is pressed again.

Figure 80: Control Panel of the Loop Pump

4. Start-up of the Dosing Pumps for Acid (P1), Base (P2) and Feed (P3)

4.1. Connect the inlet lines of the pumps to the media storage tanks and check if the suction hoses are submerged in the fluid.

4.2. Remove the outlet lines of the pumps from their port on the lid and put them in beakers. That way, the actuation procedure can be monitored more easily and the ventilation time is reduced.

4.3. Power up the pumps and set them to full capacity. The setpoint (100% flow) for the feed pump can be entered via the PCS. Since the acid and base pump work digitally, they are powered by pressing "ON" in Lucullus or at the Siemens-box. Their flow rate can be adjusted manually by turning the control wheel on the pumps to 100%.

4.4. Once fluid runs from the outlet lines into the beakers in significant amounts, the pumps can be vented by unscrewing the plug of their ventilation holes, shown in Figure 81. Several drops should now spray from the holes with each stroke of the pumps.

4.5. Screw in the plug again. The pumps should now be less noisy.

4.6. Connect the outlet lines with the Tri-Clamp ports on the lid.

4.7. Adjust the pumps' capacities to the desired values.

4.8. The dosing pumps are now operational. Make sure that their reservoirs are always filled because if they get empty during operation and the pumps suck in air, they have to be vented again. For that, the process or at least the gassing has to be stopped for a short time.
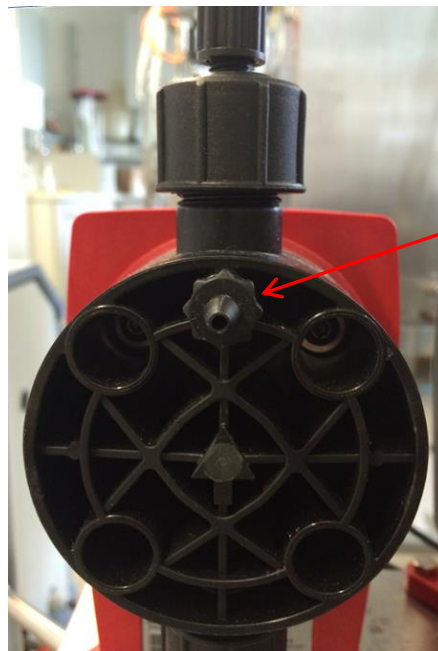

Figure 81: Dosing Pumps: Ventilation Plug

5. Start-up of the Aeration

5.1. Make sure that the gassing line is tightly connected to the pressure reducer (V1), MFC (FRC 019) and the check valve (V2). The MFC has to be placed well above the reactor lid to avoid contamination with the broth if a backflow due to hydrostatic pressure occurs when the check valve fails.

5.2. Before starting the aeration, check if all ports on the lid are closed. Elsewise, the fluid could overflow. However, if the open aperture on the lid is big enough, e.g. the excess port, and the gas flow is low, the pressure can be released sufficiently and no overflow occurs.

5.3. Set the inlet flow of air to 100% (30 L/min) via the PCS (Lucullus or Siemens-box).

5.4. Slightly open the compressed air supply by the faucet and adjust the pressure reducer to a pressure above 3 bar to be able to operate in the full pressure range of the plant.

5.5. A red light is now shining on the MFC. It indicates that the flow is lower than the entered target value. Now, the inlet air flow has to be increased by means of the compressed air faucet until the colour of the light switches to green. Then, the required flow of 30 L/min is reached and the MFC is ready to operate in its whole flow range.

5.6. Adjust the aeration rate to the desired value by the PCS. Set the flow to 0 to shut off the gassing.

6. Start-up of the Pressure Control

6.1. Install the pressure control valve in the off-gas line by the compression fittings. The mounting direction of the valve is indicated by an arrow on the housing and has to be minded. Be careful because the device gets extremely hot during operation.

7. Sanitization (with 0.5 molar NaOH-Solution at 50°C)

7.1. Open all valves in the loop and adjust the 3-way ball valve (V11) so that all three lines are open (see Figure 83, right).

7.2. Open the excess port on the lid.

7.3. Rinse the interior of the vessel with water.

7.4. Fill the reactor with 0.5 molar NaOH-solution through the excess port by using a funnel (see Figure 82). The liquid level has at least to be above the inlet nozzle of the loop so that the loop pump can work.

7.5. Close the excess port on the lid.

7.6. Start the circulation of the fluid by activating the loop pump.

7.7. Enter the temperature setpoint of 50°C on the temperature control unit in the switchboard.

7.8.   Start slightly aerating the reactor to increase the mixing and prevent overheating.

7.9.   Once the set temperature is reached, sanitize for one hour.

7.10. Meanwhile, flush the three dosing pumps with base. In order to do that, their inlet pipes have to be put in a NaOH-tank and then they have to be powered up until fluid flows out of their outlet lines.

7.11. Shut off the aeration and the loop pump.

7.12. Drain the system from the base by opening the drain valve below the reactor. Open the excess port on the lid to decease the drainage time.

7.13. Fill the rector with demineralized water and flush it again for several minutes. Drain it again and repeat this procedure to remove all residues from the cleaning agent.

Figure 82: Procedure to Fill the Reactor via the Excess Port on the Lid

8. Fermentation Preparation

8.1.   Adjust the loop valves so that the fluid either flows through the bypass line (batch mode; Figure 83 left) or through the membrane module (continuous mode; Figure 83 right) by adjusting the shut-off valves V8, V9 and the 3-way ball valve V11. The dots on the handle of the 3-way ball valve indicate which lines are open.

8.2.   Open the hatch of the switchboard and calibrate the pH-probe with the transmitter inside the switchboard. For that, the sensor has to be removed from the flow cell and put into two reference solutions with defined pH-values of 4 and 7. Close the hatch.

8.3.   Calibrate the off-gas analyser and connect it to the off-gas line. Depending on the gassing rate, either the whole gas flow can be led through the analyser or the flow has to be split by means of the two off-gas valves (V4, V5).

8.4.   Fill the reactor with culture medium via the excess port on the lid. The level has at least to be above the inlet nozzle of the loop so that the loop pump can work.

8.5. Close the excess port on the lid.

8.6. Start the circulation of the fluid by activating the loop pump and adjust the capacity.

8.7. Start the aeration by adjusting the inlet air flow via the PCS.

8.8. Set the reactor pressure to the target value by the PCS by entering the opening of the pressure control valve's aperture in percent.

8.9. Enter the set temperature on the temperature control unit in the switchboard.

8.10. DO-calibration: Once all the fermentation parameters are set and constant, the DO-calibration can be started by setting the upper limit for the two DO-probes via the PCS (100% DO). Next, shut off the inlet air and replace it with a nitrogen flow. Once the DO-concentration in both probes is constant, the lower calibration point (0% DO) is reached and can be set with the PCS.
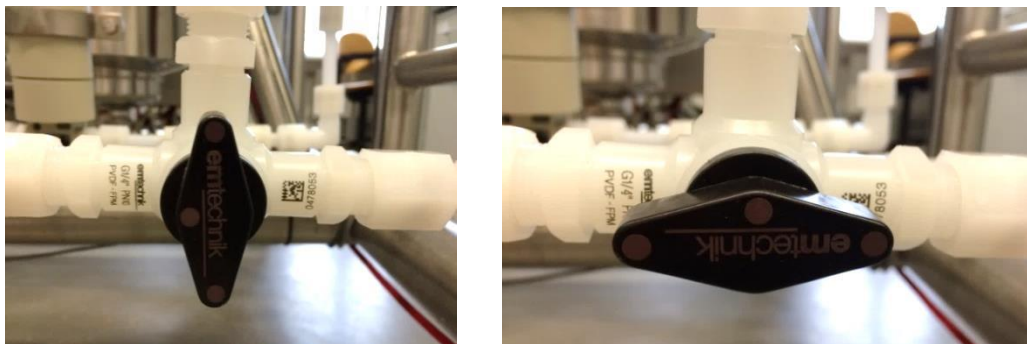
Figure 83: Position of 3-Way Valve for Batch (left) and Continuous Mode (right)

9. Inoculation (with 1 L Inoculum)

9.1. Turn off the loop pump and the gassing if activated.

9.2. Open the excess port on the lid.

9.3. Drain approximately 2 L of culture media through the drain valve (V15).

9.4. Start gassing with the flow rate chosen for the fermentation. As a result, the fluid level in the reactor rises due to the gas holdup.

9.5. Fill in the inoculum through the excess port on the lid.

9.6. Add the drained culture media until the level signal switches from 0 to 1. This is indicated in Lucullus. That way, the fermentation is started with a working volume of exactly 15 L in the reactor.

9.7. Add anti-foam agent via the open port if necessary.

9.8. Stop the gassing and close the excess port on the lid.

9.9. Start the air flow again and turn on the loop pump.

10. Starting the Process Control Program

10.1. Start the process control program and the data recording in Lucullus.

10.2. Enter the desired setpoints for pH-value, temperature, pressure, flow rates, etc. and the timer for level control.

10.3. Start the fermentation.

11. **Procedure to Open the Anti-Foam/Excess Port During Operation**

11.1. Shut off the gassing.

11.2. Once the reactor pressure has sunk to 0 barg, indicated by the manometer on the lid, the port can be opened without an overflow of liquid.

11.3. Add anti-foam-agent.

11.4. Close the port and then start the aeration again.

12. **Shutdown**

12.1. Stop the Lucullus operation.

12.2. Enter a low temperature setpoint below the ambient temperature (e.g. 10°C) on the temperature control unit to prevent further heating.

12.3. Shut off the gassing and the loop pump. Wait until the reactor is completely depressurized.

12.4. Open the excess port on the lid.

12.5. Drain the broth via the drain valve (V15).

12.6. Sanitize reactor, loop, dosing pumps, and the dosing lines with 0.5 molar NaOH-solution at 50°C as described in section 7 of this manual.

12.7. Enter a low temperature setpoint below the reactor temperature (e.g. 10°C) on the temperature control unit to prevent heating at the next start-up of the plant.

12.8. Press the red button on the side of the switchboard to shut down the 230 V AC power supply.

12.9. Turn the main switch to "Off" and disconnect the yellow power cable.

13. **Final Cleaning**

13.1. Disconnect all ports on the lid.

13.2. Remove the safety valve with its discharge line. About 1.5 m space above the reactor is required for that task and the rack has probably to be moved.

13.3. Open the four metal clamps that seal the lid by unscrewing them.

13.4. Remove the three metal dosing pipes from the reactor lid.

13.5. Detach the lid.

13.6. Manually clean all removed parts and areas of the reactor that still show signs of contamination after sanitization.

13.7. Inspect the inside of the reactor and the dissembled components for signs of corrosion.

13.8. Reassemble the parts to the reactor.

8.1.1 Manual for Loop Tubing Assemblage

The loop tubing mainly consists of PVDF compression fittings from EM-Technik GmbH. Each connection is made up of the following five parts:
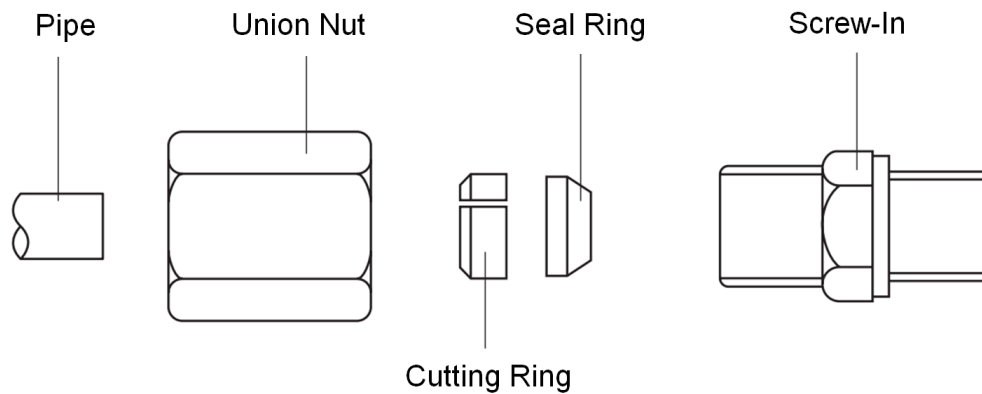
Figure 84: EM-Technik GmbH Compression Fitting Parts [32]

The assemblage of an EM-Technik compression fitting on a pipe is depicted in Figure 85 and described below:

1. Arrange the five parts in the order displayed in Figure 84. Mind the orientation of the cutting and seal ring.
2. Put the union nut and both rings on the end of the pipe. Depending on the size of the fitting, approximately 1 cm of the pipe has to stick out at the end of the tube after the seal ring.
3. Insert the pipe's end into the screw-in.
4. Slide the union nut towards the screw-in and bolt them together with two wrenches. Thereby the hex on the screw-in has to be fixed.
5. Connect the compression fitting with another part of the loop tubing.
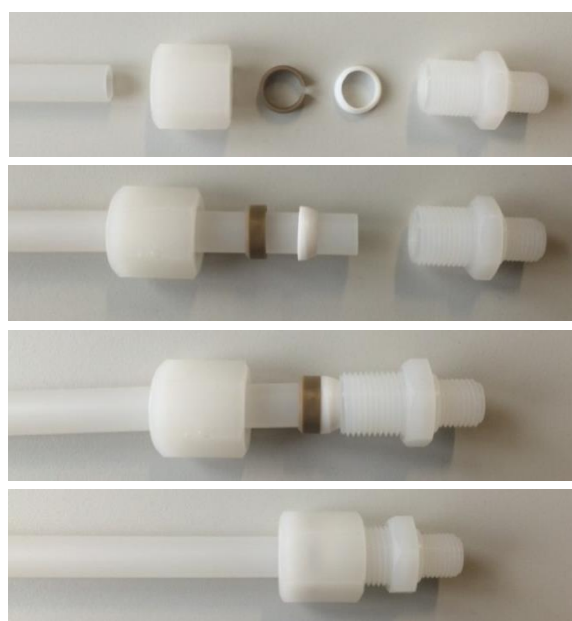
Figure 85: EM-Technik GmbH Compression Fitting Assemblage

The EM-Technik compression fittings with thread connections do not have to be sealed. However, all other parts of the plant with threads, like the pressure sensors and their adapter pieces as well as the level switch, have to be sealed with Teflon tape or with thread seal tape.

Furthermore, when bolting a compression fitting with thread connection to another one, the second fitting has to be fixed on the hex of its screw-in by a wrench. That way, they cannot unscrew each other.

9   Summary and Outlook

A worldwide unique, corrosion-resistant airlift bioreactor setup for the cultivation of halophiles on pilot-scale was designed and implemented. The system can be pressurized and is equipped with a cell retention system to increase the productivity. The process was scaled up from a 1 L stirred tank reactor bioreactor that is used for biotechnological treatment of industrial waste water by halophilic microorganisms by the department of bioprocess engineering of the Vienna University of Technology.

The main targets of this master thesis were the design and construction of the novel plant as well as to make it operational. The main challenge in the design phase was the selection and especially the combination of equipment that is suitable for the highly corrosive medium as well as pressure-resistant. Another essential task was the development of a novel, efficient control approach to maintain a constant liquid level in the vessel.

After assembly of the pilot plant, test fermentations with a halophilic strain at non-sterile conditions were performed to demonstrate the operability of the system. In a batch fermentation, an exponential cell growth could be observed and in the subsequent continuous fermentation with cell retention, a steady state could be achieved by programmed flow controllers. Despite the fact that a preliminary version of the automation approach was used for both test runs, sufficient control accuracy could be reached.

Both test fermentations could not be executed with overpressure because it was found that the foam formation significantly increases with the reactor pressure and the gassing rate. Hence, an efficient method for foam control has to be implemented in order to operate the plant at elevated pressure. Furthermore, a new way to control the membrane flows has to be realized since it was found that the general equation for transmembrane pressure is not feasible for this application.

The next steps in the development of the pilot process will be to implement the final control approach and to optimize the control parameters. Once the plant is fully developed and automated, the flows can be increased until the designed throughput is achieved. Then, the novel pilot plant will serve for the investigation of the long-term stability of the biological system of halophiles, robust bioprocess quantification and eventually be used for upscaling to industrial plants. Initially, the studies on industrial waste water treatment will be continued on a larger scale with the target to purify 50 L industrial effluent per day. But the versatile plant will also be able to be utilized for other processes with halophiles like the production of bacteriorhodopsin. In addition, it will be examined whether this new reactor technology may be used for other extremophile processes and in other fields of biotechnology, particularly the biorefinery.

10   References

[1] **Deive, F. J., E. López, A. Rodríguez, M. A. Longo, M. Á. Sanromán.** Targeting the Production of Biomolecules by Extremephiles at Bioreactor Scale. *CHEMICAL ENGINEERING & TECHNOLOGY, September 2012: DOI: 10.1002/ceat.201100528.*

[2] **Lorantfy, Bettina, Seyer, Bernhard and Herwig, Christoph.** Stoichiometric and Kinetic Analysis of Extreme Halophilic Archaea on Various Substrates in a Corrosion Resistant Bioreactor. *New Biotechnology Volume 31, Number 1, January 2014: 80-89: DOI:10.1016/j.nbt.2013.08.003.*

[3] **Mahler, Nicole and Herwig, Christoph.** Aufreinigung salzbelasteter Abwässer mit halphilen Organismen. *Wasser + Abwasser Industrie.* Modernisierungsreport 2015/2016.

[4] **Ventosa, Antonio and Nieto, Joaquin.** Biotechnological applications and potentialities of halophilic microorganism. *World Journal of Micribiology and Biotechnology, January 1995: DOI: 10.1007/BF00339138.*

[5] **Margesin, Rosa and Franz, Schinner.** Potential of halotolerant and halophilic microorganisms for biotechnology. *Extremophiles (2001) 5:73–83, DOI: 10.1007/s007920100184.*

[6] **McGenity, Terry.** http://www.microbiologysociety.org/. *The immortal, halophilic superhero: Halobacterium salinarum – a long-lived poly-extremophile.* [Online] [Cited: 17 05 2016.] http://www.microbiologysociety.org/all-microsite-sections/microbiology-today/index.cfm/article/A2E0A8E8-A416-4F3C-92301F31A595FFB5.

[7] **Tromans, Desmond.** Oxygen solubility modeling in inorganic solutions: concentration, temperature and pressure effects. *Hydrometallurgy 50 (1998) 279-296.*

[8] **Lorantfy, Bettina, Ruschitzka, Paul and Herwig, Christoph.** Investigation of physiological limits and conditions for robustbioprocessing of an extreme halophilic archaeon using external cell retention system. *Biochemical Engineering Journal 90 (2014) 140-148.*

[9] **Ruschitzka, Paul.** Integrated bioprocess characterization and optimization studies for highly saline industrial wastewater treatment with extreme halophiles in laboratory scale: Institut für Verfahrenstechnik, Umwelttechnik und Techn. Biowissenschaften der Technischen Universität Wien, 2014.

[10]. **Träger, Michael et al.** Comparison of Airlift and Stirred Reactors for Fermentation with Aspergillus niger. *JOURNAL OF FERMENTATION AND BIOENGINEERING Vol. 68, NO. 2, 112-116. 1989.*

[11] **Chmiel, Horst.** *Bioprozesstechnik.* Heidelberg : Spektrum Akademischer Verlag, 3. Auflage 2011. ISBN 978-3-8274-2476-1.

[12] **Krahe, Martin.** *Biomedical Engineering: Reprint from Ullmann's Encyclopedia of Industrial Chemistry.* s.l. : Bioengineering AG, 8336 Wald, Switzerland.

[13] **Merchuk, J. and Gluz, M.** www.bioreactorsciences.com. *BIOREACTORS, AIR-LIFT REACTORS.* [Online] [Cited: 17.04.2016] http://www.bioreactorsciences.com/uploads/1/8/5/9/18594674/bioreactors_air-lift_reactors_merchuk_gluz.pdf.

[14] **Warnock, James and Al-Rubeai, Mohammed.** Bioreactor systems for the production of. *BIOTECHNOLOGY AND APPLIED BIOCHEMISTRY.* 2006.

[15] **Präve, Paul et al.** *Handbuch der Biotechnologie.* München Wien : R.Oldenburg Verlag, 1994. ISBN 3-486-26223-8.

[16] **Merchuk, Jose.** Airlift Bioreactors: Review of Recent Advances. *THE CANADIAN JOURNAL OF CHEMICAL ENGINEERING, June 2008: DOI: 10.1002/cjce.5450810301.*

[17] **Pall Corporation.** Einführung in die Tangentialflussfiltration für Anwendung im Labor und der Verfahrensentwicklung. *http://www.pall.de/.* [Online] [Cited: 07.05.2016.] http://www.pall.de/main/Laboratory/Literature-Library-Details.page?id=34212.

[18] **GE Healthcare Life Sciences.** Cross Flow Filtration Handbook. *http://www.gelifesciences.com/.* [Online] [Cited: 07.05.2016] http://www.gelifesciences.com/webapp/wcs/stores/servlet/catalog/en/GELifeSciences-at/products/AlternativeProductStructure_16071/#.

[19] **Plastics International.** Food Handling and Equipment. *http://www.plasticsintl.com/.* [Online] [Cited: 22.04.2016] http://www.plasticsintl.com/food_compliant_materials.html.

[20] **Professional Plastics.** http://www.professionalplastics.com/. [Online] [Cited: 22.04.2016.] http://www.professionalplastics.com/de/FDAApprovedPlasticMaterials.html.

[21] **Hezayen, F.F. et al.** Polymer production by two newly isolated extremely halophilic archaea: application of a novel corrosion-resistant bioreactor. *App Microbiol Biotechnol (2000) 54: 319-325.*

[22] **Reichhold LLC.** www.reichhold.com. *FRP Material Selection Guide.* [Online] [Cited: 23.04.2016] http://www.reichhold.com/corrosion/docs/Materials%20Selection%20Guide%20Final %20Version.pdf.

[23] **Kain, Vivekanand.** Corrosion-Resistant Materials. *Functional Materials: Preparation, Processing and Applications, 2012, Pages 507-547.*

[24] **Hoar, T.P. and Mears, D.C.** Corrosion-resistant alloys in chloride solutions: materials for surgical implants. October 1966. DOI: 10.1098/rspa.1966.0220

[25] **Kopeliovich , Dmitri.** www.substech.com. *Corrosion and oxidation.* [Online] [Cited: 17.05.2016] http://www.substech.com/dokuwiki/doku.php?id=corrosion_and_oxidation.

[26] **HAYNES International Inc.** www.haynesintl.com. [Online] [Cited: 19.04.2016] https://www.haynesintl.com/pdf/h2019.pdf.

[27] **Qin-Ying, Wang et al.** Microstructures, mechanical properties and corrosion resistance of Hastelloy. *Journal of Alloys and Compounds 553 (2013) 253–258.* 2012.

[28] **Rollbusch, Philipp et al.** Hydrodynamik in Hochdruckblasensäulen. *Chemie Ingenieur Technik 2013, 85, No. 7, 1107-1111.*

[29] **Ruzicka, M. et al.** Homogeneous–heterogeneous regime transition in bubble columns. *Chemical Engineering Science 56 (2001) 4609-4626.*

[30] **Contreras, Antonio et al.** Influence of sparger on energy dissipation, shear rate, and mass transfer to sea water in a concentric-tube airlift bioreactor. *Enzyme and Microbial Technology 25 (1999) 820-830.*

[31] **VDI-Gesellschaft Verfahrenstechnik und Chemieingenieurwesen (GVC).** *VDI-Wärmeatlas, 11. Auflage.* Düsseldorf : VDI-Gesellschaft Verfahrenstechnik und Chemieingenieurwesen, 2013. ISBN 978-3-642-19980-6.

[32] **EM-Technik GmbH.** http://www.em-technik.de/. [Online] [Cited: 10.05.2016] http://www.em-technik.de/assets/catalog/de/EM-Technik-DE.pdf.

[33] **Mettler-Toledo GmbH.** http://int.mt.com/. *InPro 3250 / 3250SG / 3250i pH Probes.* [Online] [Cited: 11 05 2016.] http://int.mt.com/int/en/home/products/Process-Analytics/pH-probe/pH-ORP-probe/InPro-3250.html.

[34] **Mettler-Toledo GmbH.** http://us.mt.com/. [Online] [Cited: 10.05.2016] http://us.mt.com/dam/MTPRO/PDF/FF/FF_M200_EasyLine_PP_Analytical_en_5212 1503_Oct13.pdf.

[35] **ALMATEC Maschinenbau GmbH.** http://www.almatechnik.ch/. [Online] [Cited: 11.05.2016] http://www.almatechnik.ch/downloads/de/02_Quattroflow/02_QF150SU/02_Manual%20QF150SU.pdf.

[36] **Lutz-Jesco GmbH.** http://www.lutz-jesco.com/. [Online] [Cited: 11.05.2016] http://www.lutz-jesco.com/produkte/dosierpumpen/magnet-membrandosierpumpen/magdos-la.html.

[37] **Lutz-Jesco GmbH.** http://www.lutz-jesco.com/. [Online] [Cited: 11.05.2016] http://www.lutz-jesco.com/produkte/dosierpumpen/magnet-membrandosierpumpen/magdos-lb.html.

[38] **Brooks Instrument LLC.** http://www.brooksinstrument.com/. [Online] [Cited: 11.05.2016] http://www.brooksinstrument.com/products/mass-flow-controllers/thermal-elastomer-sealed/gf40-series.

[39] **GE Healthcare Life Sciences.** http://www.gelifesciences.com/. *Laboratory and Pilot Scale Microfiltration Hollow Fiber Cartridges.* [Online] [Cited: 11.05.2016] http://www.gelifesciences.com/webapp/wcs/stores/servlet/catalog/en/GELifeSciences-at/products/AlternativeProductStructure_16073/56410311.

[40] **Bürkert Contromatic GmbH.** www.buerkert.at. *Typ 2871 - Direktwirkendes 2/2-Wege-Standard-Proportionalventil.* [Online] [Cited: 11.05.2016] https://www.buerkert.at/de/type/2871.

[41] **Bürkert Contromatic GmbH.** www.buerkert.at. *Typ 8605 - Ansteuerelektronik für Proportionalventile.* [Online] [Cited: 11.05.2016] https://www.buerkert.at/de/type/8605.

[42] **Bürkert Contromatic GmbH.** www.buerkert.at. *Typ 6712 - 2/2-Wege schnellschaltendes Magnetventil mit Medientrennung.* [Online] [Cited: 11.05.2016] https://www.buerkert.at/de/type/6712.

[43] **Endress+Hauser GmbH.** http://www.at.endress.com/. *Grenzstanddetektion Liquiphant FTL50.* [Online] [Cited: 11.05.2016] http://www.at.endress.com/de/produkte-feldinstrumentierung/F%C3%BCllstandmesstechnik/Vibronik-Liquiphant-FTL50.

[44] **HAMILTON Bonaduz AG.** http://www.hamiltoncompany.com/. *VisiFerm DO.* [Online] [Cited: 13.05.2016] http://www.hamiltoncompany.com/products/process-analytics/intelligent-sensors/dissolved-oxygen/visiferm-do.

[45] **Riba Edelstahl.** http://www.riba-edelstahl.de/. *Chemische Beständigkeit der nichtrostenden Stähle.* [Online] [Cited: 13.05.2016] http://www.riba-edelstahl.de/services/produkte/techinfo/chemischebestaendigkeit.pdf.

[46] **Endress+Hauser GmbH.** http://www.at.endress.com/. *Omnigrad S TR88 Modulares RTD Thermometer.* [Online] [Cited: 11.05.2016] http://www.at.endress.com/de/produkte-feldinstrumentierung/Temperaturmesstechnik-thermometer-transmitter/Modulares-RTD-Thermometer-TR88?highlight=TR88.

[47] **Georg Fischer Rohrleitungssysteme GmbH.** http://www.gfps.com/. *2450 Pressure Sensor.* [Online] [Cited: 11.05.2016] http://www.gfps.com/country_US/en_US/products/sensors/pressure-sensors/2450.html.

[48] **Polytetra GmbH.** http://www.polytetra.de/. [Online] [Cited: 08.05.2016] http://www.polytetra.de/fileadmin/user_uploads/Download/Prospekte/01_POLYTETRA_Wtauscher_D.pdf.

[49] **KAISER+KRAFT GmbH.** http://www.kaiserkraft.at/. *Raumspartank.* [Online] [Cited: 14.05.2016] http://www.kaiserkraft.at/lagereinrichtungen/tanks-tonnen-faesser/raumspartank/p/M8511/?article=574716&imageCode=AA00574716FF&ff_id=574716&ff_title=Raumspartank&ff_query=Raumspartank&ff_pos=6&ff_origPos=9&ff_page=1&ff_pageSize=48&ff_origPageSize=48&ff_sim.

[50] **Schwarzer Rührtechnik GmbH.** http://www.schwarzer-ruehrtechnik.de/. *Kunststoffbehälter mit oder ohne Rührwerk.* [Online] [Cited: 11.05.2016] http://www.schwarzer-ruehrtechnik.de/pages/kunststoff-dosierbehaelter-mit-oder-ohne-ruehrwerk.php.

[51] **Leibniz-Institut DSMZ-Deutsche Sammlung von Mikroorganismen und Zellkulturen GmbH.** Halomonas sp. *www.dsmz.de.* [Online] [Cited: 22.05.2016] https://www.dsmz.de/catalogues/details/culture/DSM-7328.html?tx_dsmzresources_pi5%5breturnPid%5d=304.

[52] **Routledge, Sarah.** Beyond de-foaming: the effects of antifoams on bioprocess. *Computational and Structual Biotechnologie Journal: Volume No: 3, Issue: 4, October 2012: DOI:10.5936/csbj.201210014*

[53] **Isidoro Camacho-Córdova, David.** Estimation of bacterioruberin by Raman spectroscopy. *APPLIED OPTICS.* Vol 53, Issue 31, 2014, 7470-7475: DOI: 10.1364/AO.53.007470

11   Index of Figures

12 Index of Equations

13   Index of Tables

14   Index of Appendixes

15   Index of Abbreviations

Abbreviation	Description
AC	Alternating Current
ALR	Airlift Reactor
B	Bleed Stream
BP	Bleed Pump
CFF	Cross Flow Filtration
CO_2	Carbon Dioxide
DC	Direct Current
DO	Dissolved Oxygen
FDA	USA Food and Drug Administration
FP	Feed Pump
GRP	Glass Fibre Reinforced Plastic
H	Harvest Stream
H/D	Height to Diameter Ratio
HCl	Hydrochloric Acid
HP	Harvest Pump
HPLC	High-Pressure Liquid Chromatography
k_La	Volumetric Oxygen Transfer Coefficient
LP	Loop Pump
M	Molar
MF	Membrane Module
N_2	Nitrogen
NaCl	Sodium Chloride
NaOH	Sodium Hydroxide
O_2	Oxygen
OD	Optical Density
OTR	Oxygen Transfer Rate
PAT	Process Analytical Technology
PCS	Process Control System
PE	Polyethylene
PEEK	Polyetheretherketone
PFD	Process Flow Diagram
PHA	Polyhydroxyalkanoates
PP	Polypropylene
PSU	Polysulfone
PTFE	Polytetrafluoroethylene
PVDF	Polyvinylidene fluoride
PWM	Pulse Width Modulation
STR	Stirred Tank Reactor
TMP	Transmembrane Pressure
TOC	Total Organic Carbon
URS	User Requirement Specifications
vvm	Gas Flow per Unit of Liquid Volume per Minute

16   Index of Variables

Symbol	Description	Unit
a	Specific Contact Area	m²/m³
A_{cooler}	Required Heat Transfer Area of the Off-gas Cooler	m²
$A_{Membrane}$	Required Membrane Area	m²
c_{O2}^*	Dissolved Oxygen Concentration in Equilibrium	g/L
c_{O2}	Dissolved Oxygen Concentration	g/L
c_{pA}	Specific Heat Capacity of Dry Air	kJ/kg/K
c_{pS}	Specific Heat Capacity of Steam	kJ/kg/K
D	Dilution Rate	h⁻¹
d_{min}	Minimally Required Loop Tubing Diameter	mm
F_B	Bleed Flow	L/h
F_M	Feed Flow	L/h
F_P	Permeate Flow	L/h
h	Specific Enthalpy	kJ/kg
h_{in}	Specific Enthalpy of the Off-gas Entering the Cooler	kJ/kg
h_{out}	Specific Enthalpy of the Off-gas Leaving the Cooler	kJ/kg
H_L	Liquid Height before Gassing	m
H_{tot}	Liquid Height while Gassing	m
H_{O2}	Henry Constant of Oxygen	L*bar/g
J	Flux Rate	L/m²/h
k	Heat Transfer Coefficient	W/m²/K
k_L	Mass Transfer Coefficient of the Liquid Phase	m/h
$k_L a$	Volumetric Oxygen Transfer Coefficient	h⁻¹
K_v	Flow Coefficient	L/h
m_G	Mass of Dry Air	kg
m_W	Mass of Water in Humid Air	kg
OTR	Oxygen Transfer Rate	g/L/h
OD	Optical Density	1
p_1	Pressure of the Membrane's Feed Side	bar
p_2	Retentate Pressure	bar
p_3	Permeate Pressure	bar
p_{O2}	Partial Pressure of Oxygen	bar
p_s	Saturated Vapour Pressure	bar
p_{tot}	Total Pressure	bar
$\dot{Q}$	Heat Flow	W
R	Recirculation Ratio	1
s	Substrate Concentration	g/L
s_{in}	Substrate Concentration in the Feed	g/L

TMP	Transmembrane Pressure	bar
V_G	Gas Bubble Volume	L
$\dot{V}_G$	Off-gas Flow Rate	m³/s
$\dot{V}_{Loop}$	Flow Rate Loop	L/h
V_{tot}	Total Volume	L
$\dot{V}_{TM}$	Transmembrane Flow Rate	L/h
w_{max}	Maximum Allowable Flow Velocity	m/s
x	Biomass Concentration	g/L
Y	Water Load of Humid Air	kg/kg
y_{O2}	Amount-of-Substance Fraction of Oxygen	%
$Y_{X/S}$	Biomass Yield	1
ΔT_{log}	Middle Logarithmic Temperature Difference	K
Δh_V	Enthalpy of Vaporization	kJ/kg
ε	Gas Holdup or Voidage	%
Δm_{ges}	Mass Balance Gap	g
Δm_i	Change in Mass of the Stream i	g
Δm_{Feed}	Change in Mass of the Feed Tank	g
$\Delta m_{Acid/Base}$	Change in Mass of the Acid/Base Tank	g
Δm_{Bleed}	Change in Mass of the Bleed Tank	g
$\Delta m_{Filtrate}$	Change in Mass of the Filtrate Tank	g
$\Delta m_{Samples}$	Change in Mass caused by Sampling	g
$m_{i,End}$	Mass of the Stream i at the Start of the Period	g
$m_{i,Start}$	Mass of the Stream i at the End of the Period	g
μ	Specific Growth Rate	h⁻¹
μ_{max}	Maximum Specific Growth Rate	h⁻¹
ρ_G	Off-gas Density	kg/m³
θ	Air Temperature	°C

Appendix

Appendix 1: Initial User Requirements Specification

User Requirements Specification, 15L Bioreaktor für Halophile	
Beschreibung der Anforderung	
1	**Lieferumfang**
1.1	Kontext: Die Anlage ist für die Kultivierung von salztoleranten Mikroorganismen gedacht. Dabei wird die Produktivität durch Druckerhöhung und durch eine direkt im Kreislauf gekoppelte Zellrückhaltung mittels einer Mikrofiltrationsmembran erhöht. Das System ist aufgrund der hohen Salzkonzentration korrosionsfest auszuführen. Dabei können verschiedene Materilien von Stahl bis Plastik und glasfaserverstärktem Kunststoff (GFK) zum Einsatz kommen. Der Angebotsumfang ist hauptsächlich mechanischer Natur, die Sensoren und Aktoren werden in einem Steuerkasten geführt, wo die Signale abgegriffen werden können. Die Automation und Regelung wird durch die TU Wien durchgeführt.
1.2	Die Anbotsanfrage bezieht sich auf den gesamten Inhalt des strichpunktierten Bereichs im Prozessflussdiagramm (siehe Anhang 1 PFD).
2	**Prozessflüssigkeiten**
2.1	Feed: 20% NaCl-Lösung mit definierten oder komplexen Medien (siehe Prozess Fluss Diagramm (PFD) [1])
2.2	Säure [2], Max 1 M HCl
2.3	Base [3] Max 3 M NaOH, oder NH4OH
2.4	Produkt Strom 1: zellfreies Produkt in 20%-NaCl [12]
2.5	Produkt Strom 2: Produkt in Zellsuspension in 20%-NaCl [13]
2.6	Begasung: Druckluft [4]
2.7	Antischaummittel: Struktol J673 oder äquivalent [manuelle Zugabe]
3.	**Anlagen und Funktionsbeschreibung**
3.1	**Allgemeine Anforderungen**
3.1.1	Die Halo Pilotanlage soll für Upscalingprozesse bei der Halophilen Fermentation dienen.
3.1.2	Während der Fermentation wird kontinuierlich ein Solestrom mit verschiedenster Zusammensetzung zugeführt und soll im Reaktor durch die Halophile in Biomasse, CO2 und ein Zielprodukt (intrazellulär) umgewandelt werden. Der Produktstrom 1 soll über ein Hohlfasermembranmodul (eventuell auch andere Lösung z.B. Kassette) von den Zellen abgetrennt werden
3.1.3	Die Anlage soll zu demonstrativen Zwecken mobil gestaltet werden.
3.1.4	Reinigung der Fermenteranlage erfolgt chemisch.
3.1.5	Mit der Anlage soll es möglich sein, einen Batch- sowie kontinuierlichen Betrieb, mit und ohne Zellrückhaltung,
3.1.6	Sterilisation der Fermenteranlage ist nur bei Kulturenwechsel nötig und kann daher chemisch durchgeführt werden.
3.1.7	Sie soll einem Überdruck von 3 bar ü standhalten können (inkl. aller Leitungen).
3.1.8	Die Anlage muss korrosionsbeständig sein, da mit ~20%-NaCl-lösung gearbeitet wird.
3.2	**Funktionen**
3.2.1	Batch Betrieb
3.2.2	Phase der kontinuierlichen Kultur, ohne Zellrückhaltung.
3.2.3	Phase der kontinuierlichen Kultur, ohne Zellrückhaltung aber mit Zirkulation über den Bypass bzw. das Membranmodul.
3.2.4	Phase der kompletten Zellrückhaltung, ohne Bleed, in welcher Biomasse aufkonzentriert wird.
3.2.5	Phase der geregelten Zellrückhaltung, mit Bleed, in welcher die Biomasse auf einer konstanten Konzentration gehalten wird.
3.2.6	Filtrat und Zellsuspension parallel entnehmen (kontinuierlicher Betrieb)
3.2.7	Temperierung Kulturbrühe 20°C bis 50°C
3.2.8	Druckregelung bis 3 bar Überdruck
3.2.9	pH-Regelung mittels Zugabe von Base oder Säure
3.2.10	Probennahme
3.2.11	pO2 Regelung mittels Druck und Begasung
3.2.11	Alle Behälter im laufenden Betrieb leeren/nachfüllen, zwei Behälter wechselweise für Medium und Produktstrom 1
3.2.12	Schaumkontrolle über manuelle Antifoamzugabe
3.2.13	Reinigbarkeit / Hygiene der Anlage: Zellkreislaufverrohrung soll selbstentleerend sein --> Gefälle

4.	**Technische Daten und Ausführung**	
4.1	**Betriebsdaten und Bereiche**	
4.1.1	Arbeitsvolumen	15 L, Reaktorgeometrie siehe Anhang 5
4.1.2	Fermentationstemperatur	20 – 50°C (± 0,2°C)
4.1.3	Fermentationsüberdruck	3 bar ü (± 0,1 bar)
4.1.4	Belüftungsrate Prozessluft Sparger	0,1 – 2 vvm
4.1.5	pH	2 – 12 (± 0,05) i.d.R. pH 7
4.1.6	pO_2	0 – 100 % (± 1%)
4.1.7	NaCl Gehalt	5 - 25%
4.1.8	Medium Zugabe [1]	0 - 3 L/h (i.d.R 2,5 L/h)
4.1.9	Prudukt Strom 1 / Filtrat [12]	0 - 3 L/h (i.d.R. 1,68 L/h)
4.1.10	Produkt Strom 2 / Zell-suspension	0 - 1 L/h (i.d.R. 0,48 L/h)
4.1.11	Säure Zugabe [2]	0 - 0,1 L/h
4.1.12	Lauge Zugabe [3]	0 - 0,1 L/h
4.1.13	Antischaum Zugabe	über manuelle Zugabe etwa max. 2 mL/h
4.2	**Ausführung**	
4.2.1	**Anlagenaufbau**	
4.2.1.1	Aufbau als mobile Kompaktanlage, inkl. aller Behälter und Auffangwannen auf einem dafür eigens gefertigtem Gerüst / es kann eventuell auch ein zweites für alle Behälter geben	
4.2.1.2	Komplette Montage der Anlage durch Anlagenbauer	
4.2.1.3	Die Anlage muss so konstruiert sein, dass sie in den dafür bestimmten Raum eingebracht werden kann. Max. Türmaße 1,40 m x 2 m / Lift .	
4.2.1.4	Rahmenkonstruktion: Grundrahmen und Rohrleitungsrahmen korrosionsbeständig	
4.2.1.5	Abriebfeste Rollen (2 Lenkrollen, 2 Bockrollen)	
4.2.2	**Blasensäulereaktor**	
4.2.2.1	Behälter ist so einfach wie möglich zu halten, etwa 20L Totalvolumen Kessel mit 2 Anschlussmöglichkeiten am Boden für Begasung und Ablassventil, Deckel mit 11 Anschlussmöglichkeiten für Feed, Abluft, Base, Säure, Temperaturmessung, Antifoam, pO2 Sondensteckplatz, Füllstandsmessung, Drucksensor, fix montiertes Manometer am Deckel und ein Sicherheitsventil	
4.2.2.2	Der Prozess ist so gestaltet, dass kontinuierlich Zellsuspension aus dem oberen Reaktorbereich abgepumpt und im unteren Bereich wieder in den Reaktor gespeist wird. An diesem Zellkreislauf ist das Membranmodul angeschlossen. Der Kreislauf ist mit einem Bypass versehen, damit das Membranmodul auch während des Betriebs entnommen werden kann.	
4.2.2.3	Behältermaterial muss korrosionsbeständig sein (20% NaCl, preiswert, leicht und druckresistent)	
4.2.2.4	Vorprüfung und Abnahme durch TÜV ist erforderlich	
4.2.2.1	**Behälterdaten Reaktor**	
4.2.3.1	Totalvolumen	ca. 20 L (abhängig von Gas-Holdup)
4.2.3.2	Arbeitsvolumen	15 L
4.2.3.3	Dimensionierung	siehe Anhang 5 Behälter Geometrie
4.2.3.5	Zul. Betriebsüberdruck Kessel	-1 bis 6 bar ü
4.2.3.6	Zul. Betriebstemperatur	20 – 50 °C
4.2.3.8	Zugängigkeit	Zur Reinigung muss der Behälter leicht aus dem Gerüst demontierbar sein
4.2.2.2	**Behälterwerkstoffe**	
4.2.4.1	Behälter, Rohrleitungen	GFK, Hastelloy C-22, Emaille, Glas oder sonstiges korrosionsfestes Material
4.2.4.2	Schrauben	A4-Qualität (= Edelstahl für Hochsäureumgebungen)
4.2.4.3	Dichtungen / O-Ringe	EPDM, Viton, PTFE oder andere korrosionsfreie materialien (GFRP)

4.2.2.3	**Anschlüsse**	
4.2.5.1	Deckel	1 Stutzen für manuelle Anti-Foam Zugabe, Verschraubung PG 13 5
		1 Stutzen für Abluft
		1 Stutzen für Feed Verschraubung PG 13 5
		1 Stutzen für Base Verschraubung PG 13 5
		1 Stutzen für Säure Verschraubung PG 13 5
		1 Steckplatz für pO2- Sonde Verschraubung PG 13 5
		1 Steckplatz für Temperaturmessung, Hülse einschraubbar, in welche die Temperatursonde eingeschraubt werden kann
		1 Steckplatz für Füllstandsschalter Level Switch
		1 Steckplatz für Drucksensor
		Fix montiertes Manometer zur Sichtkontrolle
		Sicherheitsventil für Überduck
		1 Steckplatz für spätere Ergänzungen Verschraubung PG 13 5
4.2.5.2	Lateral	1 Längsschauglas zur Schaumkontrolle
4.2.5.3	Behälterboden	1 Anschlussmöglichkeit für Auslass
		1 Anschlussmöglichkeit für Begasung
4.2.5.4	Für alle Stutzen sind Blindstopfen im Lieferumfang enthalten.	
4.2.2.4	**Begasungssystem**	
4.2.2.4.1	Belüftungsrohr mit Sparger für mikrobielle Kultur, demontierbar, z.B. poröse Keramik, Begasungsrohr	
4.2.2.4.2	Druckluft Zufuhr ist vorhanden max. 6 bar	
4.2.3	**Chemikalien Behälter**	
4.2.3.1	Medium	4x 50 L Behälter aus Kunststoff
4.2.3.2	Säure	1x 5 L Behälter aus Kunststoff
4.2.3.3	Base	1x 5 L Behälter aus Kunststoff
4.2.3.4	Filtrat	4x 50 L Behälter aus Kunststoff
4.2.3.5	Zellsuspension	1x 50 L Behälter aus Kunststoff
4.2.3.5	Spezifikation	siehe Anhang 3 Equipmentliste
4.2.4	**Membranmodul**	
4.2.4.1	Das Membranmodul hat die Aufgabe die Zellen im Reaktor zurückzuhalten. Bisher wurde im Labormaßstab zu vergleichbaren Versuchen ein Hohlfasermembranmodul verwendet. Ggf. kann ein Kassettenmodul besser geeignet sein.	
4.2.4.2	Das gesamte Membranmodul soll ebenfalls korrosionsbeständig sein.	
4.2.4.1	**Technische Daten**	
4.2.4.1.1	Porendurchmesser	0,2 μm
4.2.4.1.2	Membranfläche	min 6300 cm²
4.2.4.1.3	Temperaturbereich	20 - 50 °C
4.2.4.1.4	Mindestdruck Gehäuse	3 bar Überdruck
4.2.4.1.5	Transmembraner Druck	max 3 bar ü (i.d.R. geringerer Druck über Ventil V-02 hinter Membran regelbar)
4.2.4.1.6	Transmembraner Fluss	0 - 1,5 L/h (Filtrat)
4.2.4.1.7	Tangentialfluss über Membran	8 L/(m²min)
4.2.4.1.8	Strömungsgeschwindigkeit in Rohrleitungen	1,5 m/s maximal zur Auslegung der Durchmesser
4.2.5	**Heiz-/Kühlsystem**	
4.2.5.1	elektrischer Heizmantel um Rohr, um die Betriebstemperatur konstant zu halten	
4.2.5.2	eventuell ist eine zusätzliche, leistungsstärkere Heizmatte notwendig um den Reaktor auf Betriebstemperatur zu bringen	
4.2.5.3	eventuell nachrüstbares Kühlsystem	
4.2.6	**Abluft**	
4.2.6.1	Druckregelung um Reaktordruck konstant zu halten (bis zu 3 barü)	
4.2.6.2	Abgaskühlung für Abgasmessung und Wasserabscheidung muss vorhanden sein	
4.2.6.3	Abgasmessung ist nicht Teil des Lieferumfangs	
4.2.7	**Verrohrung**	
4.2.7.1	Alle Bauteile müssen gegen 20% NaCl-Lösung beständig sein	
4.2.7.2	Alle Ventile, Armaturen und Filter sind wartungsfreundlich anzuordnen.	
4.2.7.3	Die gesamte Verrohrung, inkl.aller Einbauteile müssen einem Überduck von 3bar standhalten	
4.2.7.4	Alle Rohre sollen totvolumenfrei gestaltet werden.	
4.2.7.5	Die Rohre des Zellkreislaufs sollen ein Gefälle aufweisen, damit sie selbstentleerend sind.	

4.2.8	**Thermische Dämmung**
4.2.8.1	Der Fermenterbehälter und die Rohre des Zellkreislaufes müssen isoliert werden.
4.2.8.2	Der Dämmwerkstoff muss asbestfrei sein.
4.2.8.3	Armaturen werden nicht isoliert.
5.	**Elektro-, Mess- und Regeltechnik, Automation**
5.1	**Steuerung**
5.1.1	Alle Aktoren (Pumpen, Heizung, …) und Sensorenanschlüsse (pH-Sonde, Druckmessgerät, Temperaturfühler, ...) sollen an einem gemeinsamen Schaltkasten zusammengeführt werden, der als Schnittstelle zu allen höheren Regelungsebenen zu sehen ist
5.1.2	Lucullus wird als Prozessleitsystem verwendet.
5.1.3	SPS ist keine zu integrieren
5.2	**HMI**
5.2.1	Ein HMI stellt eine zukünftige Erweiterung der Anlage dar
5.3	**Steuerschrank / Energieversorgung / Netzausfall / Schutzarten**
5.3.1	Der Schaltkasten wird direkt am Gerüst der Apparatur montiert.
5.3.2	Mögliche Bedienungsemente und Schnittstellen sollen in der Schrankfront oder auf einem Panel angebracht werden. Für Unterhalt und Wartung muss die Schranktüre mit den Schnittstellen und Bedienungselementen, voll geöffnet werden können.
5.3.3	Auf der Fronttür muss ein abschliessbarer Hauptschalter und ein Not-Aus angebracht werden.
5.3.4	Im Schaltkasten sind zu integrieren: Analoge und digitale Signalschnittstelle zur Datenverarbeitung (Niederspannung) Energieversorgung 230 V
5.3.5	Die Anlage soll mit einer einzigen Stromeinspeisung ausgerüstet werden. Die Unterverteilung muss innerhalb der Kompakteinheit erfolgen. Die Anschlussleistung ist im Angebot anzugeben.
5.3.6	Um Gefahrenmomente zu vermeiden, muss die Anlage bei Spannungsausfällen in einen sicheren Zustand übergehen (Fail-Safe).
5.3.7	Schutzart: ≥ IP55 für Pumpen ≥ IP54 für die anderen Komponenten (Schaltschrank, Sensoren etc)
6.	**Energien und Betriebsmittel**
6.1	Die benötigten Energien und Betriebsmittel werden mit Kabel und Schläuchen an die Anlage angeschlossen.
6.2	Die Energieversorgung soll wenn möglich über eine normale 230 V Leitung erfolgen

Appendix 2: Process Flow Diagram (As-Built)

Stream List

ID	1	2	3	4	5	6	7	8
Process Medium	Medium	Acid: 0,5 M HCL	Base: 0,5 M NaOH	Inlet Air	Offgas before pressure control	Offgas for gas analysis	Offgas	Cell retention loop inlet
Temperature (°C)	Ambient temperature	Ambient temperature	Ambient temperature	Ambient temperature	up to 50°C	Ambient temperature	Ambient temperature	up to 50°C
Pressure (bar)	6 barg	6 barg	6 barg	6 barg	3 barg	Ambient pressure	Ambient pressure	3 barg
Operation Mode	continuous	intermittent	intermittent	continuous	continuous	continuous	continuous	continuous
Control/ Measuring device	Mass flow	pH-Measurement (QIRC 009)	pH-Measurement (QIRC 009)	Mass flow (FRC 019)	Druckkontrolle			Flow rate
Viscosity (cP)	0,98	1	1	0,02	0,02	0,02	0,02	0,98
Density (kg/dm³)	1,17	1	1					1,2
pH (-)	7	-	14	-	-	-	-	7
Mass flow (kg/m)	max 2,25 kg/h	Ø 0,023 g/h (Steady state); max. 0,06 kg/h	Ø 0,023 g/h (Steady state); max. 0,06 kg/h	0,1-2 vvm	0,1-2 vvm			126 kg/h
Flow rate (l/h)	1,92 l/h	Ø 0,023 l/h; max. 0,06 l/h	Ø 0,023 l/h; max. 0,06 l/h	1,5-30 l/min	1,5-30 l/min			105 l/h
Properties	corrosive	corrosive	corrosive		water free			corrosive
Comment	-	-	-	-	-	contains salt	-	-

ID	9	10	11	12	13	14	15	
Process Medium	Bypass	Retentate	Cell retention loop outlet	Filtrate	Bleed	Sampling	Kühlwasser	
Temperature (°C)	up to 50°C	up to 50°C	up to 50°C	up to 50°C	up to 50°C	up to 50°C	< 15°C	
Pressure (bar)	3 barg	3 barg	3 barg	Ambient pressure	Ambient pressure	Ambient pressure	< 6 bar	
Operation Mode	continuous	continuous	continuous	continuous	continuous	intermittent	continuous	
Control/ Measuring device	-	-	-	-	Feed-Bleed control			
Viscosity (cP)	0,98	0,98	0,98	0,98	0,98	0,98	1	
Density (kg/dm³)	1,2	1,2	1,2	1,17	1,2	1,2		
pH (-)	7	7	7	7	7	7	7	
Mass flow (kg/m)	124 kg/h	124 kg/h	1,68 kg/h	0,57 kg/h				
Flow rate (L/h)	<104 l/h	<104 l/h	1,44 l/h	<0,48 l/h		max. 13 l/min		
Properties	corrosive	cell enriched	corrosive	corrosive; cell-free	corrosive			
Comment	manually controlled	-	-	-	Feed:Zellabfall rellation	Sampling	Water flow switch	

TU WIEN
Biochemical Engineering
Gumpendorferstrasse 1a
1160 Wien
Austria

Phone: +43 1 58801 166 494
Fax: +43 1 58801 166 980

PRIZE Halophile Pilot Bioreactor System

Drawing Name
Process Flow Diagram
Halophile Pilot Bioreactor System

CAD Name: D-P-PF_0001

Drawn - Date: NMA

Rev. No.	Date	Revision	by	TUWIEN	Client
04	09.05.2016	As Built	PDE		
03	05.11.2015	Control loop edit	PDE		
02	05.06.2015	Variante 1 Pumpe	NMA		
01	03.06.2015	Variante 1 Pumpe	NMA	CHE	
00	27.05.2015	First Draft Concept Design – Variante 1 Pumpe	NMA	CHE	

Appendix 3: Constructional Drawing of the Reactor Skid

Appendix 4: Stocklist

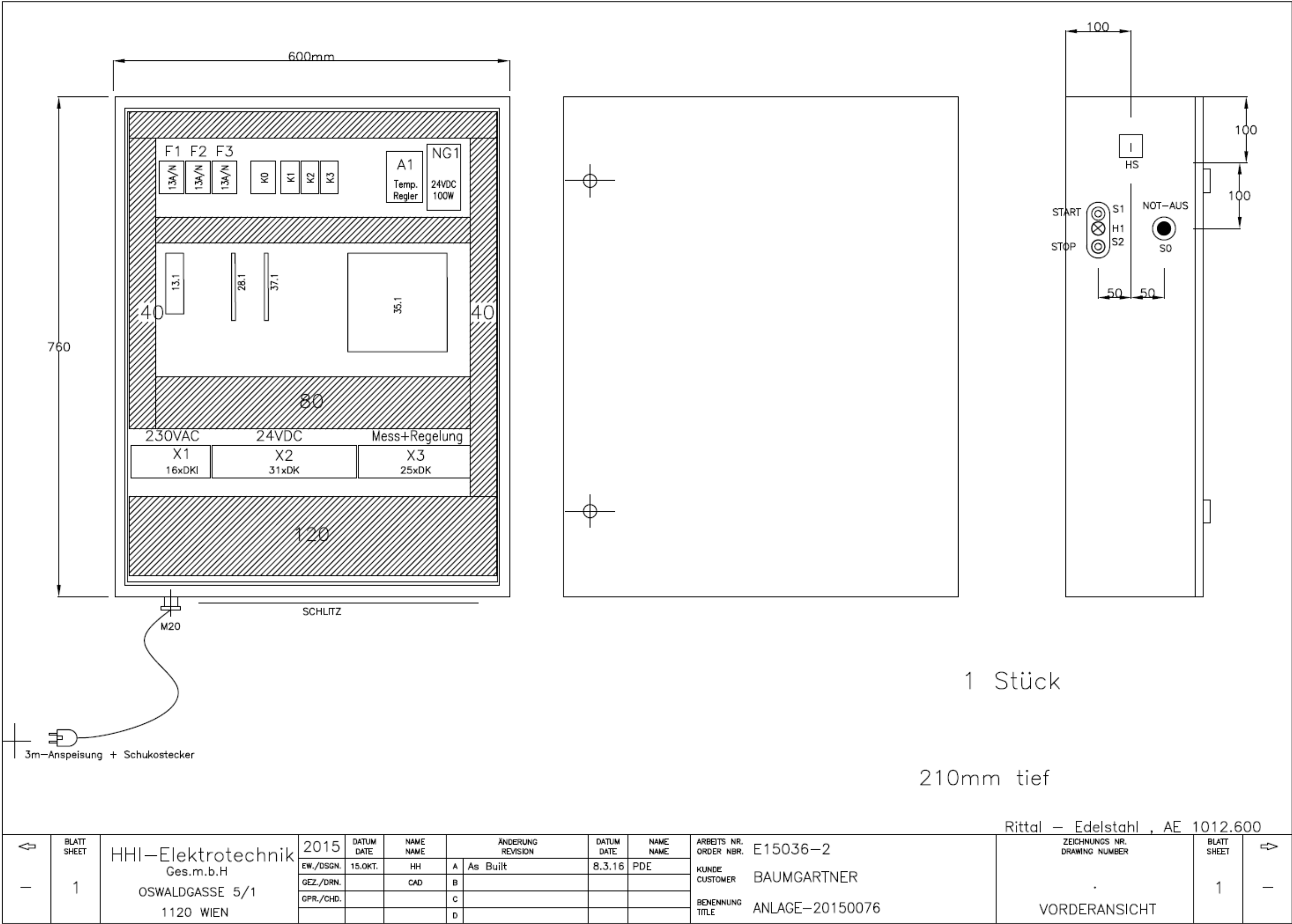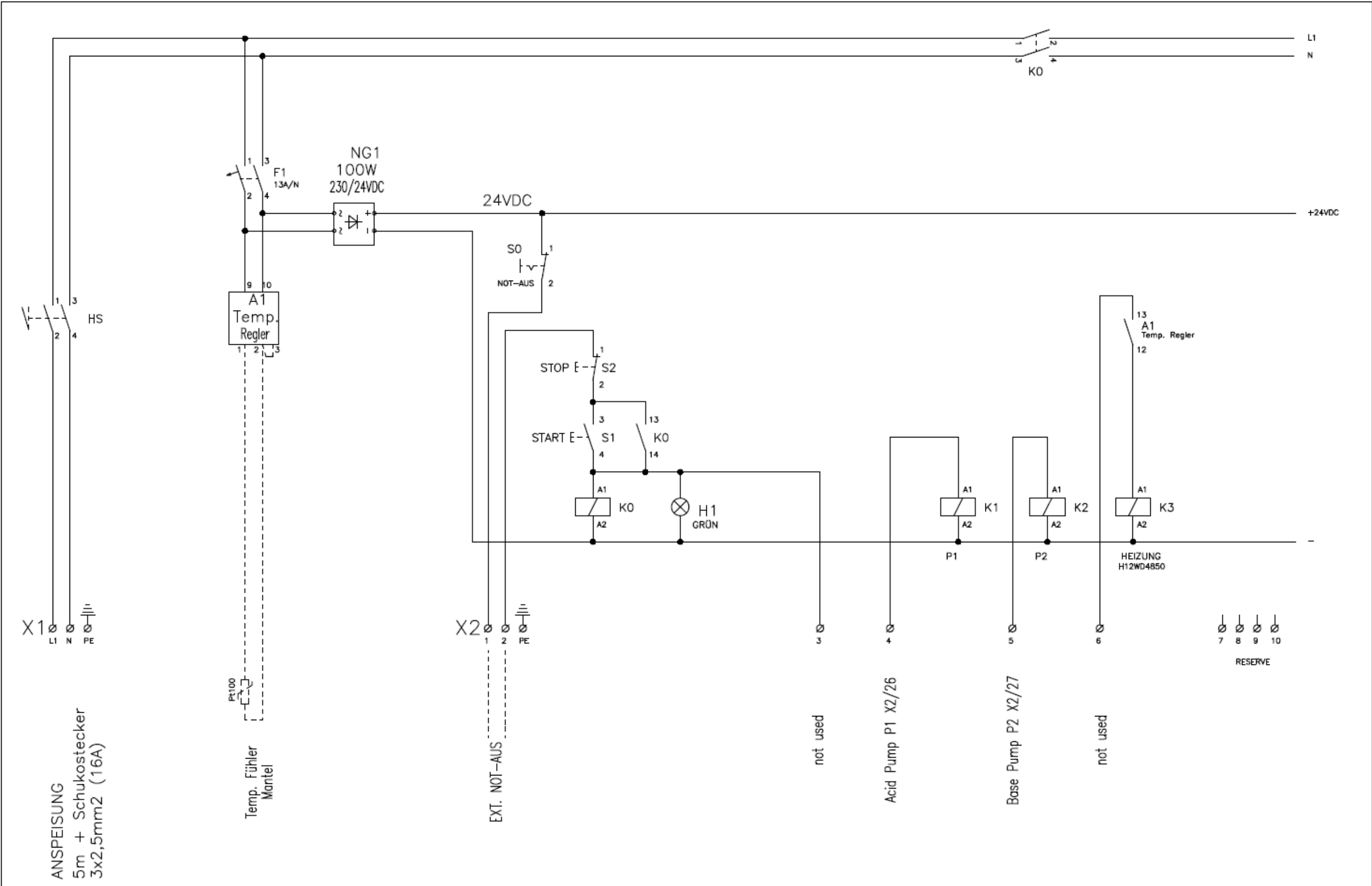| Pos.	Title	Nomenclature in PFD	Manufacturer	Type Reference	Supply Voltage	Electric Capacity [W]	Plug-In Position in Switchboard (Electrical)	Plug-In Position in Switchboard (Control)	Digital Output	Digital Input	Analogue Input	Analogue Output	Signal Type	Channel (TP 5 or Wago Box)	Material	Allowable Pressure at 50°C [barg]	Allowable Temperature [°C]	Comment
1	Reactor	C 1	Baumgartner	Pilotreaktor Halophile											2.4602 (C22)	5	90	
1.1	Sparging tube														PTFE			
1.2	Sparger		Festo	Silencer UC-M5 Type 165003											PE	10	70	10 Stk; 5 Stk Reserve
2	Acid Tank	B 1	Glas Bottle	5L Schott Bottle														Vorhanden im Haus
3	Base Tank	B 2	Glas Bottle	5L Schott Bottle														Vorhanden im Haus
4	Feed Tank	B 3	M&B Stricker	NAL-2250-0130 PP-Ballonflasche											PP			inkl. NAL-2162-0831 PP-Schraubverschluss 83B
4.1	Mixing Tank Feed		Schwarzer Rührtechnik	Dosierbehälter Typ FDE-200-SRT4-1500	230V AC	250	extern								PP			200 Liter Dosierbehälter mit Schnellmischer Rührwerk und Rollwagen
4.2	Tranfer Pump Feed & Filtrate		Ismatec	Ecoline														Vorhanden im Haus
5	Filtrate Tank	B 4	M&B Stricker	NAL-2250-0130 PP-Ballonflasche											PP			inkl. NAL-2162-0831 PP-Schraubverschluss 83B
6	Bleed Tank	B 5	Nalgene	10 L														Vorhanden im Haus
7	Acid Pump	P 1	JESCO	Magdos LB 1 PP/FPM	230V AC	18	X1 1	X2 4	x					DO Ch 3	PP/FPM	16	50	On/Off; Schaltung über Relais
8	Base Pump	P 2	JESCO	Magdos LB 1 PP/EPDM	230V AC	18	X1 2	X2 5	x					DO Ch 4	PP/EPDM	16	50	On/Off; Schaltung über Relais
9	Feed Pump	P 3	JESCO	Magdas LA 4 PP/FPM	230V AC	25	X1 3	X3 1,2				x	4-20mA	AO Ch 7	PP/FPM	16	60	inkl. Steuerungskabel PVC 2m mit Kupplung 4-polig
9.1	Backpressure Valve		JESCO	Druckhalteventil DN6											PP	16	50	noch nicht montiert
10	Loop Pump	P 4	Almatec	Quattroflow QF150S	230V AC	50	X1 4	X3 3,4				x	0-5V	AO Ch 1	1.4435	4	80	Pumpkopf nicht korrosionsbeständig
10.1	Single Use Pump Head		Almatec	QF15DISPP-3-X02											PP	3	60	3 Stk.; Sonderausführung mit Klemmring aus PETP
11	Pressure Reducer MFC	V 1																extern
12	Check Valve	V 2	emTechnik	5R200FF0414PVFP											PVDF/FPM	3,6	120	Rückschlagventil Serie 5R, mit beidseitigem G-Innengewinde, mit Feder
13	Pressure Control Valve	V 3	Bürkert	2/2-Wege-Proportionalventil Typ 2871	24V DC	5									Edelstahl	12	90	nicht korrosionsbeständig in NaCl-Lösung
13.1	Digital Control Electronics		Bürkert	Digitale Ansteuerungselektronik für Proportionalventile Typ 8605	12-24V DC	1	X2 14	X3 13,14				x	4-20mA	AO Ch 8				PWM-Signal; Montage auf Hutschiene im Schaltschrank
14	Off-gas Valve Gas Analyzer	V 4	Bürkert	Nadel-Absperrventil G1/8"											Edelstahl			nicht korrosionsbeständig in NaCl-Lösung
15	Off-gas Valve	V 5	Bürkert	Nadel-Absperrventil G1/8"											Edelstahl			nicht korrosionsbeständig in NaCl-Lösung
16	Shut-off Valve Loop In	V 6	emTechnik	6L701F0614PVFP											PVDF/FPM	6	120	Kugelhahn Serie 6L, manuell, 2-Wege
17	Sampling Valve	V 7	emTechnik	5L101G0318PVFP											PVDF/FPM	6	120	Regulierventil Serie 5L, für Schalttafeleinbau, gerade, mit beidseitigem G-Innengewinde
18	Shut-off Valve Membrane	V 8	emTechnik	6L701F0614PVFP											PVDF/FPM	6	120	Kugelhahn Serie 6L, manuell, 2-Wege
19	Shut-off Valve Bypass	V 9	emTechnik	6L701F0614PVFP											PVDF/FPM	6	120	Kugelhahn Serie 6L, manuell, 2-Wege
20	TMP Control Valve	V 10	emTechnik	5E113G60414PPFP	24V DC	5	X2 11	X3 5,6,7,8				x	4-20mA	AO Ch 6	PP/FPM	6	90	Feinstregulierventil Serie 5E mit 24V DC elektrischem Stellantrieb, mit G-Innengewinde
21	Bypass Valve	V 11	emTechnik	6L733F0614PVFP												6	120	
22	Filtrate Valve	V 12	Bürkert	Magnetventil; 0,4mm; Typ 6712	24V DC	0,9	X2 25	X3 9,10	x					DO Ch 1	PEEK	8		Kontinuierliche Ventile von Bürkert (Typ 6724) verfügbar
23	Bleed Valve	V 13	Bürkert	Magnetventil; 0,4mm; Typ 6712	24V DC	0,9	X2 24	X3 11,12	x					DO Ch 2	PEEK	8		Kontinuierliche Ventile von Bürkert (Typ 6724) verfügbar
24	Shut-off Valve Loop Out	V 14	emTechnik	6L701F0614PVFP											PVDF/FPM	6	120	Kugelhahn Serie 6L, manuell, 2-Wege
25	Drain Valve	V 15	emTechnik	6L701F0614PVFP											PVDF/FPM	6	120	Kugelhahn Serie 6L, manuell, 2-Wege
26	Safety Valve	V 16	Niezgodka	TÜV-SV-14-847 d0 10 Typ 10.2											1.4571	16	320	öffnet bei 8bar; von Baumgartner
27	Level Switch	LRC 001	Endress+Hauser	Liquifant M FTL50	19-55V DC	1,3	X2 22	X3 37,38		x				_Wago DI Ch 1	2.4602 (C22)	100	150	
28	DO-Probe Reactor	QIRC 002	Hamilton	VisiFerm DO Arc 120	24V DC	1	X2 17	X3 31,32			x		4-20mA	AI Ch 6	1.4435	12	140	inkl. Sensor Data Cable VP8 3m
28.1	Isolation Amplifier for DO-Probe		Phoenix Contact	Trennverstärker - MINI MCR-SL-I-I-SP - 2864723	24V DC													Montage auf Hutschiene im Schaltschrank
28.2	Insertion Housing for DO-Probe		Mettler Toledo	InFit761/NS/0070/PVDF D00/Vi9 Einbauarmatur											PVDF	4,8	100	
29	Thermometer Reactor	TIRC 003	Endress+Hauser	Widerstandsthermometer TR88	24V DC		X2 15	X3 15,16			x		4-20mA	AI Ch 7	1.4571		400	vorkonfiguriert auf 0-60°C; inkl. Temperaturkopftransmitter TMT180
30	Manometer Reactor	PI 004	Labom	Druckmessgerät mit Rohrfeder BA4110											1.4301	6,5	150	Messbereich: -1 bis 5bar; von Baumgartner
31	Pressure Sensor reactor	PIRC 005	Georg Fischer	Drucksensor Typ 2450 mit 1/2" Schraubnippel	12-24V DC		X2 18	X3 23,24			x		4-20mA	AI Ch 1	PVDF	3,4	85	Konfiguriert auf 0-3,4bar; inkl. Übergangsstück auf G1/2"-Gewinde
32	Pressure Sensor 1 (Stream 8)	PIRC 006	Georg Fischer	Drucksensor Typ 2450 mit 1/2" Schraubnippel	12-24V DC		X2 19	X3 25,26			x		4-20mA	AI Ch 2	PVDF	3,4	85	Konfiguriert auf 0-3,4bar; inkl. Übergangsstück auf G1/2"-Gewinde
33	Pressure Sensor 2 (Stream 10)	PIRC 007	Georg Fischer	Drucksensor Typ 2450 mit 1/2" Schraubnippel	12-24V DC		X2 20	X3 27,28			x		4-20mA	AI Ch 3	PVDF	3,4	85	Konfiguriert auf 0-3,4bar; inkl. Übergangsstück auf G1/2"-Gewinde
34	Pressure Sensor 3 (Stream 12)	PIRC 008	Georg Fischer	Drucksensor Typ 2450 mit 1/2" Schraubnippel	12-24V DC		X2 21	X3 29,30			x		4-20mA	AI Ch 4	PVDF	3,4	85	Konfiguriert auf 0-3,4bar; inkl. Übergangsstück auf G1/2"-Gewinde
35	pH-Probe	QIRC 009	Mettler Toledo	InPro3250i/SG/120				X3 17,18			x		4-20mA	_Wago AI Ch 2	Glas	4	140	
35.1	Transmitter pH-Probe		Mettler Toledo	Transmitter M400	230V AC		X1 10											vorhanden im Haus
35.2	Flow Cell pH-Probe		Mettler Toledo	Durchflussarmatur easyFlow 23											PSU	7	130	Anschluss NPT 1/4"-Gewinde
36	Temperatur Loop	TIRC 010	Mettler Toledo	InPro3250i/SG/120				X3 19,20			x		4-20mA	_Wago AI Ch 1				Temperaturmessung mit pH-Sonde
37	DO Probe Loop	QIRC 011	Hamilton	VisiFerm DO Arc 120	24V DC	1	X2 16	X3 33,34			x		4-20mA	AI Ch 5	1.4435	12	140	inkl. Sensor Data Cable VP8 3m
37.1	Isolation Amplifier for DO-Probe		Phoenix Contact	Trennverstärker - MINI MCR-SL-I-I-SP - 2864723	24V DC													Montage auf Hutschiene im Schaltschrank
37.2	Flow Cell DO-Probe		Mettler Toledo	Durchflussarmatur easyFlow 23											PSU	7	130	Anschluss NPT 1/4"-Gewinde
38	Feed Balance	WIRC 012	Bloderer	SSP 300	230V AC		extern	extern; Lantronix Box										max. 300kg; Genauigkeit 10g
39	Acid Balance	WIR 013			230V AC		extern	extern; Lantronix Box										Vorhanden im Haus
40	Base Balance	WIR 014			230V AC		extern	extern; Lantronix Box										Vorhanden im Haus
41	Filtrate Balance	WIRC 015	Bloderer	SSP 300	230V AC		extern	extern; Lantronix Box										max. 300kg; Genauigkeit 10g
42	Bleed Balance	WIRC 016			230V AC		extern	extern; Lantronix Box										Vorhanden im Haus
43	Gas Analyzer CO2	QR 017																Gasanalysator extern
44	Gas Analyzer O2	QR 018																Gasanalysator extern
45	MFC Air In	FRC 019	Brooks	MFC GF040CXXC-0008030L-T6PV S4-XXXXXX-00C	24V DC	7	X2 23	X3 39,40,41,42			x	x	4-20mA	AI Ch 8; AO Ch 5	1.4401	10	50	0-30l/min
46	Water Flow Switch	FDS 020																extern
47	Heating Pad	W 1	Winkler		230V AC	1000		X3 35,36				x	0-10V	AO Ch 2			180	Anschluss Temperaturregler und Halbleiterrelais
47.1	Temperature Controller		Winkler	Mikroprozessorgesteuerter Temperaturregler WRH00141-230XW117	230V AC	4											50	Hutschienenmontage
48	Offgas Cooler	W 2																Noch nicht bestellt
49	Kill Switch									x								Anschluss an PLS fehlt!
50	Membrane	F 1	GE Healthcare	Mikrofiltrationsmembran CFP-2-E-9A											PS	5,2	80	2 Stk. Vorhanden; TMP max 1bar
51	Tubing															3,6	120	

Appendix 5: Stocklist of the Tubing Parts from EM-Technik GmbH

No.	Function	Designation	Part Number EM-Technik	Used Amount	Reserve	Connection 1	Connection 2	Connection 3	Material	Allowable Temperature [°C]	Allowable Pressure [barg]	Pressure Reduction factor at 50°C	Allowable Pressure at 50°C [barg]	Comment
1	Ersatzteil Verrohrung	Dichtring für die Serien 2N und 2D	2N006P38PT		10	D4			PTFE	150	6	0,6	3,6	
2	Ersatzteil Verrohrung	Dichtring für die Serien 2N und 2D	2N006P40PT		10	D6			PTFE	150	6	0,6	3,6	
3	Ersatzteil Verrohrung	Dichtring für die Serien 2N und 2D	2N006P48PT		20	D12			PTFE	150	6	0,6	3,6	
4	Ersatzteil Verrohrung	Schneidring für die Serien 2N und 2D	2N007P38PK		5	D4			PEEK	250	10	0,6	6	
5	Ersatzteil Verrohrung	Schneidring für die Serien 2N und 2D	2N007P40PV		5	D6			PVDF	130	10	0,6	6	
6	Ersatzteil Verrohrung	Schneidring für die Serien 2N und 2D	2N007P48PV		10	D12			PVDF	130	10	0,6	6	
7	Ersatzteil Verrohrung	Anschlusssatz für die Serien 2N und 2D (Dichtring, Schneidring und Überwurfmutter)	2N010P38PV		2	D4			PVDF	130	10	0,6	6	
8	Ersatzteil Verrohrung	Anschlusssatz für die Serien 2N und 2D (Dichtring, Schneidring und Überwurfmutter)	2N010P40PV		2	D6			PVDF	130	10	0,6	6	
9	Ersatzteil Verrohrung	Anschlusssatz für die Serien 2N und 2D (Dichtring, Schneidring und Überwurfmutter)	2N010P48PV		2	D12			PVDF	130	10	0,6	6	
10	Anschluss Dosierleitungen an Deckel	Gerade Aufschraubverschraubung mit Rohranschluss Serie 2N und G-Innengewinde	2N100FG3814PV	6	2	D04	G1/4"		PVDF	130	10	0,6	6	
11	Anschluss Ventil Filtrat und Bleed	Gerade Aufschraubverschraubung mit Rohranschluss Serie 2N und G-Innengewinde	2N100FG3818PV	3		D04	G1/8"		PVDF	130	10	0,6	6	
12	Verschluss Membran	Gerade Aufschraubverschraubung mit Rohranschluss Serie 2N und G-Innengewinde	2N100FG4014PV	1		D06	G1/4"		PVDF	130	10	0,6	6	
13	Anschluss T-Stück Bypass	Gerade Aufschraubverschraubung mit Rohranschluss Serie 2N und G-Innengewinde	2N100FG4814PV	1	2	D12	G1/4"		PVDF	130	10	0,6	6	
14	Anschluss Probenahmeventil	Gerade Einschraubverschraubung mit Rohranschluss Serie 2N und G-Außengewinde	2N100MG3818PV	1		D04	G1/8"		PVDF	130	10	0,6	6	
15	Verschluss Membran Filrat	Gerade Einschraubverschraubung mit Rohranschluss Serie 2N und G-Außengewinde	2N100MG4014PV	1		D06	G1/4"		PVDF	130	10	0,6	6	
16	Anschluss Schlauchtüllen	Gerade Einschraubverschraubung mit Rohranschluss Serie 2N und G-Außengewinde	2N100MG4018PV	2	4	D06	G1/8"		PVDF	130	10	0,6	6	
17	Anschluss Kugelhähne	Gerade Einschraubverschraubung mit Rohranschluss Serie 2N und G-Außengewinde	2N100MG4814PV	10	3	D12	G1/4"		PVDF	130	10	0,6	6	
18	Anschluss Flusszellen	Gerade Einschraubverschraubung mit Rohranschluss Serie 2N und NPT-Außengewinde	2N100MN4814PV	4		D12	NPT1/4"		PVDF	130	10	0,6	6	
19	Anschluss Ventil Probenahme und Bleed	Gerade Einschraubverschraubung mit Rohranschluss Serie 2N und UNF-Außengewinde	2N100MU3812PV	4		D04	UNF1/4"-28		PVDF	130	10	0,6	6	
20	Anschluss Membran Filtrat	Gerade Verschraubung mit beidseitigem Rohranschluss Serie 2N	2N100P4015PV	1	1	D06	D1/2"		PVDF	130	10	0,6	6	
21	Übergang Dosierleitungen	Gerade Verschraubung mit beidseitigem Rohranschluss Serie 2N	2N100P4038PV	7	3	D06	D04		PVDF	130	10	0,6	6	
22	Anschluss Membran Filtrat	Gerade Verschraubung mit beidseitigem Rohranschluss Serie 2N	2N100P4815PF	1		D1/2"	D12		PFA	200	10	0,8	8	
23	Anschluss Loop-Pumpe	Winkel-Aufschraubverschraubung mit Rohranschluss Serie 2N und G-Innengewinde	2N200FG4814PV	1	1	D12	G1/4"		PVDF	130	10	0,6	6	
24	Winkelverschraubung Loop	Winkel-Einschraubverschraubung mit Rohranschluss Serie 2N und G-Außengewinde	2N200MG4814PV	1	3	D12	G1/4"		PVDF	130	10	0,6	6	
25	Winkelverschraubung Druckluftleitung	Winkelverschraubung mit beidseitigem Rohranschluss Serie 2N	2N200P40PV	4	4	D06	D06		PVDF	130	10	0,6	6	
26	Winkelverschraubung Loop	Winkelverschraubung mit beidseitigem Rohranschluss Serie 2N	2N200P48PV	9	1	D12	D12		PVDF	130	10	0,6	6	
27	Abzweigung Manometer	T-Aufschraubverschraubung mit Rohranschluss Serie 2N und G-Innengewinde	2N300FG4812PV	4		D12	D12	G1/2"	PVDF	130	10	0,6	6	
28	Abzweigung Probenahme und Bleed	T-Einschraubverschraubung mit Rohranschluss Serie 2N und G-Außengewinde	2N300MG4814PT	2		D12	D12	G1/4"	PTFE	150	6	0,6	3,6	
29	Tri Clamp Klammer	Verschlussklammer für Tri-Clamp-Anschluss Serie 3C	3C001SE1	4		TC 25			1.4308					
30	Tri Clamp Klammer	Verschlussklammer für Tri-Clamp-Anschluss Serie 3C	3C001SE3	2		TC 50.5			1.4308					
31	Tri Clamp Dichtung	Flansch-Abdeckdichtung für Tri-Clamp-Anschluss Serie 3C	3C002EP2	2	2	TC50,5			EPDM	140				
32	Tri Clamp Dichtung	Flansch-Abdeckdichtung für Tri-Clamp-Anschluss Serie 3C	3C002EP4	4	6	TC 25			EPDM	140				
33	Anschluss Membran neu entleerbar	Tri-Clamp Verschraubung Serie 3C mit G-Innengewinde	3C100FG5014PV		2	TC 50,5	G1/4"		PVDF	130	6	0,6	3,6	
34	Anschluss Dosierleitungen an Deckel	Tri-Clamp Verschraubung Serie 3C mit G-Innengewinde	3C100MG2514PV	5	2	TC25	G1/4"		PVDF	130	6	0,6	3,6	
35	Anschluss Entleerung	Tri-Clamp Verschraubung Serie 3C mit G-Außengewinde	3C100MG3414PV	1		TC34	G1/4"		PVDF	130	6	0,6	3,6	
36	Anschluss Entleerung	Tri-Clamp Verschraubung Serie 3C mit G-Außengewinde	3C100MG3438PV		1	TC34	G3/8"		PVDF	130	6	0,6	3,6	Fehlbestellung
37	Anschluss Offgasleitung an Deckel	Tri-Clamp Verschraubung Serie 3C mit Rohranschluss Serie 2N	3C100PN2540PV	1		TC25	D06		PVDF	130	6	0,6	3,6	
38	Verbindung Reaktor/ Loop	Tri-Clamp Verschraubung Serie 3C mit Rohranschluss Serie 2N	3C100PN2548PV	1	3	TC 25	D12		PVDF	130	6	0,6	3,6	
39	Anschluss Reaktor und Membran	Tri-Clamp Verschraubung Serie 3C mit Rohranschluss Serie 2N	3C100PN5048PV	2		TC 50.5	D12		PVDF	130	6	0,6	3,6	
40	Verschlussschraube G1/2"	Verschlussschraube Serie 3F mit G-Außengewinde, mit O-Ring	3F130G12PV	1	1	G1/2"			PVDF	130	10	0,6	6	
41	Verschlussschraube G1/4"	Verschlussschraube Serie 3F mit G-Außengewinde, mit O-Ring	3F130G14PV	1	1	G1/4"			PVDF	130	10	0,6	6	
42	Übergang Probenahmeventil	Reduziernippel Serie 3F mit G-Außengewinde und G-Innengewinde	3F134GG1814PV	1		G1/8"	G1/4"		PVDF	130	10	0,6	6	
43	Abzweigung Bypass	T-Stück Serie 3F mit allseitigem G-Außengewinde	3F333GG14PV	1		G1/4"	G1/4"	G1/4"	PVDF	130	10	0,6	6	
44	Schlauchtülle	Gerade Einschraubtülle Serie 3T mit G-Außengewinde	3T150MG4014PV		2	D04	G1/4"		PVDF	130	10	0,6	6	
45	Schlauchtülle	Gerade Einschraubtülle Serie 3T mit G-Außengewinde	3T150MG4318PV	3	3	D06	G1/8"		PVDF	130	10	0,6	6	
46	Durchflussmesser Bypass	Durchflussmesser Serie 4L, mit rückseitigem G-Innengewinde und Ventil	4L200G230414PVFP		1	G1/4"	G1/4"		PVDF/FPM	130	3	0,6	1,8	Durchflussmenge 10-100l/h
47	Regelventil Loop	Feinstregulierventil Serie 5E mit 24V DC elektrischem Stellantrieb, mit G-Innengewinde	5E113G60414PPFP	1		D04	G1/4"	G1/4"	PP/FPM	90	10	0,6	6	
48	Probenahmeventil	Regulierventil Serie 5L, für Schalttafeleinbau, gerade, mit beidseitigem G-Innengewinde	5L101G0318PVFP	1		DN03	G1/8"	G1/8"	PVDF/FPM	120	10	0,6	6	
49	Rückschlagventil vor Sparger	Rückschlagventil Serie 5R, mit beidseitigem G-Innengewinde, mit Feder	5R200FF0414PVFP	1		DN03	G1/4"	G1/4"	PVDF/FPM	120	6	0,6	3,6	
50	Kugelhahn Loop	Kugelhahn Serie 6L, manuell, 2-Wege	6L701F0614PVFP	5		DN06	G1/4"	G1/4"	PVDF/FPM	120	10	0,6	6	
51	3-Wege-Kugelhahn Bypass	Kugelhahn Serie 6L, manuell, 3-Wege, horizontal, mit T-Bohrung	6L733F0614PVFP	1		DN06	G1/4"	G1/4"	PVDF/FPM	120	10	0,6	6	
52	Dosierleitung	Rohr	SL100S20PV10	17m	3m	DN02/04			PVDF	130				
53	Druckluftleitung	Rohr	SL100S40PV10	2m	8m	DN04/06			PVDF	130				
54	Rohrleitung Loop	Rohr	SL100S48PV10	7m	3m	DN10/12			PVDF	130				

Appendix 6: Circuit Diagram of the Switchboard

L1
N
K0

NG1
100W
230/24VDC
F1
13A/N

24VDC
+24VDC

S0
NOT-AUS

A1
Temp.
Regler

HS

STOP E- S2

START E- S1   K0

A1
Temp. Regler

A1 K0 A2

H1
GRÜN

A1 K1 A2
A1 K2 A2
A1 K3 A2

P1   P2   HEIZUNG
H12WD4850

X1   X2
L1 N PE   1 2 PE   3   4   5   6   7 8 9 10

RESERVE

Pt100

ANSPEISUNG
5m + Schukostecker
3x2,5mm2 (16A)

Temp. Fühler
Mantel

EXT. NOT-AUS

not used

Acid Pump P1 X2/26

Base Pump P2 X2/27

not used

BLATT SHEET	HHI–Elektrotechnik Ges.m.b.H OSWALDGASSE 5/1 1120 WIEN	2015	DATUM DATE	NAME NAME		ÄNDERUNG REVISION	DATUM DATE	NAME NAME	ARBEITS NR. ORDER NBR.	E15036-2	ZEICHNUNGS NR. DRAWING NUMBER	BLATT SHEET	
1		EW./DSGN.	15.OKT.	HH	A	As Built	8.3.16	PDE	KUNDE CUSTOMER	BAUMGARTNER	.	1	2
		GEZ./DRN.		CAD	B								
		GPR./CHD.			C			BENENNUNG TITLE	ANLAGE-20150076				
					D								

⇦	BLATT SHEET	HHI−Elektrotechnik Ges.m.b.H OSWALDGASSE 5/1 1120 WIEN	2015	DATUM DATE	NAME NAME	ÄNDERUNG REVISION	DATUM DATE	NAME NAME	ARBEITS NR. ORDER NBR.	E15036−2	ZEICHNUNGS NR. DRAWING NUMBER	BLATT SHEET	⇨
				EW./DSGN.	15.OKT.	HH	A	As Built	8.3.16	PDE	KUNDE CUSTOMER	BAUMGARTNER			
1	2			GEZ./DRN.		CAD	B						2	3
				GPR./CHD.			C				BENENNUNG TITLE	ANLAGE−20150076		
							D							

L1
N

F3
13A/N

K3

+24VDC
−

Pressure Control Valve V3

DO Probe Reactor QIRC 002

DO Probe Loop QIRC 011

13.1   GND   X3/14
         4−20mA X3/13

28.1   GND   X3/32
         4−20mA X3/31

37.1   GND   X3/34
         4−20mA X3/33

X1   L N PE
        16

X2   + −   + −   + −   + −   + −   + −   + −
     11   12   13   14   15   16   17

HEIZUNG

Control Valve Loop V10

RESERVE

RESERVE

Control Electronics for
Pressure Control Valve V3

Thermometer Reactor TIRC 003

Isolation Amplifier for
DO Probe Reactor QIRC 002

Isolation Amplifier for
DO Probe Loop QIRC 011
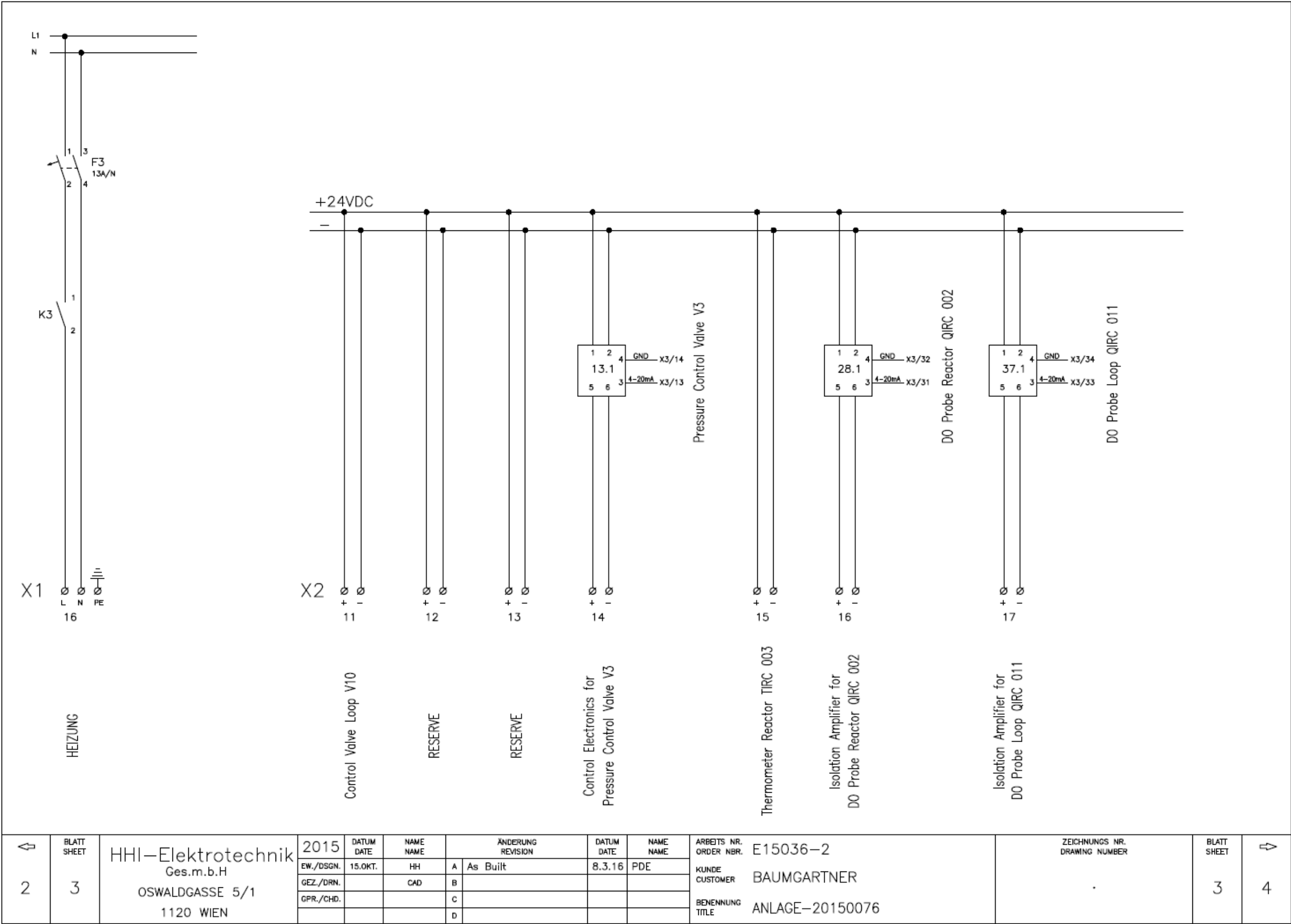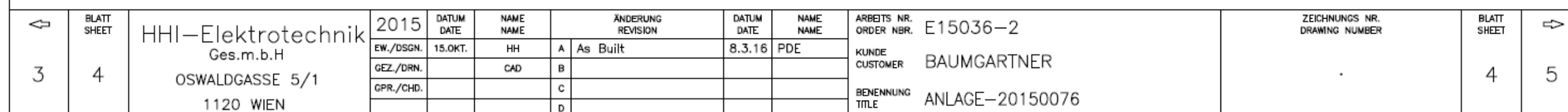
	BLATT SHEET	HHI−Elektrotechnik Ges.m.b.H OSWALDGASSE 5/1 1120 WIEN	2015	DATUM DATE	NAME NAME	ÄNDERUNG REVISION	DATUM DATE	NAME NAME	ARBEITS NR. ORDER NBR.	E15036−2	ZEICHNUNGS NR. DRAWING NUMBER	BLATT SHEET	
2	3			EW./DSGN.	15.OKT.	HH	A As Built	8.3.16	PDE	KUNDE CUSTOMER	BAUMGARTNER	·	3	4
				GEZ./DRN.		CAD	B							
				GPR./CHD.			C			BENENNUNG TITLE	ANLAGE−20150076			
							D							

+24VDC
−

X2

+ −	+ −	+ −	+ −	+ −	+ −	+ −	+ −	+ −	+ −
18	19	20	21	22	23	24	25	26	27

Reactor Pressure PIRC 005

Pressure 1 (Stream 8) PIRC 006

Pressure 2 (Stream 10) PIRC 007

Pressure 3 (Stream 12) PIRC 008

Level Switch LRC 001

MFC Air In FRC 019

Filtrate Valve V12

Bleed Valve V13

Acid Pump P1

Base Pump P2

	BLATT SHEET	HHI−Elektrotechnik Ges.m.b.H OSWALDGASSE 5/1 1120 WIEN	2015	DATUM DATE	NAME NAME	ÄNDERUNG REVISION		DATUM DATE	NAME NAME	ARBEITS NR. ORDER NBR.	E15036−2	ZEICHNUNGS NR. DRAWING NUMBER	BLATT SHEET	
3	4			EW./DSGN.	15.OKT.	HH	A	As Built	8.3.16	PDE	KUNDE CUSTOMER	BAUMGARTNER	.	4	5
				GEZ./DRN.		CAD	B								
				GPR./CHD.			C				BENENNUNG TITLE	ANLAGE−20150076			
							D								

X3

Terminal blocks 1–36

Terminal	Label	Reference
1 2	Feed Pump P3 AO 4–20mA	
3 4	Loop Pump P4 AO 0–5V	
5 6	Control Valve Loop V10 AO 4–20mA	
7 8	Control Valve Loop V10 AI 4–20mA not used	
9 10	Filtrate Valve V3 DO	
11 12	Bleed Valve V4 DO	
13 14	Pressure Control Valve V3 AO 4–20mA	13.1 (3 4) Control Electronics for Pressure Control Valve V3
15 16	Thermometer Reactor TIRC 003 AI 4–20mA	
17 18	pH Probe QIRC 009 AI 4–20mA	35.1 (5 6) Transmitter pH–Probe QIRC 009
19 20	Temperature Loop TIRC 010 AI 4–20mA	35.1 (7 8) Transmitter pH–Probe TIRC 010
21 22	RESERVE	
23 24	Reactor Pressure PIRC 005 AI 4–20mA	
25 26	Pressure 1 (Stream 8) PIRC 006 AI 4–20mA	
27 28	Pressure 2 (Stream 10) PIRC 007 AI 4–20mA	
29 30	Pressure 3 (Stream 12) PIRC 008 AI 4–20mA	
31 32	DO Reactor QIRC 002 AI 4–20mA	28.1 (3 4) Isolation Amplifier for DO Probe Reactor QIRC 002
33 34	DO Loop QIRC 011 AI 4–20mA	37.1 (3 4) Isolation Amplifier for DO Probe Loop QIRC 011
35 36	Heating Pad W1 AO 0–10V	

SHEET 4 / BLATT SHEET 5	HHI–Elektrotechnik Ges.m.b.H OSWALDGASSE 5/1 1120 WIEN	2015	DATUM DATE	NAME NAME	ÄNDERUNG REVISION	DATUM DATE	NAME NAME	ARBEITS NR. ORDER NBR. E15036–2	ZEICHNUNGS NR. DRAWING NUMBER
		EW./DSGN.	15.OKT.	HH	A As Built	8.3.16	PDE	KUNDE CUSTOMER BAUMGARTNER	BLATT SHEET 5 / 6
		GEZ./DRN.		CAD	B				
		GPR./CHD.			C			BENENNUNG TITLE ANLAGE–20150076	
					D				

X3

| | 37 38 | 39 40 | 41 42 | 43 44 | 45 46 | 47 48 | 49 50 | 51 52 | 53 54 | 55 56 | 57 58 | 59 60 |

Level Switch LRC 001 DI

MFC Air In FRC 019 AO 4-20mA

MFC Air In FRC 019 AI 4-20mA

RESERVE

RESERVE

RESERVE

RESERVE

RESERVE

RESERVE

RESERVE

RESERVE

RESERVE

⇦	BLATT SHEET	HHI—Elektrotechnik Ges.m.b.H OSWALDGASSE 5/1 1120 WIEN	2015	DATUM DATE	NAME NAME	ÄNDERUNG REVISION	DATUM DATE	NAME NAME	ARBEITS NR. ORDER NBR. E15036—2	ZEICHNUNGS NR. DRAWING NUMBER	BLATT SHEET	⇨
5	6			EW./DSGN. 15.OKT.	HH	A As Built	8.3.16	PDE	KUNDE CUSTOMER BAUMGARTNER		6	—
				GEZ./DRN.	CAD	B				.		
				GPR./CHD.		C			BENENNUNG TITLE ANLAGE—20150076			
						D						